WADC TECHNICAL REPORT 57-344
PART V

DEVELOPMENT OF NIOBIUM-BASE ALLOYS

RICHARD T. BEGLEY
WILLIAM N. PLATTE
ALLEN I. LEWIS
ROBERT L. AMMON

RESEARCH LABORATORIES
WESTINGHOUSE ELECTRIC CORPORATION

SEPTEMBER 1961

MATERIALS CENTRAL
CONTRACT No. AF 33(616)-6258
PROJECT No. 7351

AERONAUTICAL SYSTEMS DIVISION
AIR FORCE SYSTEMS COMMAND
UNITED STATES AIR FORCE
WRIGHT-PATTERSON AIR FORCE BASE, OHIO

600 - December 1961 - 14-552 & 553

FOREWORD

This report was prepared by personnel of the Research Laboratories of the Westinghouse Electric Corporation under USAF Contract AF 33(616)-6258. This contract was initiated under Project No. 7351, "Metallic Materials", Task No. 73512, "Refractory Metals". The contract was administered under the direction of the Materials Central, Directorate of Advanced Systems Technology, Wright Air Development Division, with Lt. C. S. Hartley acting as project engineer.

This report describes the results of research conducted during the period 1 June 1959 to 31 July 1960.

Among those who contributed to the experimental work described in this report were R. Palmquist, H. G. Kohute, R. Kramer, W. N. Pryle, R. Hovan, and E. Vandergrift.

ABSTRACT

The effect of oxygen and nitrogen additions on the hardness, workability, strain-hardening characteristics, and recrystallization behavior of niobium was determined. Nitrogen additions were found to be detrimental to cold rolling characteristics. Hardness, workability, and mechanical property data for Nb-C alloys were obtained. Grain boundary carbides were found to be very detrimental to cold workability. Carbon additions increased the ductile-brittle transition temperature range of niobium.

Mechanical property data were obtained for many binary, ternary and quaternary niobium base alloys. Re, W, and Mo additions increased the ductile brittle transition of niobium. A number of alloys were prepared by the consumable electrode arc melting process. Ingot breakdown was accomplished by high energy rate extrusion (Dynapak). The results of Dynapak extrusion were very encouraging.

Several high strength alloys were investigated. One alloy, Nb-10W-5V-1Zr, had excellent room temperature ductility and ultimate tensile strengths of 64, 800 psi and 29, 450 psi at 1205 C (2200 F) and 1315 C (2400 F) respectively.

Welding data for a number of Nb-base alloys are also presented.

PUBLICATION REVIEW

This report has been reviewed and is approved.

FOR THE COMMANDER:

I. Perlmutter
Chief, Physical Metallurgy Branch
Metals and Ceramics Laboratory
Materials Central

TABLE OF CONTENTS

LIST OF FIGURES

LIST OF FIGURES (Cont'd)

LIST OF FIGURES (Cont'd)

LIST OF FIGURES (Cont'd)

LIST OF FIGURES (Cont'd)

LIST OF TABLES

LIST OF TABLES (Cont'd)

INTRODUCTION

This report summarizes research conducted on niobium and its alloys during the period 1 June 1959 to 31 July 1960. The work described in this report is an extension of earlier research (1 January 1956 thru 1 June 1959) described in WADC TR 57-344, Parts I, II, and IV.

The research program was undertaken to evaluate the potentialities of niobium-base alloys as high temperature materials. The initial work was largely devoted to studies of the properties of commercial and high purity niobium to provide the background data necessary for a systematic investigation of niobium-base alloys. This included studies of low temperature flow and fracture characteristics, elevated temperature tensile and stress-rupture properties, recrystallization behavior, rolling and recrystallization textures, oxidation studies, weldability, and melting and purification techniques. Subsequent work was concentrated on the evaluation of the workability, mechanical properties, and welding characteristics of a number of niobium-base alloys. The intent of this work was to provide some systematic data on alloying effects and strengthening mechanisms, rather than the development of alloys for specific engineering applications.

In the current program, the effects of interstitial elements on the properties of niobium were investigated. The mechanical properties and welding characteristics of a number of niobium-base alloys were evaluated. Several of the more promising alloys were prepared by consumable electrode arc-melting for more extensive evaluation.

Manuscript released by authors January 3, 1961 for publication as a WADC Technical Report.

EFFECTS OF INTERSTITIAL ELEMENTS ON THE PROPERTIES OF PURE NIOBIUM

Commercial niobium may contain significant quantities of the interstitial elements oxygen, nitrogen, carbon, and hydrogen. The presence of interstitial impurities has a pronounced effect on the properties of body-centered cubic metals. Among the more important manifestations of interstitial impurity effects are strain-aging, which arises from the interaction of mobile interstitial solute atoms and moving dislocations; and deleterious effects on low temperature and ductility and workability which are associated with the presence of dissolved interstitial impurities or precipitated interstitial-metal compounds. It has also been observed that the interaction of interstitial elements with alloy additions resulting in dispersion hardening contributes significantly to the high temperature strength of refractory metals such as molybdenum and niobium.

In the current work, the effects of oxygen and nitrogen on the hardness, workability, recrystallization behavior, and strain hardening of niobium were explored in some detail. Additional studies of the effect of carbon additions on the hardness, workability and low temperature mechanical properties of niobium were also carried out.

Niobium-Oxygen

Literature. The solid solubility of oxygen in niobium is quite high compared to that of most of the other refractory metals. Seybolt[1] reported the solid solubility to be 0.25 and 1.0 w/o at 775 and 1100 C respectively. Recent work by Elliott[2] indicates a solubility of 0.25 w/o at 500 C, and a maximum solid solubility of 0.72 w/o at 1915 C. Three oxides, NbO, NbO_2 and Nb_2O_5 exist in the system. A eutectic reaction occurs between α-Nb primary solid solution and NbO at 10.5 w/o oxygen and 1915 C.

Oxygen has a pronounced effect on room temperature tensile properties of niobium. Tottle[3] has reported that increasing the oxygen content of niobium from 0.03 w/o to 0.41 w/o raises the ultimate tensile strength from 41,100 psi to 131,250 psi. Several investigators[4, 5, 6] have observed repeated yielding and the return of the yield point on aging in niobium. Earlier work[6] in this program indicated that oxygen is the interstitial element responsible for the observed strain-aging phenomena.

Materials and Experimental Procedure. The base material used for this study was obtained from the Union Carbide Metals Company in the form of small beads, approximately 1/8 inch in diameter. The chemical analysis of this material is listed in Table 1.

Table 1. Chemical Analysis of Niobium

Lot No.	Analysis (w/o)					
	0	N	C	Ta	Ti	B
EM-5	0.045	0.011	0.022	0.5	0.01	0.0001

The interstitial impurity level of this material was considerably higher than desirable for a study of the effects of specific interstitial elements. Material of low oxygen and nitrogen content was subsequently prepared by vacuum levitation melting 10 gram pellets cold pressed from the as-received material. Earlier work had shown that purification of niobium with respect in volatile impurities could be achieved by levitation melting in vacuum. Typical purification data are listed in Table 2. As can be seen, considerable oxygen removal occurs after only 15 seconds in the molten state. The oxygen level generally decreases as the residence time in the molten state increases.

Table 2. Purification of Niobium by Vacuum Levitation Melting

Time Molten (seconds)	Analysis (w/o)		
	0	N	C
Starting Matl.	0.038	0.013	0.012
15	0.0092	0.0120	-----
30	0.0035	0.0080	0.0110
60	0.0065	0.0120	0.0050
120	0.0030	0.0080	-----
120	0.0022	-----	-----

Removal of nitrogen and carbon proceeds at a slower rate than that of oxygen. The scatter in the analytical data is probably due to inhomogeneity of the starting material. Violent gas evolution was observed in melting some of the samples while others behaved in a quiet manner indicating that the as-pressed pellets vary considerably in gaseous impurity level. The principal mechanism of oxygen removal is the evaporation of NbO from the melt, for the reduction in carbon content does not correspond to its removal as CO. The required equilibrium oxygen pressure over the melt is evidently much too

low for oxygen removal in the elemental form. The purification reactions which occur during vacuum levitation melting niobium are very similar to those observed by Smith, Hunt and Hanks[7] in electron beam melting. By analogy with the result of electron beam melting, considerable removal of volatile metallic impurities such as vanadium, iron and chromium should also be obtained during vacuum levitation melting since the melting pressures are essentially the same (1×10^{-5} to 1×10^{-4} mm of Hg.).

High purity material was prepared by levitation melting the cold pressed compacts and holding them fully molten for 30 to 60 seconds. This was sufficient time to reduce the carbon, oxygen and nitrogen level to 0.01 w/o or less. Several specimens were floated in the molten state for 2 minutes in order to prepare niobium extremely low in oxygen and nitrogen.

Niobium-oxygen alloys were prepared by levitation melting the pre-melted buttons in high purity argon containing varying partial pressures of oxygen. Oxygen was supplied to the melting chamber from a tank of Sigma argon (4.89 mol % O_2, 95.11 mol % A) which was then diluted with high purity argon to achieve the desired partial pressure of oxygen. This technique of gas doping was chosen for several reasons.

1) It was desired to determine the effect of gaseous impurities on the properties of as-cast niobium. The samples produced were cast in the form of miniature sheet bars (1/2 inch x 1/4 inch by 3/4 inch) which were well suited for rolling experiments.

2) The large surface to volume ratio of the molten samples and the vigorous electromagnetic stirring action of the field provided very homogeneous alloys.

3) A relatively large number of samples could be prepared quickly and easily in existing equipment.

It was found that by keeping the time in the molten state constant and varying the partial pressure of oxygen, a suitable range of oxygen levels could be obtained. Oxygen concentrations varying from 0.0123 to 0.409 w/o were achieved (by using partial pressures of oxygen ranging from 5μ Hg to 30 mm Hg).

Particular care was taken to insure reliable results of the vacuum fusion oxygen analyses. The method used has been described by Harris[8]. The accuracy of this technique is very good, as shown by the results of isotopic addition studies conducted by Harris, Hickam and Loeffler[9]. Most of the Nb-O alloys were analyzed for nitrogen to determine if contamination had occurred during melting. With one exception, the nitrogen analyses were below 0.01 w/o. The exception was the 0.137 w/o oxygen alloy, which contained 0.032 w/o nitrogen.

The VPN hardness of each of the alloys was determined by making hardness impressions on a ground and polished surface of the as-cast sheet bars. An average of three or more impressions was used. Workability was evaluated by cold rolling on a 2 high Stanat mill, using reductions of about 10% per pass.

Hardness and Workability. The effect of oxygen additions on the as-cast hardness of niobium is shown in Figure 1. Relatively small additions of oxygen have a rather pronounced effect in raising the as-cast hardness. Raising the oxygen level from 0.0076 w/o to 0.104 w/o increased the as-cast hardness from 66 VPN to 152 VPN. At the high concentrations the hardness data agree quite well with results reported by Seybolt[1] and Tottle[3]. Metallographic examination showed all the specimens to be single phase.

The results of cold rolling Nb-O alloys are tabulated in Table 3. Alloys containing up to 0.137 w/o oxygen were cold rolled to 75% reduction with good results. Alloys of higher oxygen level failed during rolling by brittle transgranular cleavage. Workability data obtained on 10 gram samples cannot, of course, be applied directly to commercial or semi-commercial size ingots, where large

Table 3. Workability of Levitation Melted Niobium-Oxygen Alloys

w/o Oxygen	Results of Cold Rolling
0.0076	75% Reduction. Excellent
0.0123	75% Reduction. Excellent
0.028	75% Reduction. Excellent
0.093	75% Reduction. Excellent
0.104	75% Reduction. Excellent
0.121	75% Reduction. Minor edge tears. Good.
0.137	75% Reduction. Minor edge tears. Good.
0.212	Cracked after 25% reduction
0.381	Cracked severely on first pass
0.409	Cracked severely on first pass

differences in grain size, cooling rate, homogeneity and purity with respect to other contaminants may be expected. The data are useful, however, in providing quantitative information concerning the effect of oxygen on workability under rather ideal conditions. These results illustrate the rather remarkable tolerance of Nb to oxygen level compared to most of the other refractory metals.

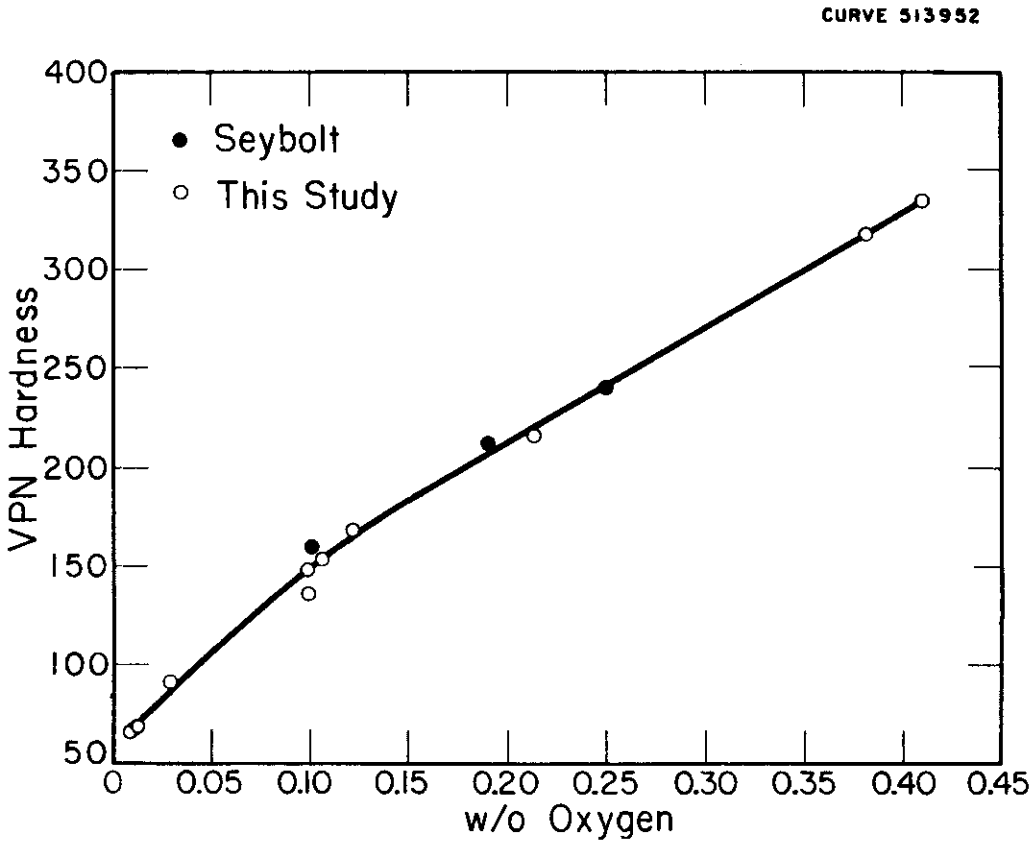

Fig. 1 -Effect of oxygen on the as-cast hardness of niobium.

Strain-Hardening. The effect of oxygen additions on the strain hardening of niobium is shown in Figure 2, where hardness is plotted as a function of percent reduction by cold rolling. Oxygen additions significantly increase the rate of strain hardening of niobium with small amounts of deformation. However, the hardness increment after 75% reduction (as-rolled hardness minus as-cast hardness) is virtually the same for low oxygen and high oxygen alloys.

Recrystallization. The recrystallization behavior of Nb-O alloys was studied by means of 1 hour isothermal anneals at temperatures ranging from 900 C to 1300 C. The progress of recrystallization was followed by hardness measurements and metallographic examination. Isochronal softening curves for specimens cold rolled 75% are shown in Figure 3. The results of metallographic examination are listed in Table 4.

Table 4. Recrystallization Data for Niobium-Oxygen Alloys[a]

Specimen No.	Oxygen (w/o)	Percent of Specimen Recrystallized Estimated from Metallographic Examination				
		Annealing Temperature °C				
		900	1000	1100	1200	1300
L-366	0.0076	B-C[b]	C	E	F	F^+
L-365	0.0123	B	B	C	E	F^+
L-360	0.028	B	C	D	F	F^+
L-359	0.093	B	C	D	D	F^+
L-358	0.104	B-[c]	B	C	C	F^+
L-375	0.121	B-	B	C	D	D-E
L-382	0.137	B	B	C	D	F

(a) 75% reduction by cold rolling, 1 hour anneals

(b) Key: A - no recrystallization
B - 1 to 10% recrystallized
C - 10 to 50% recrystallized
D - 50 to 90% recrystallized
E - 90 to 99% recrystallized
F - completely recrystallized
F - completely recrystallized with grain growth.

(c) Superscript minus sign (-) denotes low side of range.

CURVE 513950

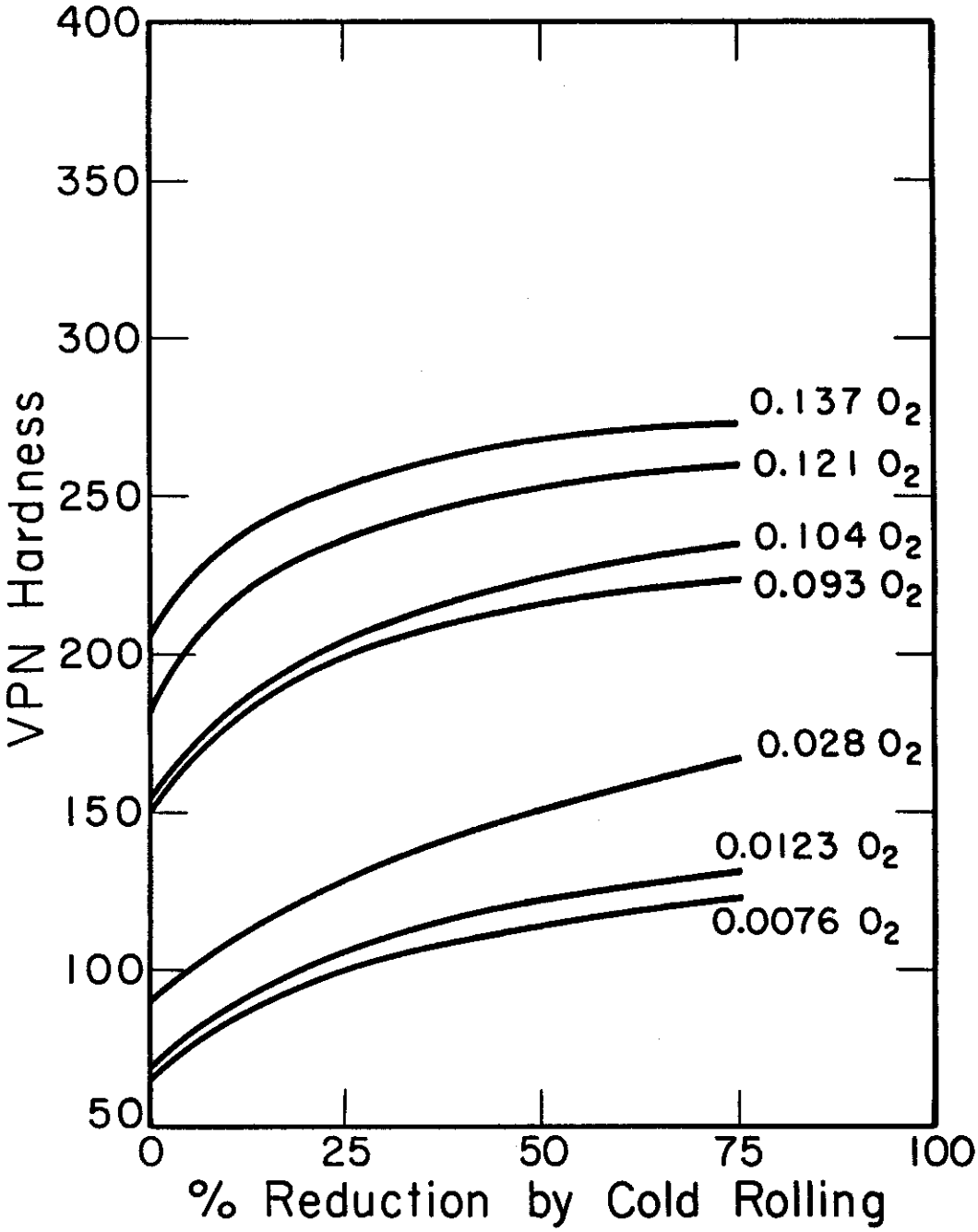

Fig.2- Effect of oxygen on the strain hardening of niobium.

CURVE 513951

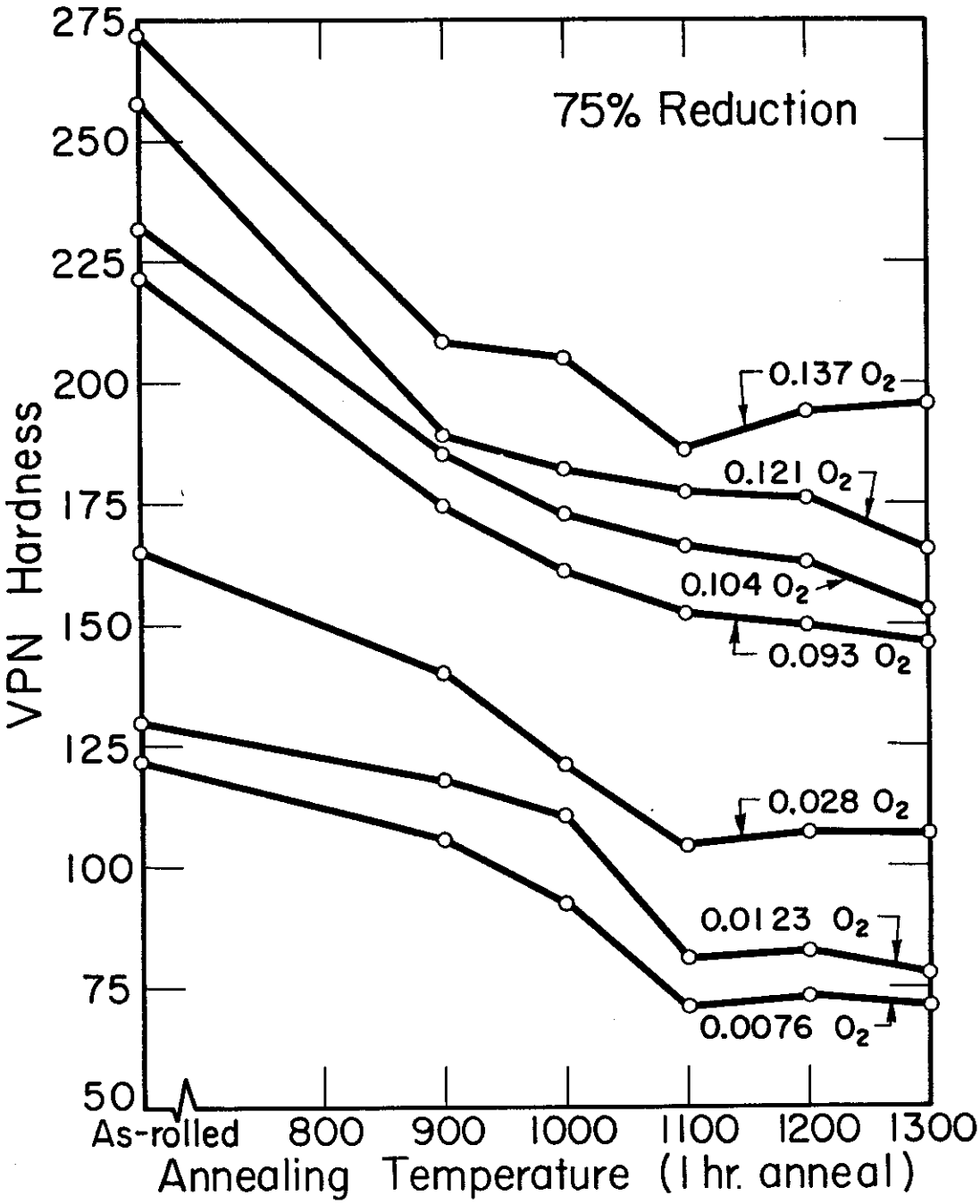

Fig.3 – Hardness as a function of annealing temperature for Nb – O alloys.

After a 1 hour anneal at 900 C, recrystallization is about 5-10% complete for most of the alloys. However, in the 0.104 and 0.121 w/o oxygen alloys only a very few new grains were observed in the cold worked matrix. Recrystallization was essentially complete for alloys containing up to 0.028 w/o oxygen after a 1 hour anneal at 1200 C. Alloys of higher oxygen level were only 50 to 75% recrystallized. After 1 hour at 1300 C all of the specimens were completely recrystallized, with the exception of the 0.121 w/o O_2 alloy. Grain growth was observed at this temperature in alloys containing up to 0.104 w/o O_2. The softening curves shown in Figure 3 are in fairly good agreement with the observed microstructures. However, as found in earlier recrystallization studies of electron beam melted niobium, considerable reduction in hardness occurs before any significant amount of recrystallization is observed in the microstructure. Oxygen additions appear to have a relatively slight effect in broadening the recrystallization range of niobium, the increase being on the order of 100-150 C for material containing about 0.12 w/o oxygen.

Niobium-Nitrogen

Literature. The solid solubility of nitrogen in niobium is considerably lower than that of oxygen. By internal friction measurements Ang and Wert[10] determined the solubility to be about 0.05 w/o at 1100 C, decreasing to about 0.005 w/o at 300 C. Hansen[11] has reviewed the information available on the Nb-N system. Three nitrides, Nb_2N, NbN, and a phase stable between 42.9 and 44.1 a/o N, have been reported. Nb_2N is close packed with interstitial nitrogen atoms. It exists over the composition range 28.6 to 33.3 a/o N. The phase stable between 42.9-44.1 a/o N has a tetragonally distorted NaCl structure. NbN exists in three forms, NbNI, NbNII, NbNIII. NbNI, stable at 50 a/o N, is hexagonal. NbNII (about 48.7 a/o N) is also hexagonal with a c/a ratio about half that of NbNI; it appears to be stable only under certain conditions of temperature and pressure. NbNIII exists from 47.1 to 48.5 N and has a NaCl type structure.

Relatively few data are available in the literature concerning the effect of nitrogen on the properties of niobium. Ang and Wert[10] investigated the effect of several aging heat treatments on the hardness and nitrogen content. However, it appears that considerable oxygen contamination of the samples may have occurred in these studies.

Material and Experimental Procedure. The base material used for this work was the same as that used in the niobium-oxygen alloy studies. The chemical composition is listed in Table I. High purity material was prepared by levitation melting 10 gram pellets in the manner described previously. Initial attempts

were made to prepare Nb-N alloys by admitting nitrogen from a liquid nitrogen dewar to the levitation melting chamber through a regulated leak. When specimens were melted in a dynamic pressure of 50 μ of N_2 a hardness increase of only 25-30 VPN was observed. Melting was then done in a static argon-nitrogen atmosphere, again using a liquid nitrogen source. Recovery of nitrogen was considerably more erratic than that of oxygen. Alloys of low nitrogen content (0.059 w/o) and specimens containing over 0.6 w/o N were prepared, but difficulty was encountered in melting alloys of intermediate nitrogen level. Subsequently a premixed tank of argon-nitrogen gas (2.01 mol % N - 97.99 mol % A) was procured in order to achieve reliable partial pressures of nitrogen in the melting atmosphere. Nitrogen analyses were obtained using the micro-Kjeldahl method. The technique used has been described by Harris[8]. Check analyses showed that the oxygen content of the low nitrogen alloys was below 0.01 w/o. High nitrogen specimens (over 0.6 w/o) had somewhat higher oxygen levels, but in all instances this was below 0.015 w/o. Subsequent evaluation of the nitrogen alloys was carried out in the same manner as for the Nb-O specimens.

Hardness and Workability. Hardness data for Nb-N alloys are plotted in Figure 4. As can be seen, nitrogen additions up to about 0.06 w/o greatly increase the as-cast hardness of niobium. At the low concentrations nitrogen is a more effective hardener than oxygen. However, additions of nitrogen greater than about 0.1 w/o had only a relatively small effect on hardness. Metallographic examination of the high nitrogen alloys showed the presence of Nb_2N needles in a niobium matrix, as shown in Figure 5. The hardness values on alloys containing up to 0.06 w/o N are representative of super-saturated solid solutions, since these alloys were single phase in the as-cast condition.

The results of rolling Nb-N alloys are listed in Table 5. Specimens containing up to 0.059 w/o N were cold rolled to 75% reduction with excellent results. Alloys containing over 0.62 w/o N cracked severely after small reduction. The fractures were mixed intergranular and transgranular cleavage. While the data are not sufficiently complete to determine the maximum nitrogen content compatable with good workability, it appears that nitrogen may be more detrimental than oxygen to the cold workability of niobium. It may be anticipated that niobium containing more than about 0.1 w/o N, roughly corresponding to the inflection point in the hardness-composition curve of Figure 4, would have poor workability. This inflection point evidently corresponds to the composition at which Nb_2N is precipitated from solid solution on casting. This composition is, of course, dependent upon the cooling rate. Casting a levitation-melted specimen corresponds to a rather rapid quench, for the samples cool to below red heat in a few seconds. With slower cooling rates, which would be encountered in commercial size heats, the nitrogen level at which Nb_2N would be precipitated on casting would be lower than that observed in this study.

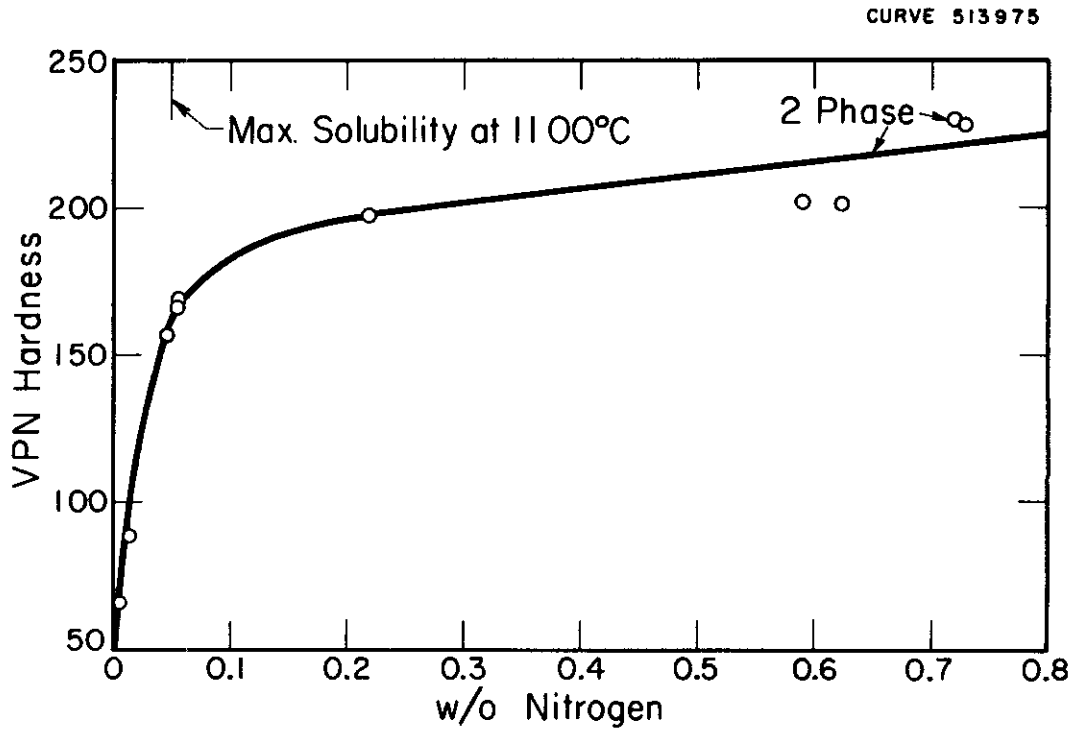

Fig.4-Effect of nitrogen on the as-cast hardness of niobium.

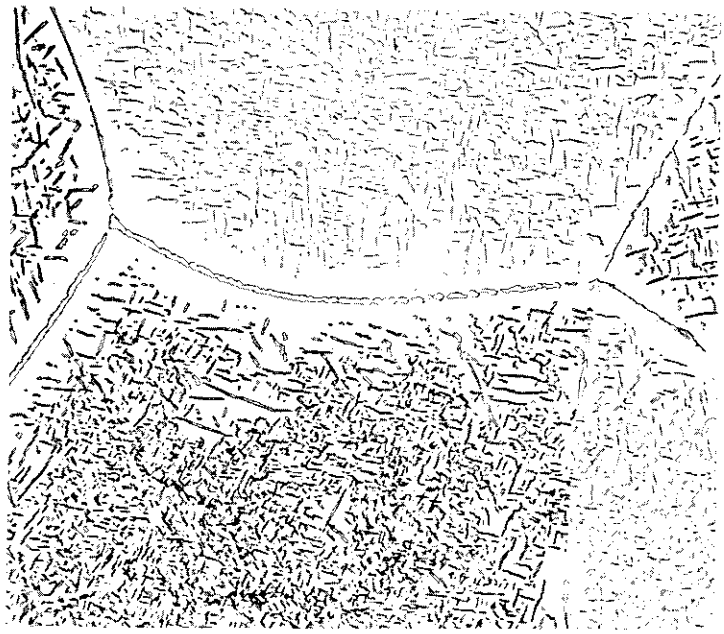

(a)

Nb–0.59 N_2 as Cast 500X

Nb_2N Needles Precipitated from Niobium Solid Solution

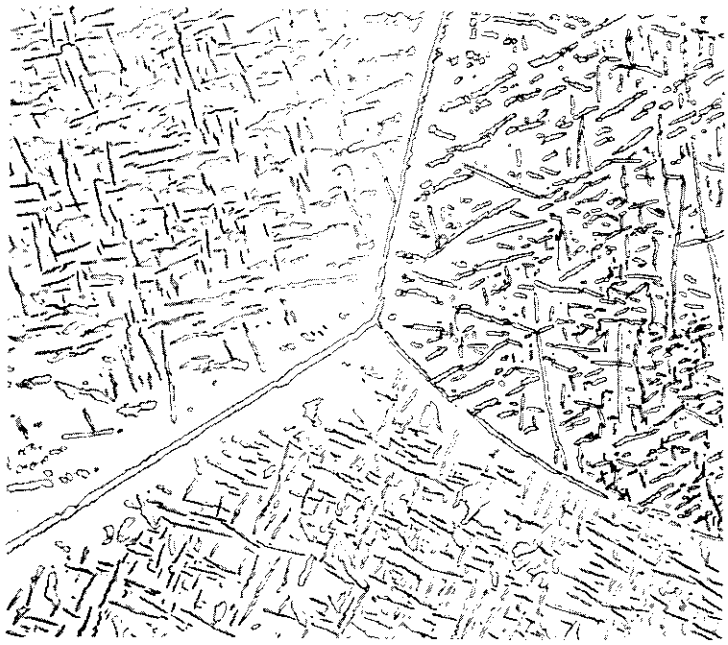

(b)

Nb–0.83 N_2 as Cast 500X

Nb_2N Needles Precipitated from Niobium Solid Solution

Fig. 5—Microstructures of niobium–nitrogen alloys.

Table 5. Workability of Levitation Melted Niobium-Nitrogen Alloys

w/o Nitrogen	Results of Cold Rolling
0.0036	75% Reduction. Excellent
0.014	75% Reduction. Excellent
0.045	75% Reduction. Excellent
0.059	75% Reduction. Excellent
0.623	Cracked up after 20% reduction
0.730	Cracked up after 10% reduction

Strain Hardening. The effect of nitrogen additions on the strain hardening of niobium is shown in Figure 6, when hardness is plotted as a function of percent reduction by cold rolling. As can be seen, nitrogen additions up to 0.059 w/o have no significant effect on the strain hardening of niobium.

Recrystallization. Recrystallization data for Nb-N alloys are summarized in Table 6. The alloys were evaluated in an identical manner to that described previously for Nb-O alloys.

Table 6. Recrystallization Data for Niobium-Nitrogen Alloys[a]

Specimen No.	Nitrogen (w/o)	Percent of Specimen Recrystallized Estimated from Metallographic Examination				
		Annealing Temperature °C				
		900	1000	1100	1200	1300
L-366	0.0036	B-C[b]	C	E	F	F^+
38V	0.010	B-[c]	B	E	E	F^+
L-392	0.045	A	B-	-	C	E
L-391	0.059	A	B-	-	C	E
45V	0.220[d]	-	B	-	-	E

(a) 75% reduction by cold rolling, 1 hour anneals

(b) Key: A - no recrystallization
B - 1 to 10% recrystallized
C - 10 to 50% recrystallized
D - 50 to 90% recrystallized
E - 90 to 99% recrystallized
F - completely recrystallized
F^+ - completely recrystallized

(c) Superscript Minus sign (-) denotes low side of range

(d) Rolled to 75% reduction at 800 C

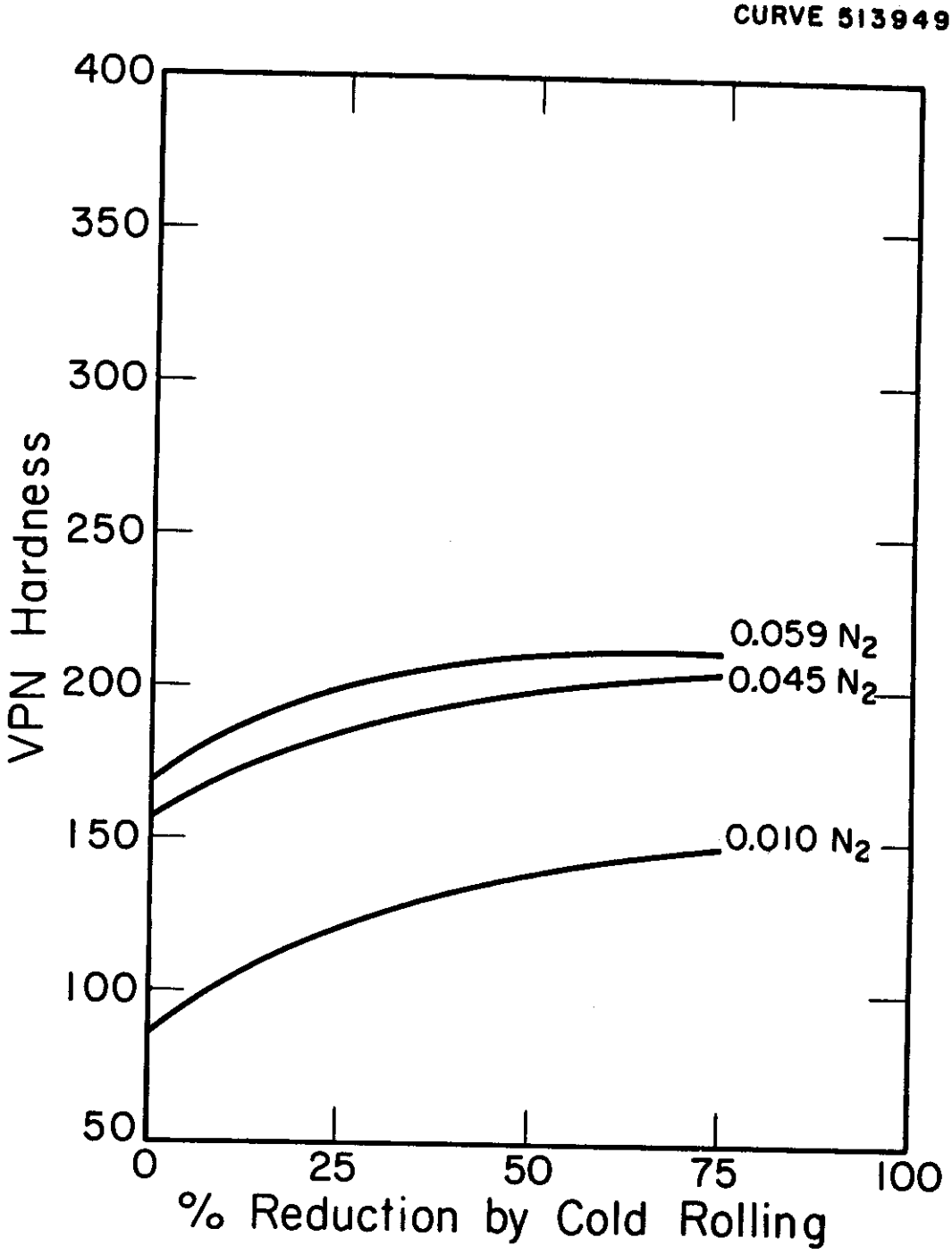

Fig.6- Effect of nitrogen on the strain hardening of niobium.

Metallographic examination of specimen containing 0.045 and 0.059 w/o nitrogen revealed that recrystallization was barely initiated after a 1 hour anneal at 1000 C. Annealing for the same period at 1200 C resulted in less than 50 percent recrystallization of the specimen. After a similar anneal at 1300 C, these specimens were still not completely recrystallized. These results indicate that nitrogen additions have a somewhat more pronounced effect than oxygen additions in raising the recrystallization temperature range of niobium.

Niobium-Carbon

Literature. Relatively little work has been reported concerning the effect of carbon on the properties of niobium. Saller, Stacy, and Porembka[13], in early studies of arc-melted niobium, observed that the cast material had fabricating characteristics different from those of the conventional powder metallurgy niobium. They related this difference in behavior in part to the presence of an unidentified grain boundary constituent in the arc melted material. It appears likely that this grain boundary phase was a carbide. Recent work by Chang[14] indicates that carbon additions have a pronounced effect on the high temperature properties of complex niobium-base alloys.

While little work has been reported concerning the effect of carbon level on the properties of niobium, the carbides of niobium have been the subject of a number of investigations. A comprehensive summary of this work has been published by Hansen.[11] The existence of two carbide phases, Nb_2C, isomorphous with Nb_2N, and cubic NbC has been confirmed by several investigators. Pouchon et al.,[15] carried out a phase diagram study. The main features of this phase diagram were:

1) A eutectic reaction between Nb and Nb_2C at 2335 C and 1.5 w/o C.

2) A low solubility of carbon in niobium, ranging from about 0.03 w/o at the eutectic temperature to about 0.016 w/o at 1200 C.

3) A peritectic reaction between liquid and NbC→Nb_2C at 3265 C.

Elliott[16] recently reported results of a study of the niobium-carbon system. This work confirmed many of the essential features of the phase diagram determined by Pouchon et al.[15] However, Elliott's results indicated a much higher solubility of carbon in niobium, ranging from 0.8 w/o carbon at the eutectic temperature to about 0.10 w/o at 1800 C. Elliott[16] determined the solubility limits of Nb_2C and NbC. For Nb_2C the range of solubility is from 5.43 to 5.83 w/o C. For NbC the range of solubility is considerably wider, ranging from 8.25 to 10.25 w/o carbon.

Experimental Procedure. Niobium-carbon alloys were prepared by conventional DC non-consumable arc melting in water cooled copper crucibles, using a tungsten electrode. Twenty gram samples containing up to 2.0 w/o carbon were melted for metallographic examination, hardness determinations, and workability evaluations; 150 gram alloys containing up to 0.5 w/o C were prepared for mechanical property studies. The samples were weighed out, cold pressed, and melted in a titanium gettered argon atmosphere. Each button was melted at least four times to insure homogeneity, and the samples were inverted after each melt.

The base material used was obtained from the Union Carbide Metals Co., in the form of small beads, approximately 1/8 inch in diameter. The composition of the niobium used is listed in Table 1. Carbon was added as a Nb - 8.62 w/o carbon master alloy. Several samples of very low carbon content were prepared by vacuum levitation melting the base material. The levitation melted samples were subsequently arc melted to provide buttons of low carbon level.

The workability of the as-cast buttons was evaluated by cold rolling and by forging at 1200 C. In the cold rolling experiments the 20 gram specimens were rolled on a 2 high Stanat mill, using reductions of about 10% per pass. The cold rolled samples were then remelted for hot working experiments. The samples were heated prior to forging in an Inconel retort inserted in a gas fired furnace. Argon was passed through the retort during the heating cycle to minimize contamination. Forging was done on a 800 lb. steam hammer, using flat dies. The dies incorporated a spacer block so that the samples would be reduced approximately 50% in thickness by a single hammer blow.

The 150 gram niobium-carbon alloys were ground to remove any surface irregularities and then jacketed in Type 304 stainless steel. The jacketed assembly was evacuated, sealed off, and rolled at 1200 C. The samples were rolled to provide sheet stock approximately 0.080 inch thick. All of the jacketed samples were reduced at least 75% in thickness by the rolling operation. No difficulty was encountered in mechanically stripping the stainless steel jackets after rolling. Flat tensile specimens were machined from the as-rolled sheet stock.

Sections of the as-cast 20 gram buttons were vacuum annealed for 12 hours at 1900 C in an induction furnace. Each sample was wrapped in niobium foil and placed in a molybdenum susceptor. Pressure was maintained at less than 5×10^{-5} mm of Hg during the annealing treatment. Temperature readings were taken with a calibrated optical pyrometer through a Pyrex sight port located above the susceptor. Corrections were made for emissivity and the transmittance of the Pyrex. At the end of the heat treatment the power was turned off and the samples were allowed to cool in the susceptor. The samples cooled to below red heat in approximately three minutes. Tensile specimens were wrapped in niobium foil and annealed for 1/2 hr. at 1450 C under conditions identical with those described above.

Particular care was taken to insure reliable hardness readings. VPN hardness values were determined for each alloy on mounted and polished metallographic samples, using a 30 kg. load. At least 3 determinations were made for each alloy. For the low carbon alloys an average of at least 8 impressions was used.

Tensile data were obtained for several niobium-carbon alloys in the temperature range -196 C to 200 C. Sheet tensile specimens, 0.050 inch thick, having a 1 inch gage length and a 0.250 inch gage width, were tested in a constant strain rate tensile machine of the type described by Manjoine, Wessel, and Pryle[17]. For tests below room temperature the specimens were cooled in gaseous nitrogen by the method of Wessel and Olleman[18]. Strain-rate was held constant at 1×10^{-3} sec^{-1}. The working and annealing treatment described previously for the 150 gram alloys resulted in a fairly uniform recrystallized grain size of approximately 520 grains/mm^2.

Results

The nominal composition, chemical analysis, and hardness of the alloys prepared for this study are listed in Table 7. Samples NC-189, 190, 246 and 247 were large buttons prepared for mechanical property studies. The remaining alloys were melted for microstructure, hardness, and workability evaluations.

Table 7. Composition and Hardness of Niobium-Carbon Alloys

Heat No.	w/o Carbon (nominal)	Analysis (w/o) O	N	C	VPN Hardness As-Cast	Annealed
NC-251	0.01	0.009	0.009	0.0085	103	72
NC-252	0.015	0.011	0.019	0.015	122	87
NC-157	0.022	0.019	0.011	0.038	134	72
NC-165	0.050	0.024	0.012	-	122	75
NC-166	0.075	0.014	0.011	0.072	117	69
NC-158	0.127	0.012	0.014	0.15	116	70
NC-159	0.30	-	-	0.28	117	75
NC-160	0.51	0.020	0.020	0.44	126	87
NC-161	0.75	-	-	-	148	97
NC-162	1.0	-	-	-	152	-
NC-163	1.5	-	-	-	151	112
NC-164	2.0	-	-	-	164	113
NC-190		-	-	0.035		
NC-189	0.10	-	-	0.10		
NC-246	0.20	0.031	0.009	0.17		
NC-247	0.50	0.018	0.028	0.53		

Microstructure. Photomicrographs of niobium-carbon alloys are shown in Figures 7 thru 12. The as-cast microstructures of the dilute carbon alloys (Figure 7) showed acicular Nb_2C precipitated primarily within the grains and at subgrain boundaries. Alloys containing up to 0.05 w/o carbon showed pronounced substructure in the as-cast condition. Evidence of this substructure remained after annealing at 1900 C, as shown in Figure 8. At carbon levels above 0.05 w/o the pronounced substructure was not observed, the precipitated Nb_2C particles were larger in size, and the carbides tended to form continuous grain boundary networks (Figures 9 and 10). On the basis of as-cast microstructures Pouchon et al.[15] suggested a maximum solubility of about 0.03 w/o C at the eutectic temperature.

Elliott[16] pack carburized pieces of Nb sheet at temperatures ranging from 1800 to 2200 C to achieve equilibrium saturation of carbon at the various carburizing temperatures. The carbide layers were removed and the samples were analyzed for carbon. These results indicated a maximum solubility of about 0.80 w/o C at the eutectic temperature (2235 C), decreasing rapidly to about 0.1 w/o at 1800 C. Elliott's results are in good agreement with the as-cast microstructures shown in Figures 10 and 11, which indicate a maximum solubility between 0.75 w/o and 1 w/o C.

Both Elliott[16] and Pouchon[15] reported the Nb-Nb_2C eutectic composition to be about 1.5 w/o C. The as-cast microstructure of Figure 12 shows the 1.5 w/o alloy to be almost entirely eutectic. A 2 w/o C alloy showed proeutectic Nb_2C in a Nb-Nb_2C eutectic matrix.

Elliott[16] indicates a solubility of approximately 0.2 w/o carbon in niobium at 1900 C. Metallographic examination of dilute carbon alloys annealed for 12 hours at 1900 C showed evidence of solution and reprecipitation of Nb_2C in the Nb matrix on cooling. Alloys containing over 0.3 w/o carbon revealed a general agglomeration of Nb_2C particles on annealing. At the Nb-Nb_2C eutectic composition, eutectic divorcement occurred during the annealing treatment.

As shown in Figure 8, a sample containing 0.0085 w/o carbon was single phase after annealing at 1900 C. This sample was subsequently annealed for 12 hours at 1200 C. Metallographic examination revealed the presence of Nb_2C after the second annealing treatment, indicating a solubility of less than 0.0085 w/o carbon in niobium at 1200 C.

Hardness. Hardness values determined on as-cast and annealed niobium-carbon alloys are listed in Table 7 and plotted as a function of carbon content in Figure 13. Increasing carbon content initially resulted in an increase in hardness, with a maximum occurring at about 0.038 w/o carbon. Hardness then decreased

Nb - 0.0085 w/o C

Nb - 0.015 w/o C

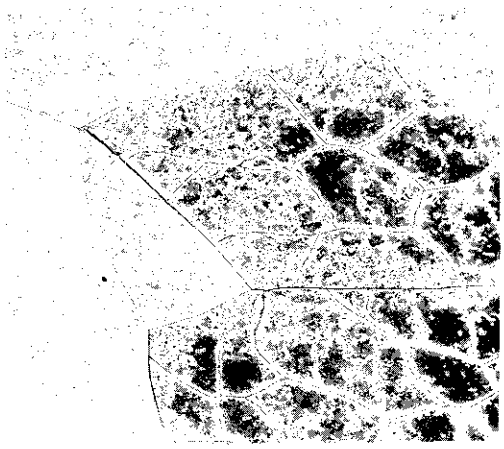

Nb - 0.038 w/o C

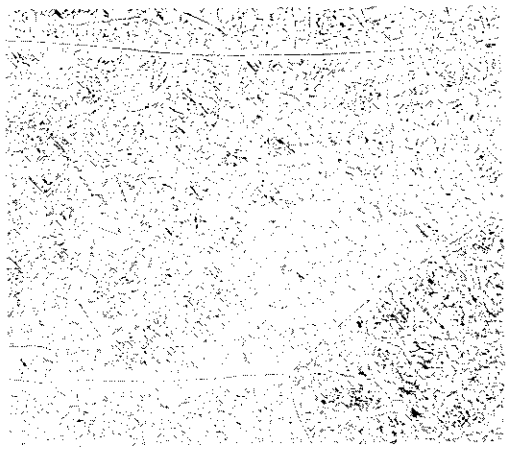

Nb - 0.05 w/o C

Fig. 7 - Microstructure of niobium low carbon alloys. As cast. 100x

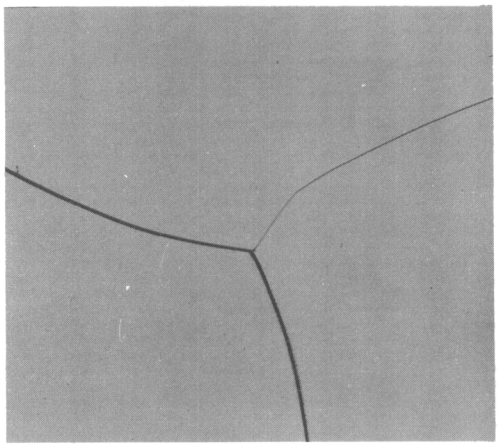

Nb - 0.0085 w/o C

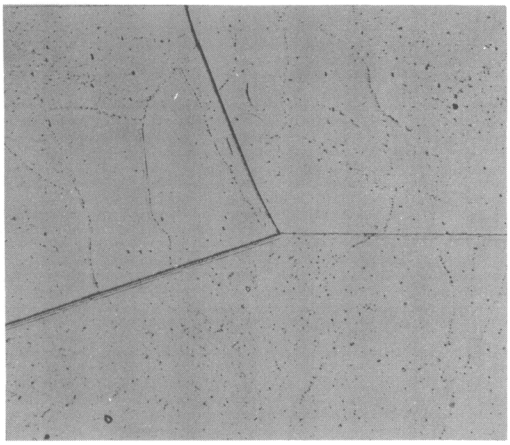

Nb - 0.015 w/o C

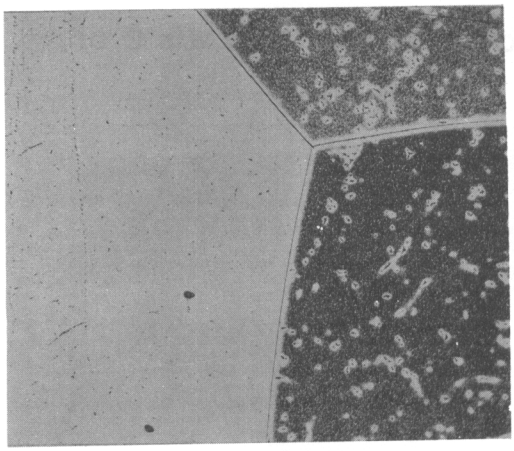

Nb - 0.038 w/o C

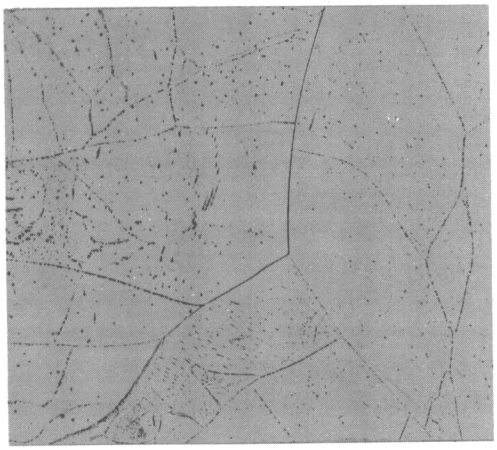

Nb - 0.05 w/o C

Fig. 8 – Microstructure of niobium - low carbon alloys. Annealed 12 hours at 1900°C. 100x

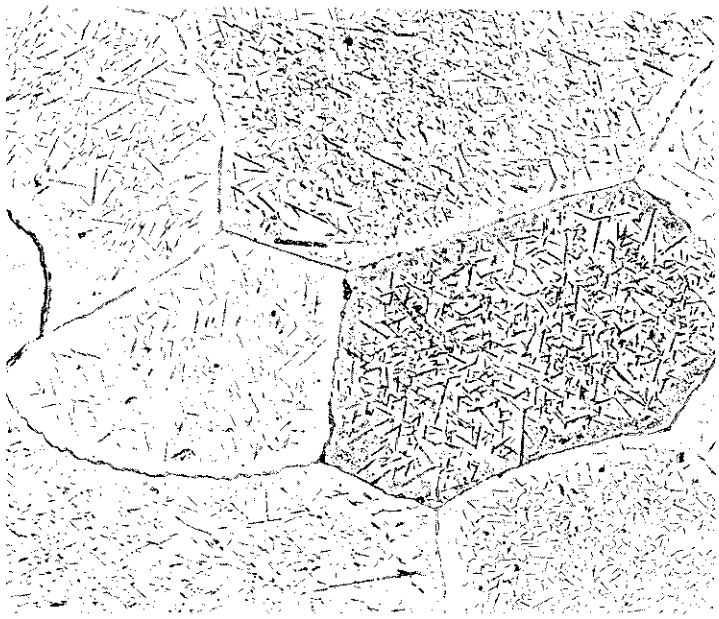

Nb-0.30 w/o C. As cast. 100x
Nb_2C precipitate in niobium solid solution.

Fig.9–Microstructure of Nb-0.30 w/o C alloy.

Nb-0.75 w/o C. As cast. 100x
Nb_2C precipitate in niobium solid solution.

Fig.10–Microstructure of Nb-0.75 w/o C alloy.

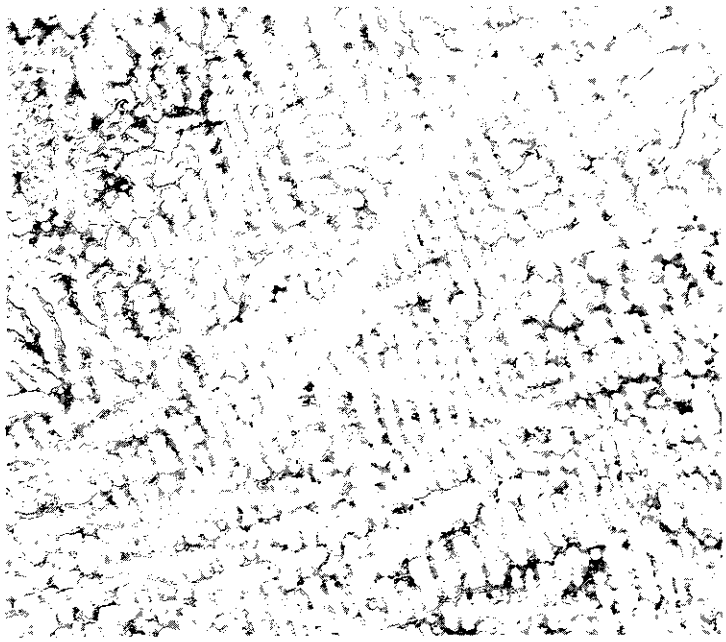

Nb - 1.0 w/o C. As cast. 100x
Pro-eutectic Nb in matrix of Nb - Nb_2C eutectic.

Fig. 11 - Microstructure of Nb - 1.0 w/o C alloy.

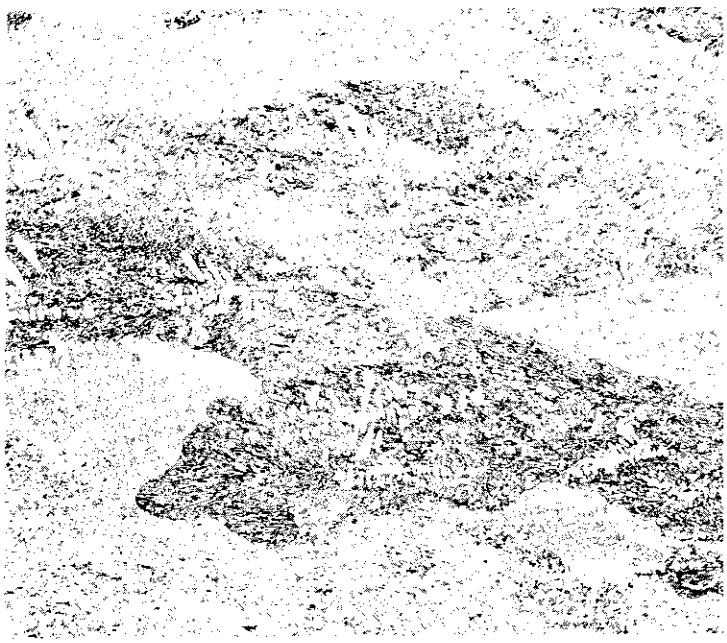

Nb - 1.5 w/o C. As cast. 100x
Small amount of pro-eutectic Nb in matrix of Nb_2C eutectic.

Fig. 12 - Microstructure of Nb - 1.5 w/o C alloy.

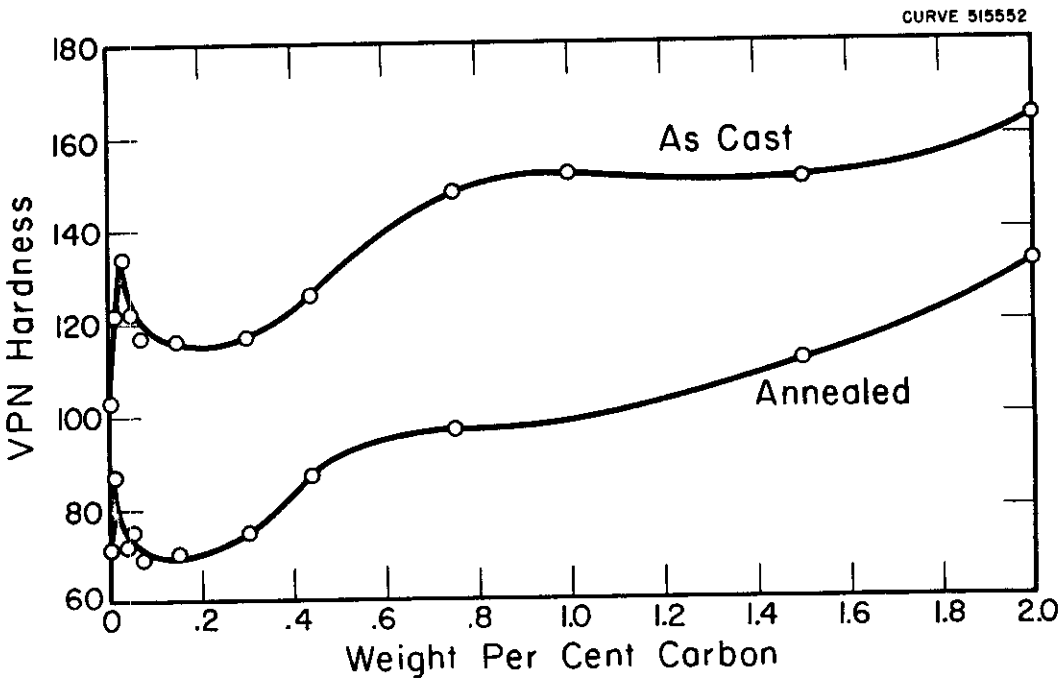

Fig.13-Effect of carbon additions on the hardness of niobium.

to a minimum at about 0.1 - 0.2 w/o carbon. Hardness increased slightly thereafter with further increases in carbon. Annealing the as-cast samples for 12 hours at 1900 C resulted in a general lowering of hardness. A slight indication of a hardness peak at 0.015 w/o carbon remained after the annealing treatment. In an attempt to duplicate the anamolous hardness peak, several additional dilute niobium-carbon alloys were prepared. Hardness values obtained for these alloys confirmed the existence of a hardness maximum at about 0.038 w/o carbon. As shown in Table 7, the oxygen and nitrogen contents of the dilute niobium-carbon alloys are virtually the same. Results described earlier in this report show that the hardness maximum cannot adequately be explained by the minor variation in oxygen and nitrogen content of the samples. The anomalous hardness peak appears to be associated with the presence of a pronounced sub-boundary network in the as-cast samples, as shown in Figure 7. Studies of nickel[19] and steel[20] have shown that the introduction of substructure by suitable working and annealing treatments results in a significant increase in flow stress. Recent work[21] has shown a relation between subgrain size and hardness in rolled and annealed aluminum. It is therefore reasonable to expect that the presence of the substructure in the niobium-carbon alloys results in an increase in hardness. This supposition is supported by the marked lowering of hardness on annealing, since the annealing treatment eliminated most of the sub-boundary network. At present no explanation is available for the pronounced substructure which occurs in the range 0.015 to 0.05 w/o carbon, and its disappearance at higher carbon levels.

Knoop hardness values were determined for several large carbide particles in the annealed 1.5 w/o and 2.0 w/o carbon alloys. Hardness values ranged from 876 to 1052 Knoop. The carbide particles were extremely brittle. Direct impressions caused them to shatter. The presence of relatively large amounts of Nb_2C in the niobium matrix contributes little to hardness. The as-cast hardness of a niobium - 2.0 w/o carbon alloy was only 164 VPN.

Workability. The results of cold rolling niobium-carbon alloys are summarized in Table 8. Specimens containing up to 0.072 w/o carbon were cold rolled to about 60% reduction in thickness with no indication of cracking. Rolling was discontinued at this point for it appeared that the specimens could be cold rolled indefinitely without difficulty. Above 0.072 w/o carbon, serious cracking occurred after small reductions. Workability tended to improve slightly near the eutectic composition (1.5 w/o C).

As shown in Figure 14, specimens containing up to 0.15 w/o carbon exhibited excellent workability on forging at 1200 C. Above 0.28 w/o carbon serious edge cracks developed. The severity of cracking decreased significantly at the eutectic composition. These results indicate that the presence of eutectic in the high carbon alloys tends to improve workability.

Table 8. Results of Working Niobium-Carbon Alloys

Heat No.	w/o Carbon	Results of Cold Rolling	Results of Forging at 1200 C
NC-157	0.038	60% reduction. Very good.	80% reduction. Very good.
NC-165	0.050 *	60% reduction. Very good.	52% reduction. Very good.
NC-166	0.072	60% reduction. Very good.	58% reduction. Very good.
NC-158	0.15	Cracked after 26% reduction.	55% reduction. Very good.
NC-159	0.28	Cracked after 22% reduction.	54% reduction. Minor edge cracks.
NC-160	0.44	Cracked after 10% reduction.	55% reduction. Serious edge cracks.
NC-161	0.75 *	Cracked after 5% reduction.	53% reduction. Serious edge cracks.
NC-162	1.0 *	Cracked after 15% reduction.	47% reduction. Edge cracks.
NC-163	1.5 *	Cracked after 20% reduction.	53% reduction. Minor edge cracks.
NC-164	2.0 *	Cracked after 12% reduction.	48% reduction. Minor edge cracks.

* Nominal composition

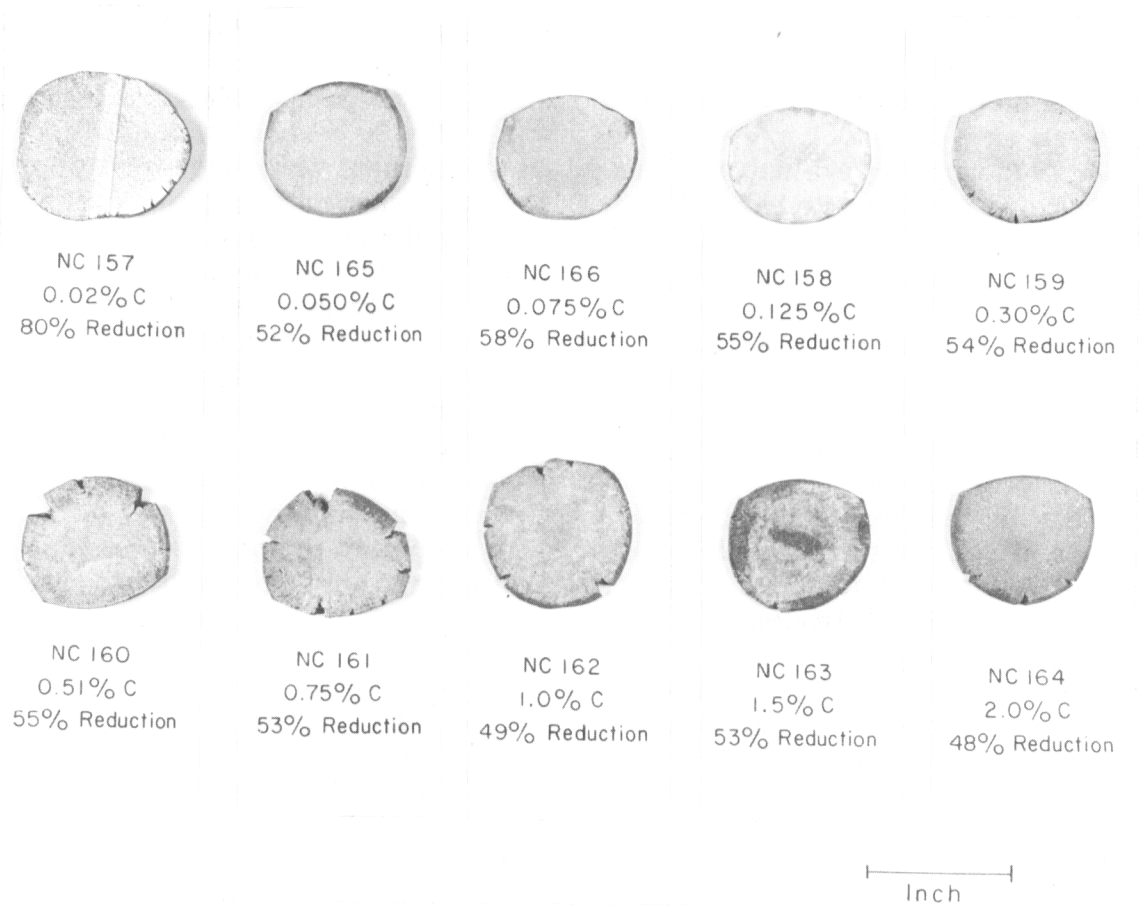

Fig. 14 – Results of forging niobium–carbon alloy at 1200 C

Carbide distribution appears to have a significant effect on workability. This is illustrated by the results of working a 2-1/2 inch diameter niobium ingot prepared by consumable electrode arc melting. The ingot (VAM-15), containing 0.012 w/o oxygen, 0.031 w/o nitrogen, and 0.076 w/o carbon, was cut in half for hot and cold working evaluations. One half of the ingot was successfully forged at 1100 C to 1 inch square bar. Attempts to cold forge the remaining half of the ingot were not successful. Many serious cracks developed after small reduction. The as-cast microstructure of ingot VAM-15 (Figure 15) shows carbide particles precipitated within the grains and at grain boundaries. Examination of the fractured surfaces of the cold forged section of the ingot showed the fracture to be predominately transgranular cleavage, but a number of grain boundary facets were observed. Typical fractographs are shown in Figures 16 and 17. Figure 16 shows a transition from intergranular fracture to transgranular cleavage at a grain boundary. Figure 17 shows the presence of carbide particles or "feathers" on a grain boundary fracture surface. X-ray diffraction analysis of residues extracted from the sample showed the precipitate to be Nb_2C. The carbide feathers appear quite similar to those observed in fractographic studies of molybdenum[22].

The workability studies indicate that the presence of Nb_2C in the grain boundaries is severely detrimental to cold workability. The fractures apparently initiate at grain boundaries and then propagate predominately by transgranular cleavage. The as-cast 20 gram buttons did not show the presence of any appreciable quantity of Nb_2C in the grain boundaries until the carbon level was increased to 0.15 w/o. With the appearance of the grain boundary carbide the cold workability became very poor.

Mechanical Property Data. In common with all body-centered cubic metals, the mechanical properties of niobium change markedly with temperature over a relatively narrow temperature range. The yield strength of niobium increases rapidly with decreasing test temperature below approximately 25 C. As the test temperature is decreased the mode of fracture changes from a ductile shear type to brittle cleavage. Recent work[12] has shown that pure polycrystalline niobium fails (in tension) by complete transgranular cleavage at temperatures below -215 C.

The mechanical property studies described in this section of the report were undertaken to provide data concerning the effect of precipitated carbide particles on the low temperature flow and fracture characteristics of niobium. More detailed studies of the effect of alloy additions on the low temperature mechanical properties of niobium are described in a subsequent section of this report. The alloys selected for evaluation ranged from 0.035 w/o to 0.53 w/o carbon. In all the samples tested the carbon content was in excess of the solid-solubility limit. Tensile tests were conducted on completely recrystallized

Nb – 0.076 w/o C As-cast 500 x
Nb_2C Precipitate in Niobium Solid Solution

Fig. 15 – Microstructure of Nb–0.076 w/o C alloy (VAM-15).

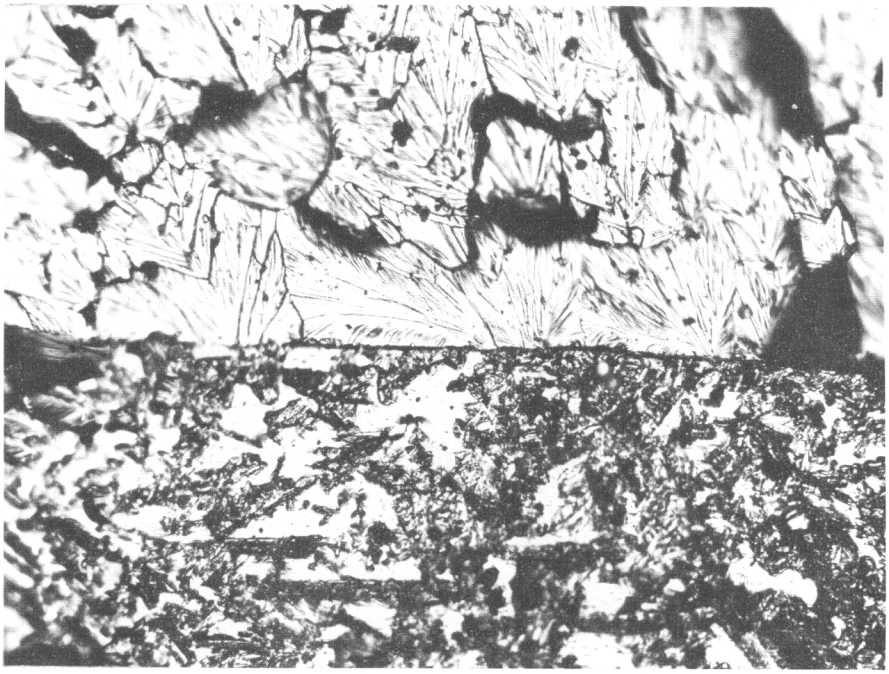

Transition from Grain Boundary Fracture (lower section) to Transgranular Cleavage Fracture.

Fig. 16 — Fractograph of Nb — 0.076 w/o C alloy (VAM-15).

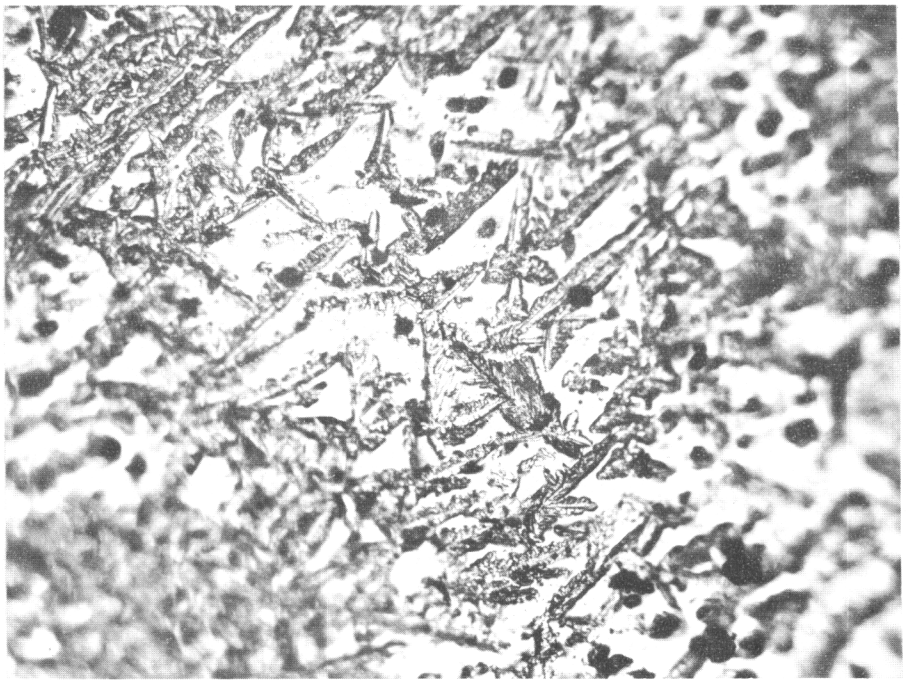

Nb_2C Feathers on Grain Boundary Fracture Surface 250x

Fig. 17 — Fractograph of Nb — 0.076 w/o C alloy (VAM-15).

samples in the temperature range from -196 C to 200 C. For the alloy of lowest carbon content the testing temperature range was extended to 300 C. The working and annealing procedures used have been described previously. No attempts were made to control the carbide size and distribution by working and annealing treatments, since this would have introduced grain size variations within the alloys evaluated. Wessel and Lawthers[23] have shown that the ductile-brittle transition of niobium is significantly affected by grain size. The grain size of all the samples was therefore maintained constant at approximately 520 grains/mm^2.

Typical microstructures of niobium-carbon tensile specimens are shown in Figure 18. The carbides in the two alloys of lowest carbon level (0.035 w/o and 0.10 w/o C) were fairly randomly distributed and tended to be spherical in shape. The average diameter of the carbide particles was of the order of 0.005 mm. Nb_2C was precipitated primarily within the grains, with a relatively small amount at the grain boundaries. Alloys of high carbon content contained somewhat more massive carbides which tended to be oblong and extended in the direction of rolling. A considerable amount of Nb_2C was present in the grain boundaries, but continuous grain boundary precipitates were not observed.

The effect of temperature on the yield and ultimate strength of the 0.035 w/o and 0.53 w/o carbon alloys is shown in Figure 19. The characteristic rapid increase in yield strength with decreasing test temperature was observed for both alloys. The effect of carbon level on the yield and ultimate strength of niobium is shown in Figure 20. The presence of carbides in the niobium matrix has essentially no effect on the yield strength of niobium at temperatures as low as -196 C. Ultimate strength appeared to increase slightly with increasing carbon content. Ultimate strength values were not obtained for the high carbon alloys at the low test temperatures since fracture occurred while the load was increasing.

The effect of carbon content on the low temperature ductility of niobium is shown in Figure 21. In the sample of lowest carbon content, no uniform elongation was observed at -196 C, but total elongation and reduction of area at fracture were still quite high. With 0.10 and 0.17 w/o carbon, ductility decreased considerably at temperatures below -100 C, although some measureable total elongation and reduction in area remained at -196 C. The 0.53 w/o carbon alloy exhibited zero uniform elongation at -100 C, and reduction in area was reduced over the entire temperature range. The general effect of increased carbon content was to decrease low temperature ductility and broaden the ductile-brittle transition range.

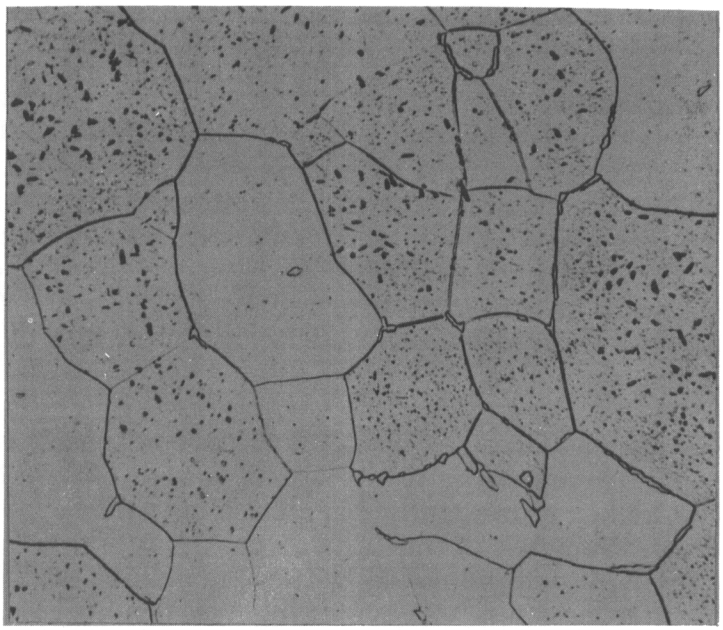

Nb - 0.035 w/o C

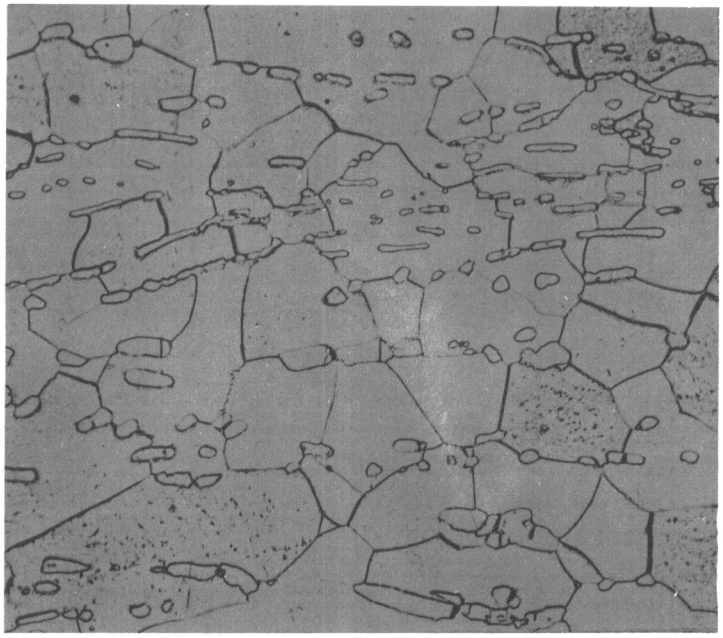

Nb - 0.53 w/o C

Fig. 18 - Microstructure of niobium - carbon sheet tensile specimens. Annealed 1/2 hour at 1450 °C. 500 x

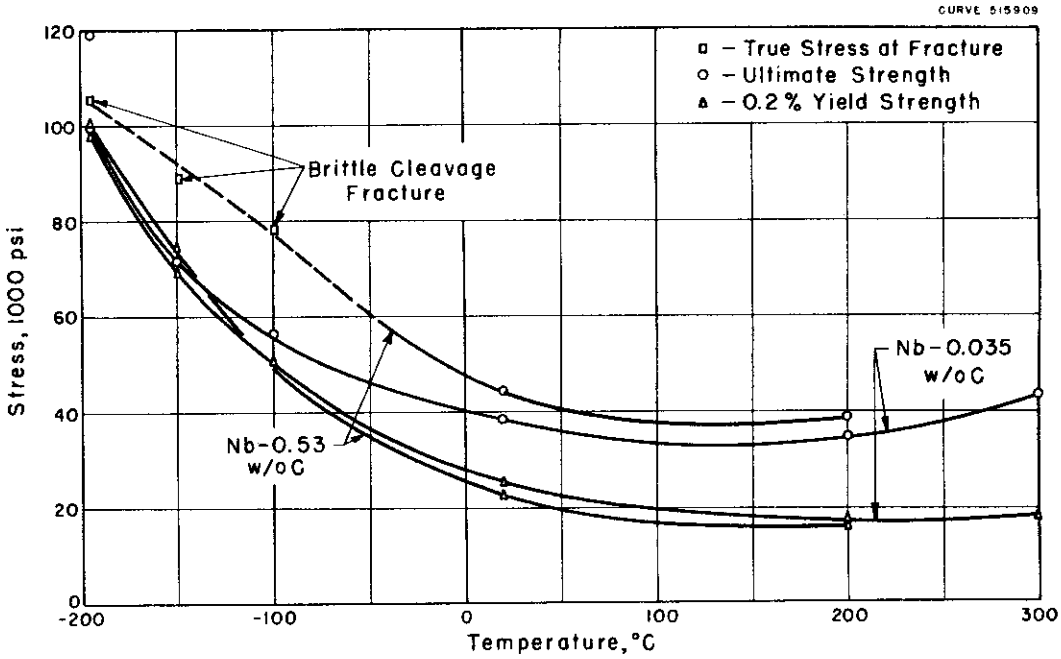

Fig.19– Effect of temperature on the yield and ultimate strength of carbon alloys.

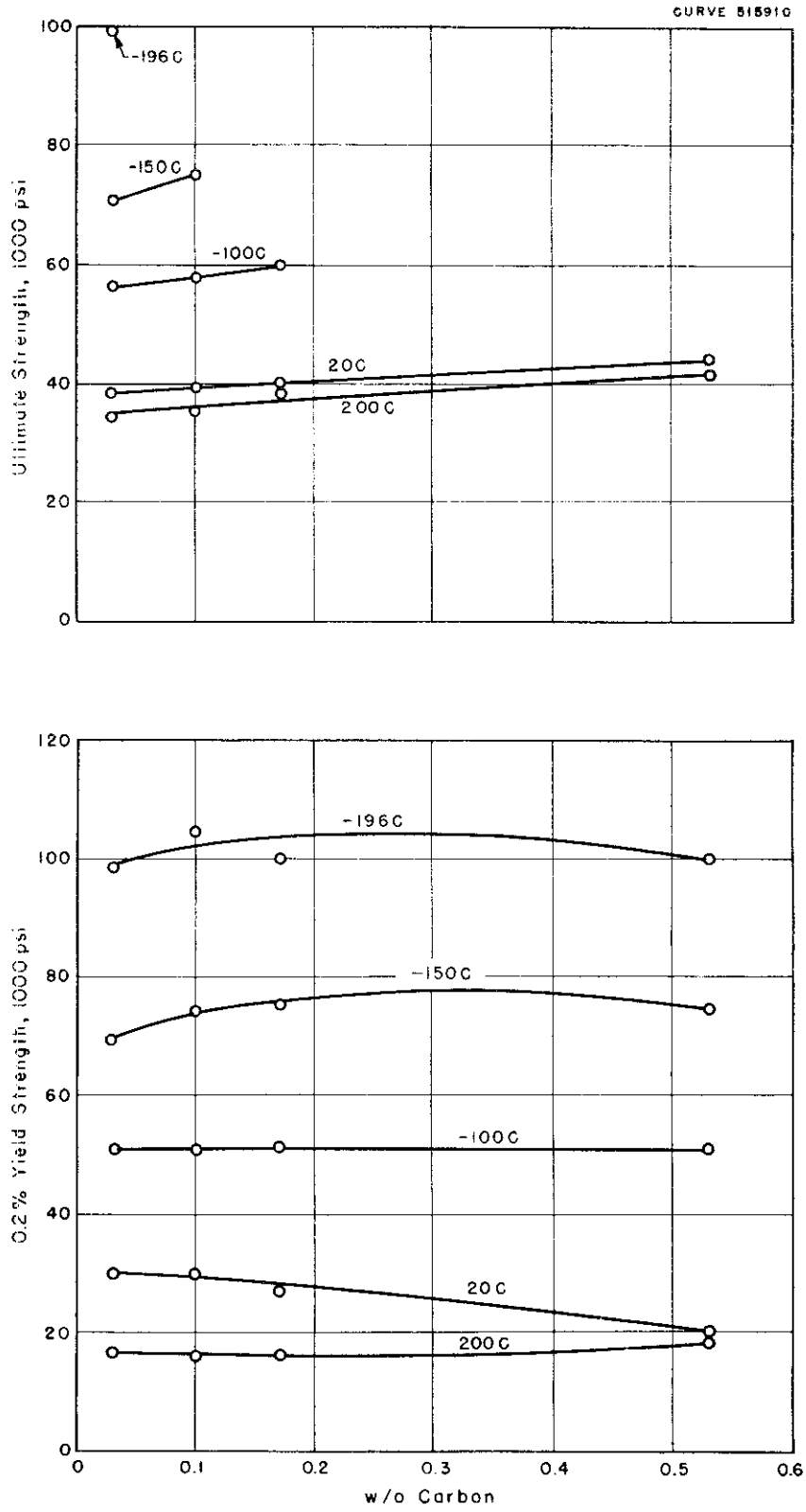

Fig. 20—Effect of carbon additions on the yield and ultimate strength of niobium.

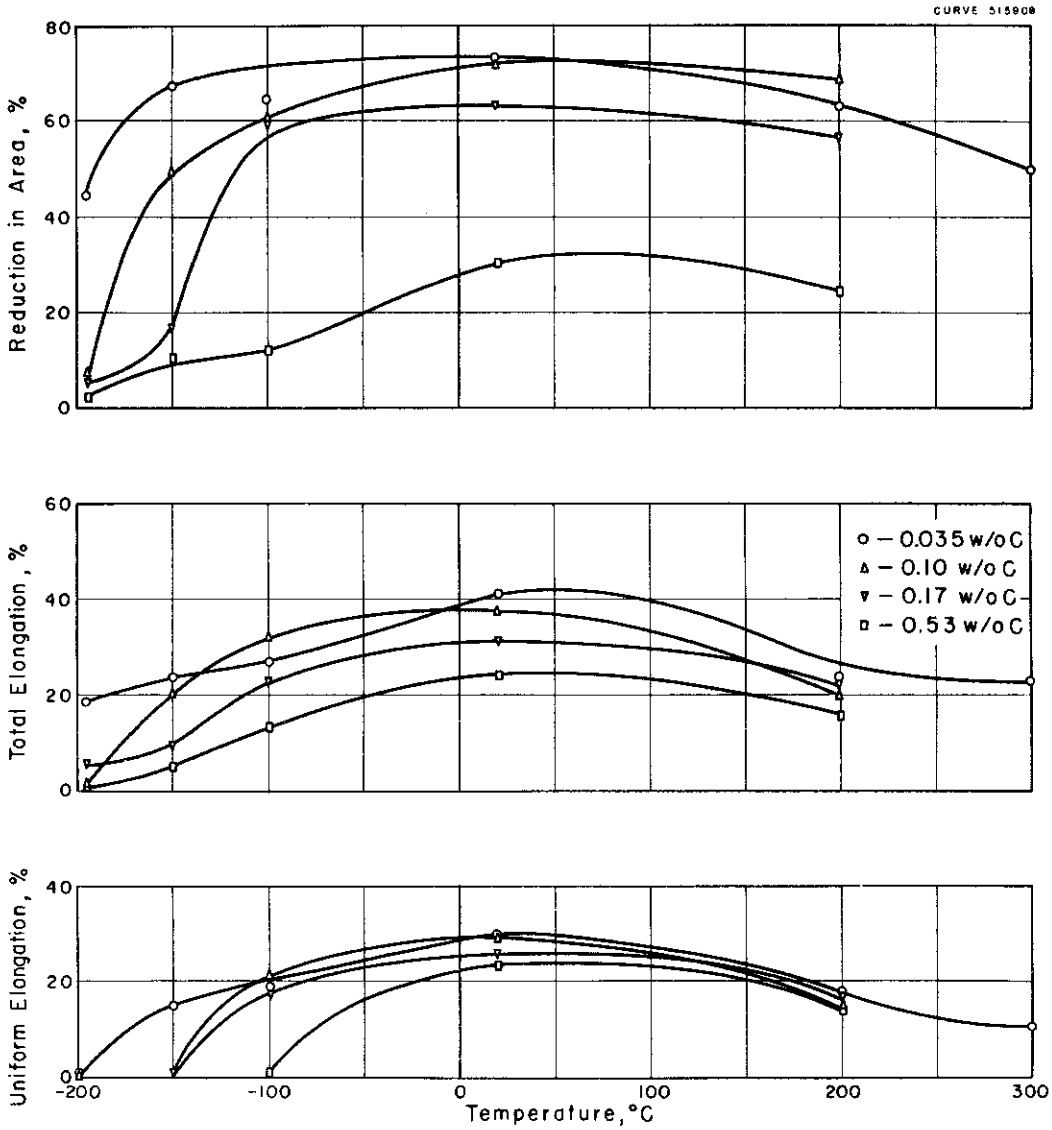

Fig.21— Effect of carbon additions on the low temperature ductility of niobium.

As the test temperature decreased the mode of fracture changed from ductile shearing to brittle cleavage. The 0.035 w/o carbon alloy showed a considerable amount of transgranular cleavage at -150 C and -196 C. Alloys of higher carbon content exhibited complete transgranular cleavage failure after extensive deformation at -150 C. Although no intergranular fracture facets were observed, the fine grain size of the samples made fractographic examination difficult. It is therefore possible that some intergranular fractures were present.

The tensile data show that the presence of dispersed carbide particles is detrimental to the low temperature ductility of niobium, but does not appreciably affect strength properties. The carbide distribution will obviously have a considerable effect on low temperature ductility. In view of the cold workability results described previously, it appears that carbides forming relatively complete grain boundary networks would be even more detrimental to tensile ductility.

MECHANICAL PROPERTIES

Earlier work in this program[24] provided data concerning the effects of binary additions of Ti, Zr, Hf, V, Cr, Mo, W, Re, Al, and Y on the microstructure, hardness, and workability of niobium. Mechanical property data were obtained at room temperature and 1095 C (2000 F) on alloys containing binary additions of Zr, Hf, V, Mo, and W. In addition, several ternary alloys and one quaternary system (Nb-Ti-Zr-Hf) were investigated. Of the binary additions studied, Zr and V were the most effective strengtheners at 1095 C (2000 F). A number of the alloys studied exhibited encouraging properties. Of particular interest were Nb-Hf and Nb-Ti-Zr-Hf alloys of rather high oxygen level. These alloys had excellent workability and attractive elevated temperature strength. The mechanical property studies described in this report are an extension of work described previously.[24] The current effort may be divided into 2 phases. Phase I involved the fabrication and evaluation of 150-200 gram binary, ternary, and quaternary alloys prepared by nonconsumable arc melting. Phase II effort was devoted to the preparation of larger heats (approximately 1.6 kg.) of promising alloys for more extensive evaluation. The purpose of this work was to determine if workability and mechanical property results obtained on small button samples could be duplicated in larger heats.

The alloy studies conducted during the present program may be summarized as follows:

Phase I

a) Binary alloy investigations were continued to determine the effect of Cr, Al, Re, and Y additions on the high and low temperature mechanical properties of niobium. Mechanical property data were also obtained on several Nb-Ti, Nb-Zr, Nb-Mo, and Nb-W alloys to complete work initiated earlier.

b) Evaluation of the workability and mechanical properties of a number of niobium ternary and quaternary alloys was carried out.

c) Studies of the effect of oxygen and carbon on the properties of niobium-base alloys were conducted. This work was aimed at understanding the strengthening effect of interstitial elements in these alloys.

Phase II

a) A number of niobium-base alloys were prepared by consumable electrode arc melting. Ingot breakdown was accomplished by high energy rate extrusion (Dynapak).

b) Secondary working experiments were carried out on the extruded samples. Tensile and hot hardness data were obtained on the material produced.

Material and Experimental Procedure

Materials. The niobium used for most of the alloys was obtained from the Union Carbide Metals Company in the form of small beads (approximately 1/8 inch diameter), roundels (approximately 1/8 inch diameter, 1/2 inch long), and 10 mesh powder. A special lot of high oxygen powder was procured from Kennametal, Inc. The chemical compositions of the various lots of niobium used are listed in Table 9. The alloy additions were of good commercial purity. The source and form of the alloy additions are listed in Table 10.

Non-Consumable Arc Melting. Samples were prepared for Phase I mechanical property studies by conventional tungsten electrode non-consumable arc melting. The melting charges were weighed out, cold pressed, and placed in water cooled copper crucibles in a multiple hearth arc furnace. The furnace chamber was evacuated to less than 5×10^{-5} mm of Hg, flushed with argon, re-evacuated, and back-filled to one atmosphere pressure with high purity welding grade argon. Mass spectrometer gas analyses were obtained on each tank of argon to insure a purity level of at least 99.99%. A titanium button was melted to getter any remaining impurities, and the samples were then melted at currents ranging from 320 to 660 amperes, straight polarity DC. Each sample was melted four to six times, and the samples were inverted after each melt. Most of the as-melted buttons were sectioned on an abrasive wheel and the melting cycle was repeated to insure homogeneity. The arc melted samples were approximately 2-1/2 inches in diameter and 3/8 inch thick, and weighed 150 to 200 grams. The niobium roundels and beads listed in Table 10 were used as the base material for the non-consumable arc-melted samples.

Considerable loss of Cr and Al occurred through evaporation when these elements were added to the melting charge in the elemental form. To alleviate this problem Nb_2Al and $NbCr_2$ master alloys were prepared by arc melting. Much better recovery was obtained when Cr and Al were added in the master alloy form.

Table 9. Chemical Analysis of Niobium

Lot. No.	Form	Source	Analysis (w/o) 0	N	C	Ta	Ti	B	Fe	H	Zr
EM-5	Beads	Union Carbide Metals	0.045	0.011	0.022	0.5	0.01	0.0001	-	-	-
EM-6	Roundels	Union Carbide Metals	0.05	0.017	0.025	0.5	0.01	0.001	-	-	-
EM-7	10 Mesh Powder	Union Carbide Metals	0.10	0.039	0.026	0.5	-	-	-	0.044	-
KM-2	20 Mesh Powder	Kennametal	0.085	0.030	0.015	0.05	0.01	-	0.01	-	0.01

Table 10. Source and Form of Alloy Additions

Alloying Element	Form	Source
Titanium	Sponge	Du Pont
Zirconium	Hf Free Sponge Crystal Bar	Carborundum Metals Foote Mineral
Hafnium	Crystal Bar	Westinghouse
Vanadium	Powder (60 mesh)	Union Carbide Metals
Chromium	Hydrogen Reduced Electrolytic Flake	Union Carbide Metals
Molybdenum	Sheet Trimmings Powder	Climax Westinghouse
Tungsten	Special High Purity Crushed Rod Wire	Westinghouse Westinghouse
Rhenium	Sheet Trimmings	Chase Brass
Aluminum	Pig (99.9% Purity)	Alcoa
Yttrium	Ingot	Michigan Chemical Corp.
Carbon	Columbium Carbide Powder	Union Carbide Metals

Consumable Electrode Arc Melting. A number of alloys were prepared by consumable electrode arc melting in order to provide sufficient material for more extensive evaluation of promising compositions. Electrodes 20 inches x 3/4 inch x approximately 7/8 inch were compacted in a double acting hydraulic press at a pressure of about 37 tsi. As-pressed electrode density ranged from 80 to 85% of theoretical. The electrodes were prepared using the niobium roundels, beads, and powder listed in Table 10. Molybdenum, tungsten, and hafnium were added in the form of wires pressed into the electrode. Zirconium was added as zirconium hydride, or as sponge in the case of alloys of high zirconium content. Vanadium was added as powder and titanium as sponge.

Most of the electrodes were vacuum sintered for 1 hour at 1500 C prior to melting. The sintering treatment did not increase electrode density, but did improve mechanical strength. Sintering also removed hydrogen from electrodes pressed from powder lot EM-7, which has a high hydrogen content.

Titanium extension pieces were welded to the electrodes, which were then melted in a laboratory arc furnace. The electrodes were melted into a 1-7/8 inch diameter water cooled copper crucible. Depending on the alloy being melted, the melting current ranged from 1700 to 2000 amperes straight polarity DC. Arc voltage was 32-34 volts. Furnace chamber pressure varied from approximately 5×10^{-4} to 3×10^{-3} mm of Hg, depending upon the gas load. One ingot (heat VAM-19) was melted into a 1-1/4 inch diameter crucible. The electrode for this ingot was made by non-consumably arc melting several alloy rods approximately 5/8 inch in diameter, and then welding the rods together.

Fabrication. The non-consumably arc melted buttons were generally fabricated by hot rolling, although pure Nb, Nb-Ti, and Nb-Y alloys were cold rolled to sheet stock. All of the hot rolled alloys were jacketed in type 304 stainless steel prior to working. The as-cast buttons were ground to remove any surface irregularities and then inserted in sections of flattened stainless steel tubing. The tube diameter was selected so that, when the tubing was flattened, the button fitted closely inside the tube. Tubing wall thickness was 1/16 inch. An evacuation tube was welded in place and the ends of the tubing were welded closed. The assembly was evacuated, flushed with argon, and pumped down to a pressure of about 10 microns Hg. The evacuation tube was then sealed off and the assembly was ready for rolling. The inside of the tubing was coated with a thin layer of alumina to prevent bonding of the can to the sample.

The canned specimens were hot rolled at temperatures ranging from 1200 to 1300 C on a 2-high Stanat mill, using reductions of about 10% per pass. The button samples were rolled to sheet stock about 0.08 inch thick. The stainless steel jackets were stripped mechanically after rolling.

One consumable electrode arc-melted ingot (VAM-19) was forged in air at 1200 C from 1-1/8 inch diameter to 7/8 x 3/8 inch bar. The as-forged bar was ground to remove the contaminated surface layer, and then canned in stainless steel. The canned assembly was rolled at 1300 C to a finished sheet size of 0.080. The jacket was removed and the sheet was subsequently cold rolled to 0.055 inch thickness.

The remaining consumable electrode arc-melted ingots were extruded in a 12 inch Dynapak machine located at the Westinghouse Blairsville Plant. Dynapak extrusion will be described in a subsequent section of this report. The extrusions were surface conditioned and forged at 1200 C to approximately 0.5 inch diameter rod.

Testing. Flat tensile specimens, 0.050 inch thick, having a 1 inch gage length and a 0.250 inch gage width, were machined from the sheet stock obtained by rolling the Phase I button samples. Round tensile specimens were machined from the extruded and forged rod stock. These specimens had a 1 inch gage length and a 0.200 inch gage diameter.

Most of the alloys were tested in the fully recrystallized condition. The machined specimens were wrapped in niobium foil, placed in a molybdenum susceptor, and annealed in a vacuum induction furnace for 1 hour at 1600 C. Pressure during annealing was below 5×10^{-5} mm of Hg. Temperatures were measured by sighting a calibrated optical pyrometer on the bottom of a hole drilled in a niobium block. The block was located inside the susceptor adjacent to the specimens. The depth of the hole was at least 5 times the diameter to insure black body conditions. Corrections were made for absorption by the Pyrex sight glass. Several of the alloys were tested in the worked and stress relieved condition. The specimens were stress-relieved by annealing 1 hour at 1095 C (2000 F) in a resistance heated vacuum tube furnace.

Low temperature tensile tests were conducted in a constant strain rate tensile machine of the type described by Manjoine, Wessel and Pryle.[17] All tests were run at a strain-rate of 1×10^{-3} sec^{-1} (360%/hr) and the load and deformation were recorded autographically. Temperatures below ambient were obtained using the technique of Wessel and Olleman.[18]

Elevated temperature tests (to 1095 C) were carried out in vacuum tensile machines similar in general construction to the stress-rupture units used in earlier work in this program.[25] The equipment and testing procedure were essentially the same as those described by Lawthers and Manjoine.[26] Testing at temperatures above 1095 C (2000 F) was done in identical machines, with the exception that the heating unit was a tungsten-wound furnace located inside the Inconel vacuum chamber. Pressure during testing was generally below 1×10^{-4} mm of Hg. The gage length of the specimens were loosely wrapped in niobium foil to minimize contamination. The strain rate was maintained at 1×10^{-3} sec^{-1}, the same as that used for the low temperature tests.

Properties of Binary Alloys

Fabrication. The results of working binary niobium-base alloys are summarized in Table II. Alloys containing up to 20 w/o Ti were cold rolled without difficulty. Nb-V, Nb-W and Nb-Re alloys were hot rolled at 1200-1300 C with satisfactory results. However, the 18 w/o Re sample was extremely brittle at room temperature and required careful handling to avoid shattering. Dilute Nb-Cr and Nb-Al alloys gave good results, but serious cracking was encountered in hot rolling alloys containing over 2.5 w/o Cr or Al. As noted in previous work,[24] poor results were obtained with alloys containing 10 and 20 w/o Zr.

Niobium-yttrium alloys were difficult to melt because of the presence of a tenacious surface film on the molten samples. The apparent high surface tension of the surface film did not permit the entire surface of the button to flow under the arc, consequently irregular shaped samples were produced. It has been proposed that the surface film is an yttrium oxide, possibly Y_2O_3.[24] However, Miller[31] has suggested that niobium and yttrium may show partial or complete liquid immiscibility, hence the film may be an yttrium rich layer. The Nb-Y alloys were very ductile and the addition of yttrium lowered the as-melted hardness indicating that yttrium is effective in gettering interstitial impurities.

Workability of Niobium-Yttrium Alloys. To determine if yttrium additions could be used to alleviate or eliminate the detrimental effect of interstitial elements on ductility, a series of alloys was prepared using niobium powder of very high oxygen and nitrogen content.

Table 11. Results of Working Binary Niobium Alloys

Heat No.	Nominal Composition (w/o)	As-Cast Hardness (VPN)	Results of Working[a] Hot Rolling	Cold Rolling
NC-112	Nb-5 Ti	154	-	-
NC-113	Nb-7.5 Ti	172	-	E
NC-195	Nb-20 Ti	192	-	G
NC-237	Nb-10 Zr	197	P	-
NC-242	Nb-20 Zr	260	P	-
NC-253	Nb-5 V	219	E	-
NC-241	Nb-20 Mo	289	F	-
NC-131	Nb-10 W	-	E	-
NC-194	Nb-10 W	149	E	-
NC-282	Nb-10 W	195	E	-
NC-243	Nb-20 W	247	G	-
NC-270	Nb-2 Re	156	G	-
NC-269	Nb-10 Re	262	G	-
NC-289	Nb-18 Re	358	F	-
NC-273	Nb-1.25 Cr	184	E	-
NC-197	Nb-2.5 Cr	203	G	-
NC-287	Nb-4.5 Cr	273	P	-
NC-274	Nb-6 Cr	299	NG	-
NC-272	Nb-0.6 Al	154	E	-
NC-238	Nb-1.5 Al	213	G	-
NC-288	Nb-2.5 Al	308	F	-
NC-256	Nb-3.1 Al	322	P	-
NC-271	Nb-3.5 Al	-	P	-
NC-211	Nb-1Y	75	Button too irregular to roll	
NC-212	Nb-2Y	82	Button too irregular to roll	
NC-267 *	Nb-1Y	92	-	G

* 50 gram button

(a) Workability Results: E - no cracks; G - minor surface cracks; F - small cracks, essentially sound; P - large cracks, NG - cracked up after small reduction.

The chemical analysis, hardness, and result of working these alloys are listed in Table 12. Figure 22 is a photograph of the cold rolled buttons. The

Table 12. Composition, Hardness and Workability of Impure Nb-Y Alloys

Heat No.	Nominal Composition (w/o)	O	N	C	Y	As-Cast Hardness (VPN)	Results of Cold Rolling
NC-202	Nb(Impure)	0.601	0.177	0.034	-	496	Cracked up on first pass
NC-203	Nb-1Y	-	-	-	-	401	Cracked after 6% reduction
NC-204	Nb-2Y	-	-	-	-	322	Cracked after 6% reduction
NC-205	Nb-5Y	0.011	-	0.074	2.01	147	Edge cracks after 59% reduction

data of Table 12 show that the addition of yttrium significantly increases the ductility of highly impure niobium by removing oxygen. With the addition of 5 w/o Y, the oxygen level was reduced from 0.601 to 0.011 w/o. There are apparently two possible mechanisms for oxygen removal. An yttrium oxide may be formed which is insoluble in niobium and floats to the surface of the melt, or an yttrium rich liquid layer is formed which has a greater affinity for oxygen. At present, analytical techniques are not available for the determination of nitrogen in Nb-Y alloys. However, the low hardness of the Nb-5 w/o Y alloys indicates that some nitrogen has also been removed during melting. These results suggest that yttrium may have some economic importance in upgrading niobium scrap such as machining chips, small reject parts, etc. during melting.

Mechanical Property Data. Tensile data were obtained for the binary alloys at room temperature and at 1095 C (2000 F). Several of the alloys were also tested in 1205 C (2200 F). In instances where material was available, a number of additional low temperature tensile tests were carried out to provide preliminary data on the ductile-brittle transition characteristics of the alloys. Tensile data for the binary alloys are listed in Table 13.

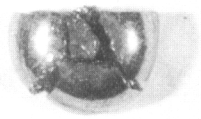

Nb
4% Red

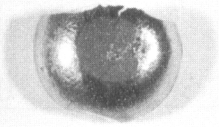

Nb - 2 w/o Y
6% Red

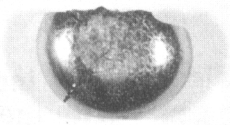

Nb - 1 w/o Y
6% Red

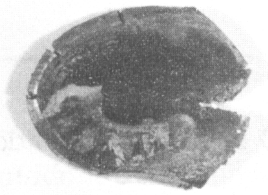

Nb - 5 w/o Y
59% Red

Fig. 22 - Effect of yttrium additions on the cold workability of impure niobium.

Low Temperature Tensile Properties. An evaluation of the room temperature properties of niobium alloys is complicated by the ductile-to-brittle transition phenomenon. The strength of unalloyed niobium begins to increase rapidly with decreasing temperature at approximately 0 C. In unalloyed niobium of the purity used in this investigation, the yield strength increases from about 25,000 at room temperature to 100,000 psi at -196 C. This highly temperature sensitive strengthening is part of the ductile-to-brittle transition phenomenon. At room temperature alloy additions can increase strength by a relatively temperature independent increment added to the strength of the pure metal, or a shift of the transition temperature range to a higher temperature. Data for two titanium and two tungsten containing alloys shown in Figure 23 indicate that solid solution additions to niobium increase room temperature strength by both mechanisms. This can be seen by comparing the strength of the 20 w/o (11 a/o) tungsten alloy at room temperature and 400 C. At room temperature the alloy addition resulted in a yield strength increase of about 60,000 psi, while at 400 C the increase is only about 25,000 psi. The 25,00 psi increment at 400 C is probably close to the true solid solution strengthening. The additional 35,000 psi increment at room temperature is due to a shift to a higher temperature of the range over which the yield strength of niobium becomes sharply temperature dependent.

Insufficient data exist to determine whether this behavior exhibited by the titanium and tungsten containing alloys (Figure 23) is characteristic of all additions to niobium or to determine the relative effect of the individual alloying element on the two strengthening mechanisms. It is important, however, to recognize that both factors can contribute to the room temperature strength of niobium-base alloys. In attempts to correlate the strengthening effect of alloying elements with various proposed theories of solid solution strengthening, only the relatively temperature independent increment should be used. This usually cannot be estimated from room temperature test data on niobium alloys, and consequently room temperature data are not sufficient to make basic studies of strengthening mechanisms. It is also important from an alloy design standpoint to know whether strengthening is due to conventional solid solution strengthening or to a shift in the transition temperature range.

Alloy additions which raise the temperature range over which the strength increases rapidly usually raise the temperature range over which the change from ductile rupture to brittle fracture occurs. The data of Figure 23 show this to be true for titanium and tungsten containing alloys. However, it is also evident that tungsten causes a much greater increase in the fracture transition temperature than titanium, when compared at alloy contents which give equivalent strength increases.

Table 13. Tensile Properties of Niobium Binary Alloys

Specimen No.	Nominal Composition (w / o)	Analysis (w / o)	Test Temperature °C	Test Temperature °F	0.2% Yield Strength (psi)	Ultimate Strength (psi)	Elongation (%) Uniform	Elongation (%) Total	Reduction in Area (%)	Annealed Hardness (VPN)	Recrystallized Grain Size (ASTM No.)
NC-112-1	Nb-5 Ti	4.33 Ti	RT	RT	50,000	60,000	18.0	26.2	68.0		5
NC-112-3	Nb-5 Ti	0.056 O_2	-100	-148	75,800	84,400	11.7	17.1	51.7	145	5
NC-112-4	Nb-5 Ti	0.009 N_2	-150	-238	103,300	108,800	14.5	20.7	45.0		5
NC-112-2	Nb-5 Ti		-196	-320	123,200	130,000	5.2	10.8	21.6		5
NC-113-1	Nb-7.5 Ti	6.83 Ti	RT	RT	52,900	62,250	15.0	19.8	51.6	156	5
NC-113-4	Nb-7.5 Ti	0.043 O_2	- 50	- 58	82,500	89,400	16.8	24.7	48.4		5
NC-113-3	Nb-7.5 Ti	0.011 N_2	-100	-148	88,400	95,100	16.1	22.7	43.8		5
NC-113-5	Nb-7.5 Ti		-150	-238	108,700	112,000	12.9	17.2	38.7		5
NC-113-2	Nb-7.5 Ti		-196	-320	124,000	133,600	5.7	8.2	22.7		5
NC-195-6	Nb-20 Ti	18.0 Ti	200	392	51,100	57,900	13.9	21.6	46.0		4-5
NC-195-1	Nb-20 Ti	0.059 O_2	RT	RT	74,550	79,700	12.9	18.5	31.4		4-5
NC-195-2	Nb-20 Ti		-100	-148	104.700	105,800	1.2	5.1	10.7		4-5
NC-195-5	Nb-20 Ti		-150	-238	116,000	134,600 *	-	1.8	5.5		4-5
NC-195-3	Nb-20 Ti		-196	-320	121,700	154,800 *	-	1.2	3.6		4-5
NC-195-4	Nb-20 Ti		-196	-320	114,200	156,700 *	-	2.0	4.0		4-5
NC-115-1	Nb-10 Zr		RT	RT	57,200	72,800	13.4	15.1	41.9		6
NC-115-3	Nb-10 Zr		RT	RT	60,450	76,500	12.6	13.1	28.3		6
NC-115-2	Nb-10 Zr		-100	-148	80,550	94,500	10.5	11.4	14.8		6
NC-115-4	Nb-10 Zr		-196	-320	109,300	124,700 *	-	0.9	0.8	164	6
NC-237-1	Nb-10 Zr		1095	2000	36,800	44,000	3.6	29.0	38.3	193	5
NC-242-1	Nb-20 Zr		1095	2000	48,000	53,000	1.2	19.9	22.3	244	4
NC-196-1	Nb-10 Hf		RT	RT	36,750	54,850	14.3	20.2	57.2		
NC-196-2	Nb-10 Hf		-196	-320	85,500	97,650	21.9	27.4	41.6		
NC-273-1	Nb-1.25 Cr		RT	RT	50,900	65,900	21.6	34.4	68.8		2
NC-273-2	Nb-1.25 Cr		-100	-148	56,900	70,000	17.9	22.4	27.1		
NC-273-3	Nb-1.25 Cr	~1.0 **	1095	2000	21,200	21,330	0.4	36.0	~100	163	1

* True Stress at fracture

** Spectrographic Analysis

Table 13. Tensile Properties of Niobium Binary Alloys (cont.)

Specimen No.	Nominal Composition (w / o)	Analysis (w / o)	Test Temperature °C	Test Temperature °F	0.2% Yield Strength (psi)	Ultimate Strength (psi)	Elongation (%) Uniform	Elongation (%) Total	Reduction in Area (%)	Annealed Hardness (VPN)	Recrystallized Grain Size (ASTM No.)
NC-197-1	Nb-2.5 Cr	1.57 Cr	RT	RT	58,100	76,100	23.9	34.1	73.6	176	3-4
NC-197-2	Nb-2.5 Cr		-100	-148	82,000	97.900	22.2	27.1	52.4		3-4
NC-197-3	Nb-2.5 Cr	1.57 Cr	1095	2000	24,500	25,940	0.5	37.9	~100	169	3-4
NC-197-4	Nb-2.5 Cr		1205	2200	15,600	16,600	8.2	55.4	~100	172	3-4
NC-150-1	Nb-5 Mo	5.03 Mo	RT	RT	43,600	52,700	21.1	27.5	82.0	149	3
NC-150-2	Nb-5 Mo		RT	RT	45,500	55,100	21.9	27.2	72.4		3
NC-150-4	Nb-5 Mo		-100	-148	69,900	77,850	18.1	24.5	54.8		3
NC-192-3	Nb-10 Mo		200	392	39,830	54,200	16.8	24.4	69.0		5
NC-192-1	Nb-10 Mo		RT	RT	56,650	-	-	6.6	6.4		5
NC-192-2	Nb-10 Mo		-100	-148	-	70,900 *	-	-	-	187	5
NC-241	Nb-20 Mo		1095	2000	36,800	43,700	1.7	5.9	53.6	248	4-5
NC-282-1	Nb-10 W	9.49 W	RT	RT	43,250	64,650	18.1	34.4	68.8		
NC-282-4	Nb-10 W		- 50	- 58	55,000	75,650	18.4	26.4	43.3		
NC-284-6	Nb-10 W		- 75	-103	59,350	80,700	19.2	21.9	25.2		
NC-284-2	Nb-10 W		-100	-148	68,000	80,650 *	0	2.5	3.4		
NC-284-3	Nb-10 W		-150	-238	83,700	94,400 *	0	1.5	3.0		
NC-284-5	Nb-10 W		-196	-390	102,900	108,750 *	0	0.4	2.2		
NC-243-3	Nb-20 W	19.9 W	400	752	45,850	75,100	13.0	16.9	50.2		5
NC-243-2	Nb-20 W		200	392	55,800	56,600	0.7	2.0	5.9		5
NC-243-1	Nb-20 W		RT	RT	81,600	82,600 *	0	0.2	1.2	220	5
NC-243-4	Nb-20 W		1095	2000	26,500	34,800	4.6	17.7	~100	241	5
NC-270-1	Nb-2 Re	1.46 Re	RT	RT	47,750	61,800	22.2	31.4	83.7		
NC-270-2	Nb-2 Re		-100	-148	53,450	65,600	21.2	29.0	56.6		
NC-270-3	Nb-2 Re		-196	-320	96,300	101,800 *	-	.7	3.0		
NC-270-4	Nb-2 Re	1.46 Re	1095	2000	12,600	14,000	3.6	26.9	~100		
NC-269-1	Nb-10 Re	7.88 Re	400	752	39,100	66,200	10.3	14.5	46.2		
NC-269-2	Nb-10 Re		200	392	52,000	58,200 *	-	0.9	2.6		

* True stress at fracture

Table 13. Tensile Properties of Niobium Binary Alloys (cont.)

Specimen No.	Nominal Composition (w / o)	Analysis (w / o)	Test Temperature °C	Test Temperature °F	0.2% Yield Strength (psi	Ultimate Strength (psi)	Elongation (%) Uniform	Elongation (%) Total	Reduction in Area (%)	Annealed Hardness (VPN)	Recrystallized Grain Size (ASTM No.)
NC-269-3	Nb-10 Re	7.88 Re	1095	2000	27,100	30,900	1.5	9.4	34.1		
NC-289-1	Nb-18 Re		400	752	-	30,450 *	0	0	0		
NC-289-2	Nb-18 Re	14.38 Re	1093	2000	41,800	45,100	1.6	6.7	-		
NC-272-1	Nb-0.6 Al	0.44 Al	RT	RT	37,820	52,700	19.4	24.2	58.0		
NC-272-2	Nb-0.6 Al		-100	-148	59,350	69,750	15.4	20.7	32.5		
NC-272-3	Nb-0.6 Al	0.44 Al	1095	2000	13,000	15,340	4.0	43.9	100		
NC-238-2	Nb-1.5 Al	1.88 Al	200	392	34,300	49,800	15.4	19.2	55.3		4-5
NC-238-1	Nb-1.5 Al		RT	RT	67,500	75,700 *	-	2.8	6.6	203	4-5
NC-238-4	Nb-1.5 Al		- 50	- 58	72,400	86,700 *	-	9.9	8.6		4-5
NC-238-3	Nb-1.5 Al		-100	-148	79,300	82,800 *	-	0.5	2.6		4-5
NC-238-5	Nb-1.5 Al	1.88 Al	1095	2000	17,600	19,200	3.3	44.1	~100	172	4
NC-238-6	Nb-1.5 Al		1205	2200	11,400	12,000	2.4	77.2	~100		4
NC-288-1	Nb-2.5 Al		RT	RT	-	60,700 *	0	0.1	4.7		
NC-288-2	Nb-2.5 Al		1095	2000	17,600	19,300	2.2	26.0	~100		
NC-267-1	Nb-1Y		RT	RT	9,680	27,950	24.8	41.6	61.9		

* True stress at fracture

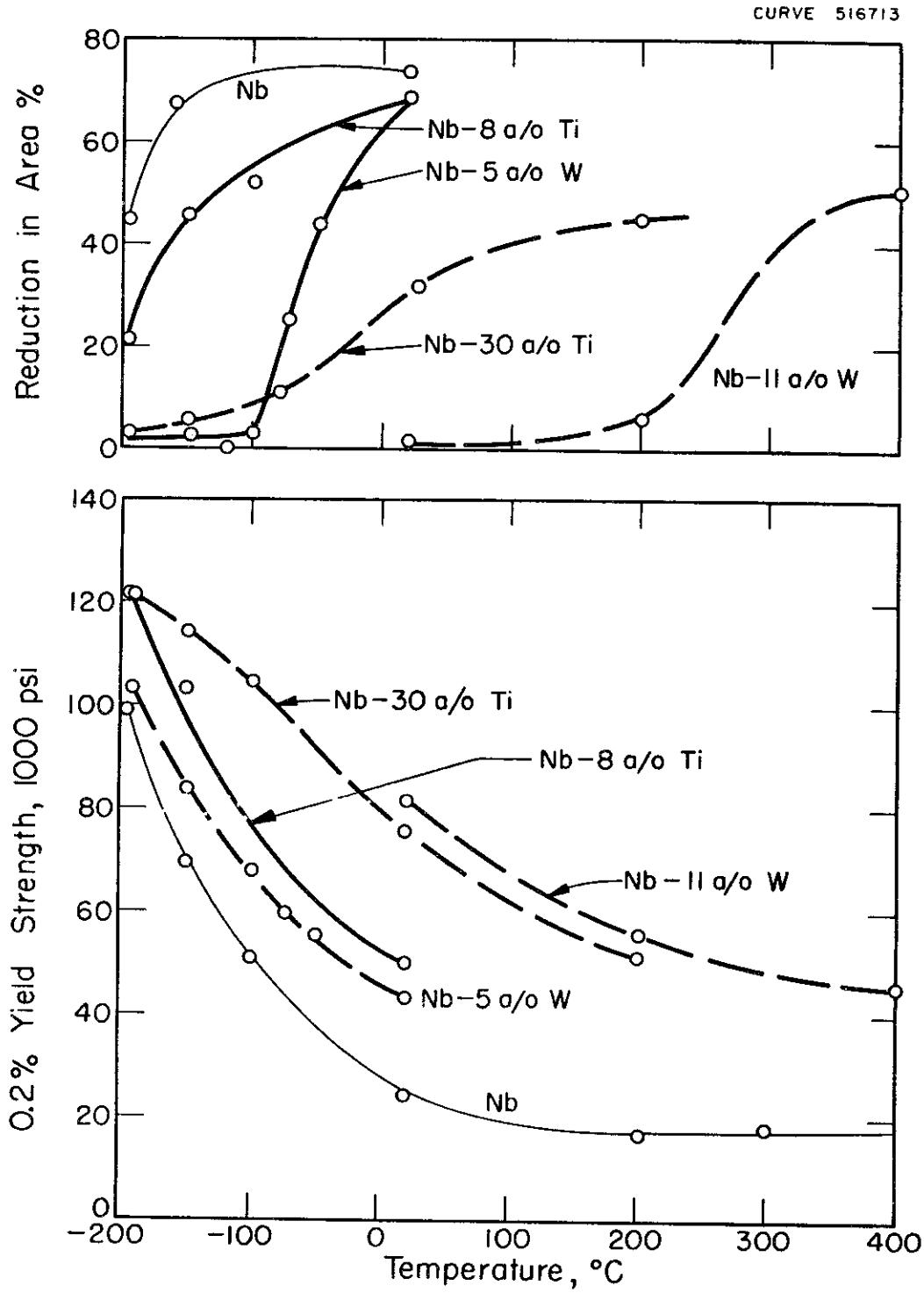

Fig.23-Effect of temperature on the yield strength and ductility of several niobium binary alloys.

Although data on the ductile-brittle transition characteristics of binary niobium alloys are limited, sufficient results are available to outline some general trends. Figure 24 shows the temperatures, as a function of atom percent alloy addition, above which the alloys exhibit over 10% reduction in area. The alloys may be grouped into two general classes: Those with Al, Re, Mo, and W, which greatly increase the fracture transition temperature; and those with titanium and hafnium, which have very little effect. Zirconium alloys are intermediate between these two groups. However, the higher zirconium content alloys are two phase at low temperatures and probably should not be compared with the solid solution alloys. Low temperature data are not available for vanadium alloys. However, room temperature data obtained previously[24] indicate that vanadium additions are not particularly detrimental to low temperature ductility. Data for chromium containing alloys are too limited to permit any conclusions to be drawn at present. It is interesting to note that rhenium, which improves the low temperature ductility of molybdenum and tungsten, has a directly opposite effect in niobium.

Fractographic examination of the low temperature tensile specimens is still in progress. Preliminary results indicate that brittle fracture occurs by transgranular cleavage. One exception has been noted in the case of the 20 w/o Ti alloy, which failed by complete intergranular separation. The reason for the intergranular failure of this alloy is not understood at present. It should be emphasized that the ductile-brittle transition phenomena are greatly influenced by purity, grain size, and prior metallurgical history. Care was exercised in maintaining these factors as constant as possible in the materials studied; however, caution should be exercised in comparing these data with results obtained on samples of widely differing purity and metallurgical history. The results of low temperature tests on the binary alloys, while fairly limited, illustrate the very significant effect of alloy additions on the ductile-brittle transition of niobium. At the present time, no adequate explanation of the effect of solute additions on the ductile-brittle transition behavior is available. However, this phenomenon is of considerable, practical and theoretical importance, and appears to be an area for fruitful study.

In an earlier report[24] data concerning the effect of Zr, Hf, V, Mo, and W additions on the room temperature tensile properties of niobium were presented. Additional data on Ti, Cr, and W alloys obtained during the current program are shown in Figures 25 and 26. The room temperature tensile data for the binary alloys are summarized in Figures 27 and 28 where the alloys are compared on an atom percent basis. In the dilute range (5 a/o or less) limited data indicate chromium to be the most effective strengthener. Beyond 5 a/o alloy addition, vanadium has the greatest effect in increasing room temperature strength.

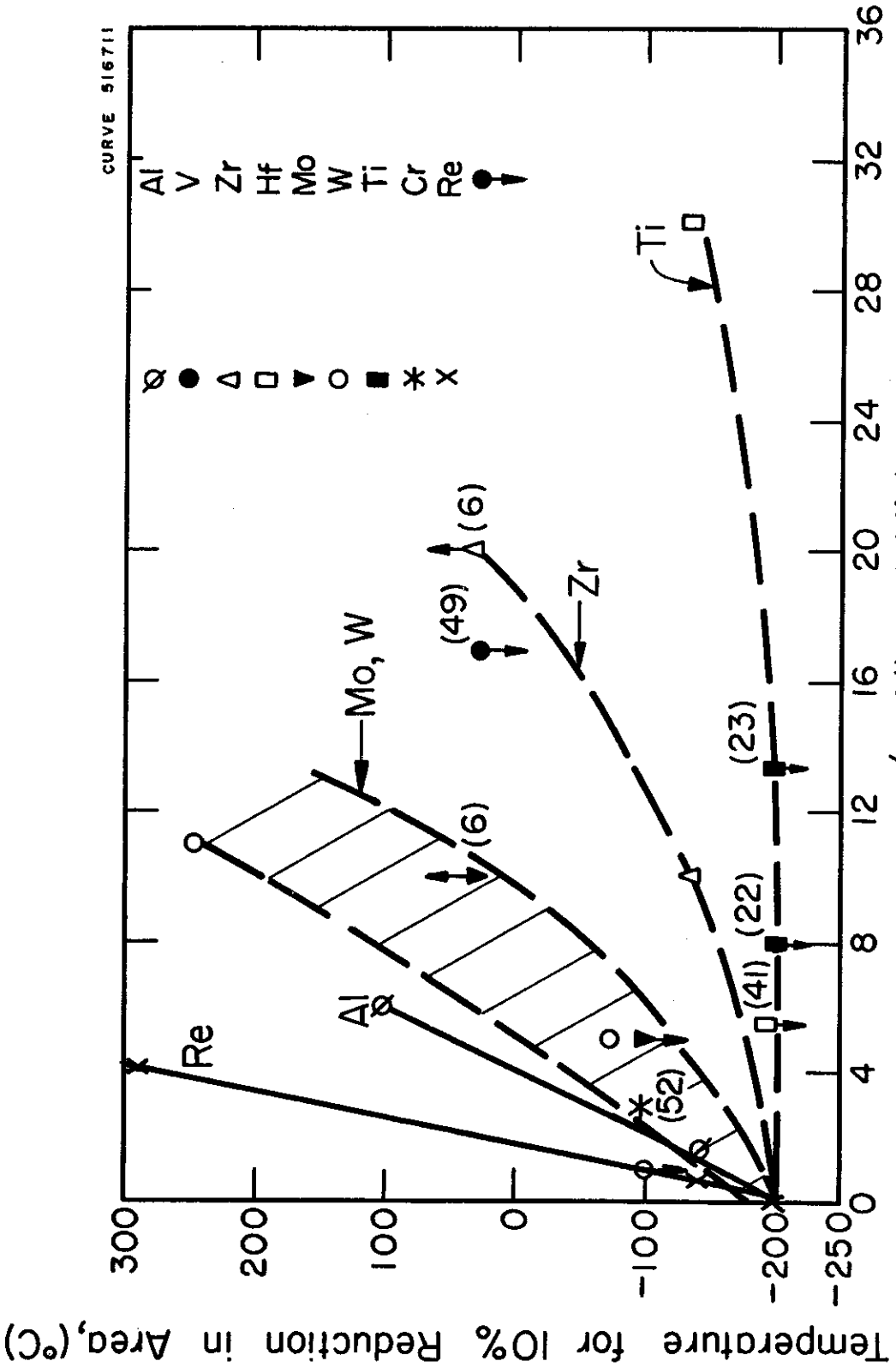

Fig.24-Effect of binary alloy additions on the transition temperature of niobium (approximate)

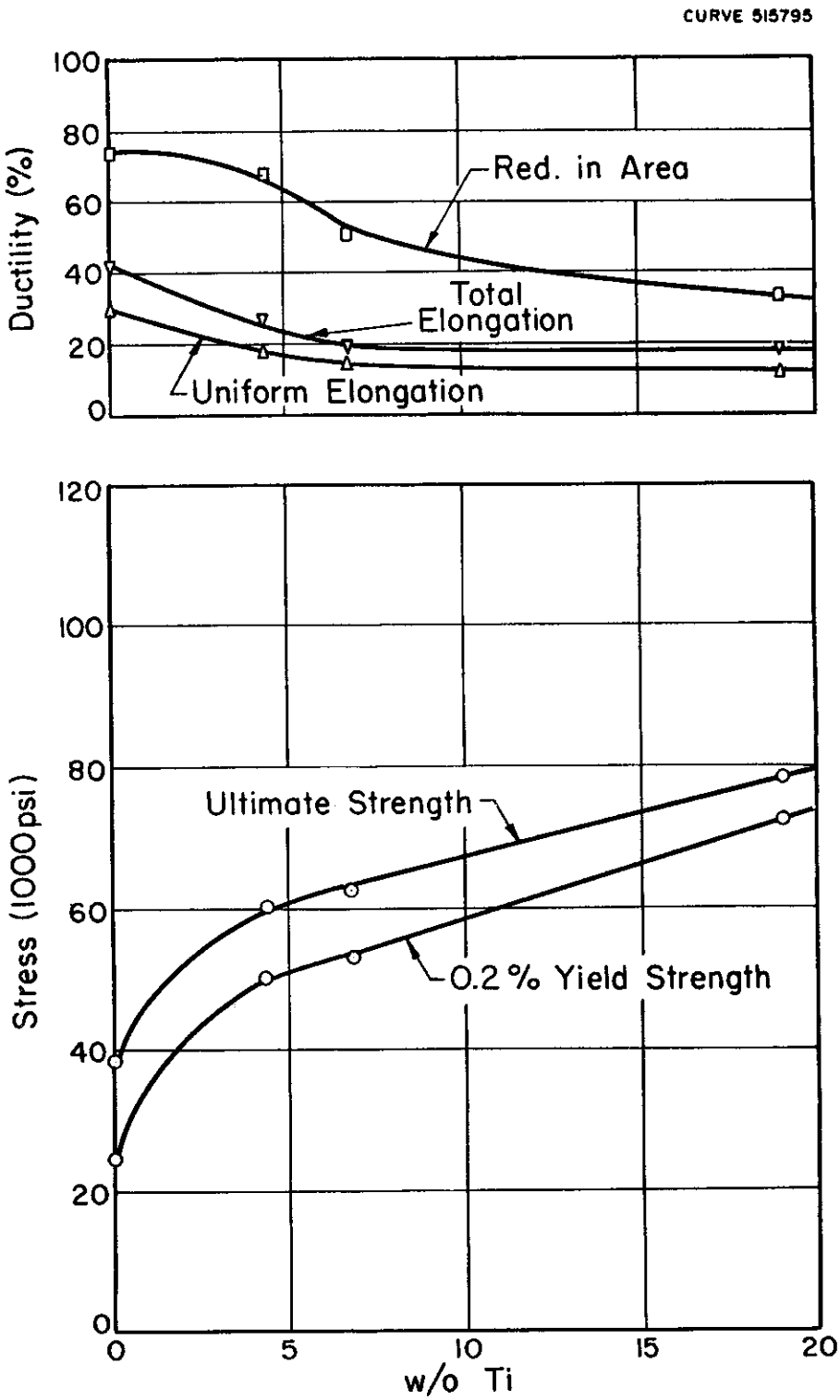

Fig. 25 – Effect of titanium additions on the room temperature tensile properties of niobium

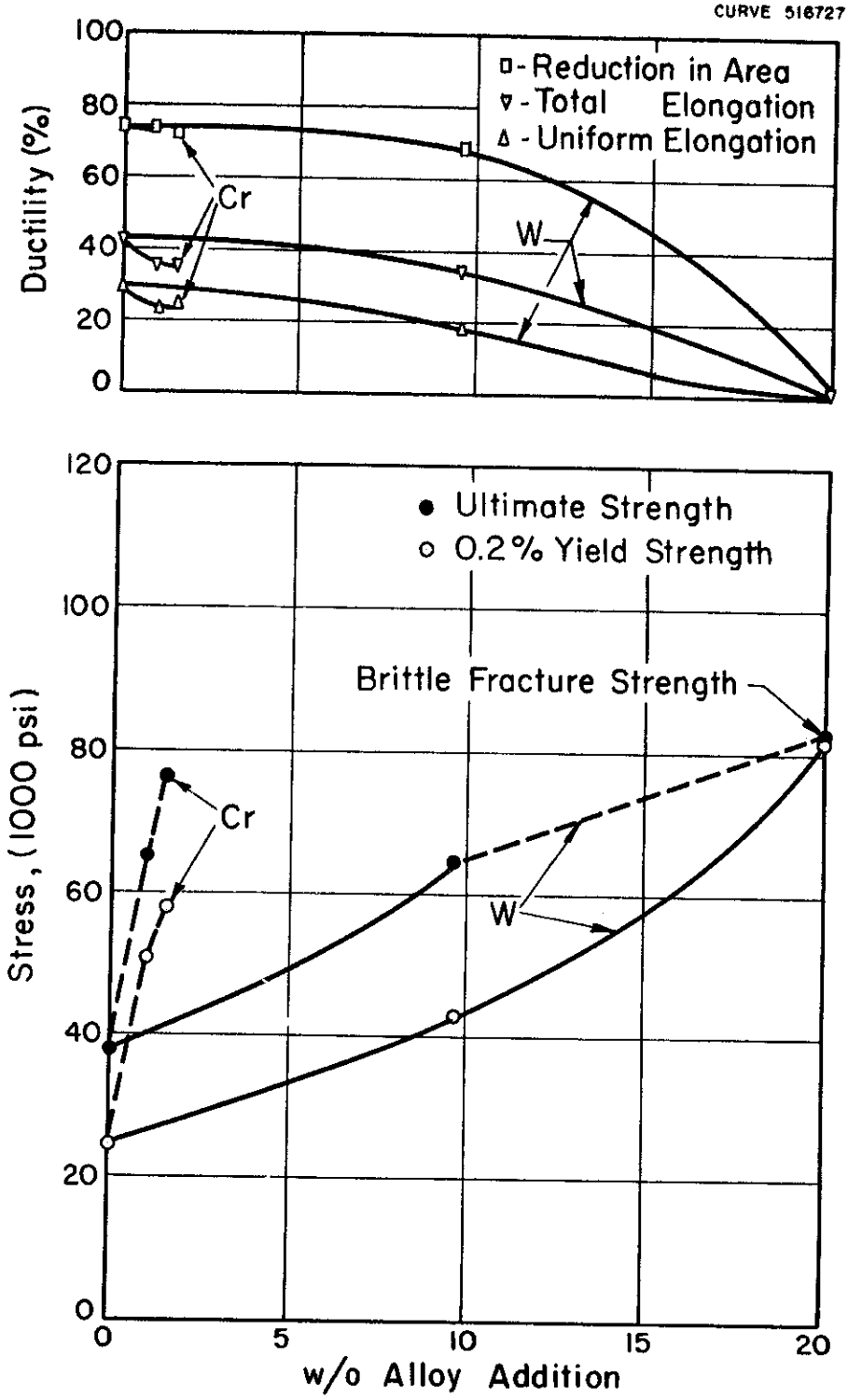

Fig. 26— Effect of chromium and tungsten additions on the room temperature tensile properties of niobium.

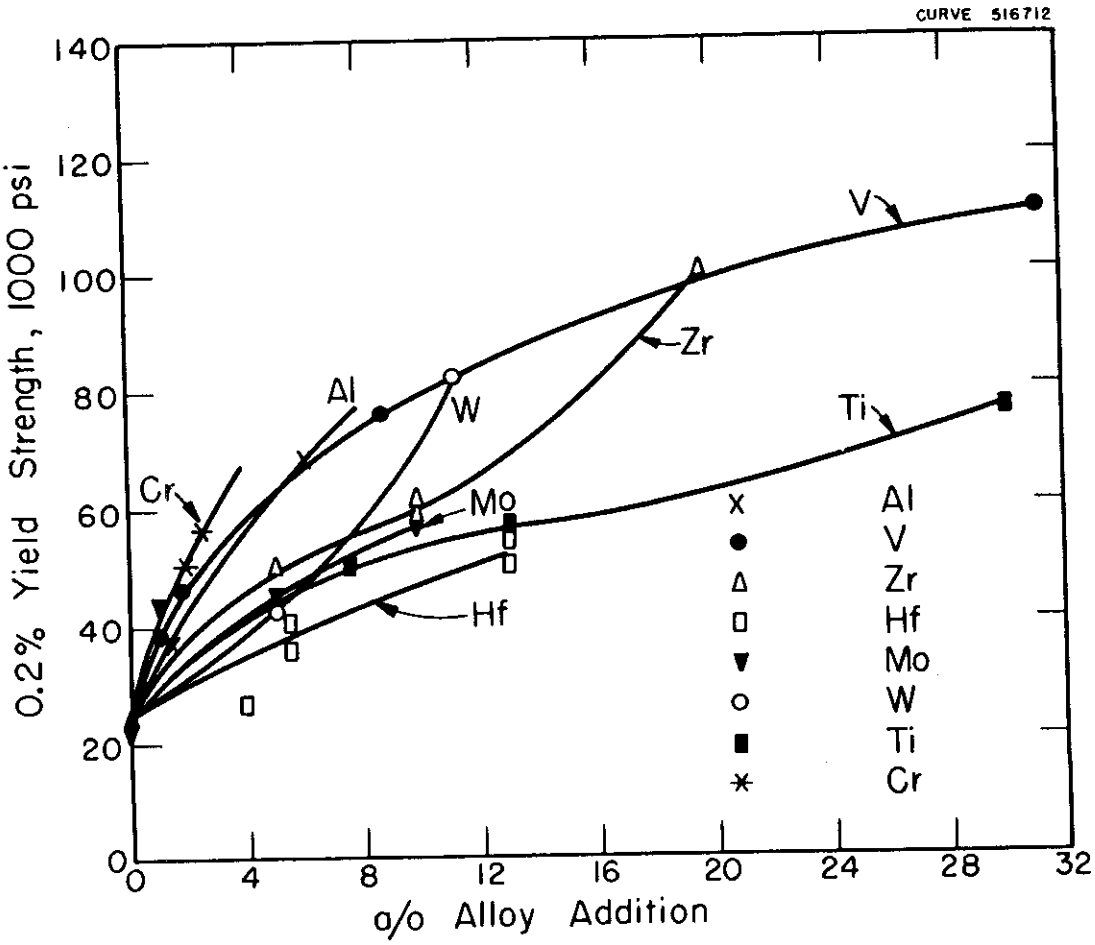

Fig.27-Effect of binary alloy additions on the room temperature yield strength of niobium.

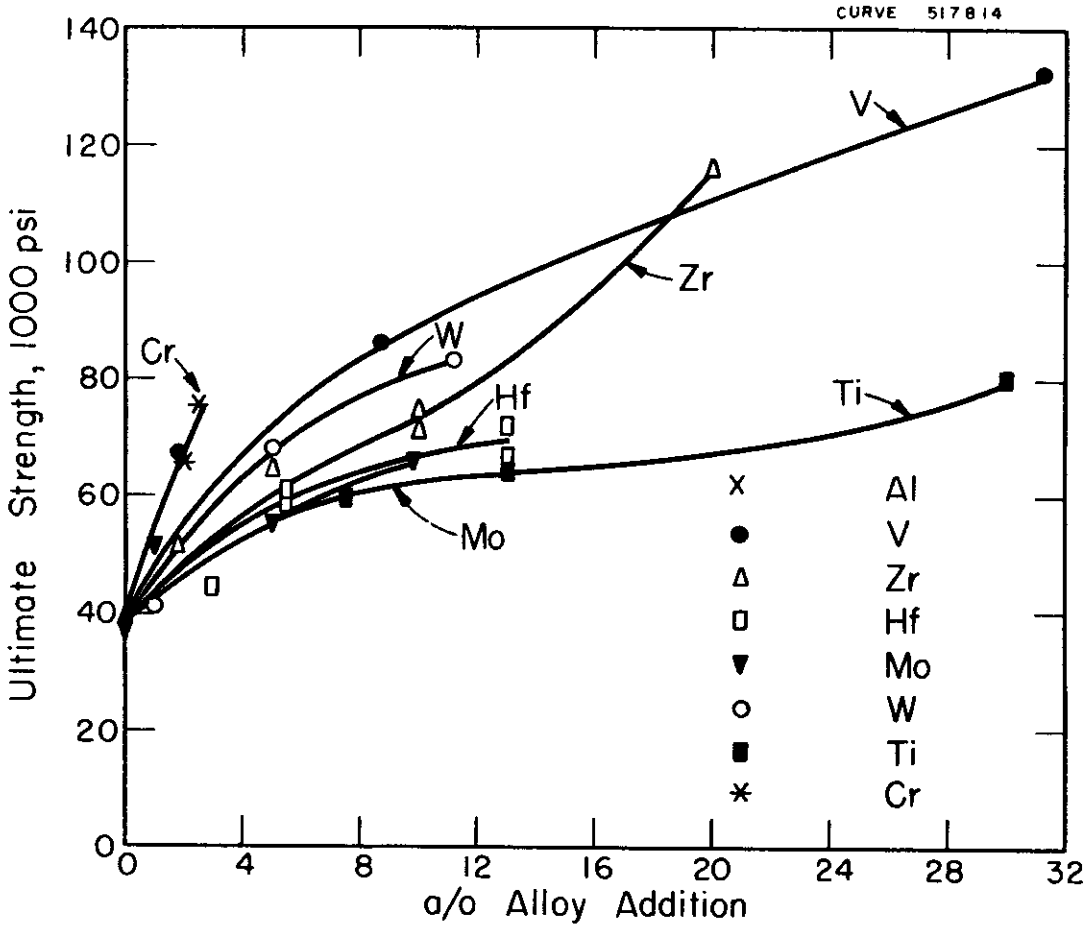

Fig. 28 – Effect of binary alloy additions on the room temperature ultimate tensile strength of niobium.

Titanium and hafnium are the least effective strengtheners. However, they also have the smallest effect in decreasing ductility. Molybdenum and tungsten are intermediate in strengthening, but the strengthening is accompanied by a decrease in ductility. At the higher additions, zirconium is an effective strengthener. However, appreciable amounts of second phase are observed in the microstructure in compositions above 10 a/o. Consequently, the 20 a/o zirconium alloy reflects some second-phase hardening.

Elevated Temperature Tensile Properties. Elevated temperature tensile data for the binary alloys are listed in Table 13. All the high temperature tests were conducted in vacuum, generally at pressures below 1×10^{-4} mm of Hg. Hardness values determined on the specimens before and after testing indicated that no contamination by gaseous impurities occurred. The effect of binary additions on the 1059 C (2000 F) tensile properties of niobium are summarized in Figures 29 and 30. These curves also includes data on binary alloys obtained previously.[24] The data are replotted on the basis of atom percent alloy addition in Figures 31 and 32. Also included are the data of Gemmel[27] for Nb-Ti alloys. The test temperature (1095 C) was slightly in excess of one-half the absolute melting temperature of pure niobium. It is therefore to be expected that appreciable solid solution strengthening would be observed in a short time tensile test. The data of Figure 31 show that, with the exception of titanium, all the alloy additions evaluated significantly increased the strength of niobium at 1095 C (2000 F). Limited data indicate the small additions of chromium are very effective in raising strength. At the higher alloy additions, Re, Zr, and V are the most potent strengtheners. Hafnium, molybdenum, tungsten, and aluminum are somewhat less effective in increasing strength. Gemmel's data for Nb-Ti alloys show that very little increase in tensile strength is obtained with titanium additions up to 15 a/o. Rhenium containing alloys had particularly high strength. Unfortunately, Re drastically reduces the low temperature ductility of niobium. On the basis of workability, low temperature ductility, and elevated temperature strength, V and Hf additions appear to be the best of the elements studied. While Mo and W are fairly attractive strengtheners, they seriously reduce low temperature ductility with additions greater than about 10 w/o. Limited data indicate that dilute Cr additions may be useful in improving elevated temperature strength.

Microstructure. Metallographic examination of the binary alloys is in progress. Preliminary results show that the Nb-Ti, Nb-Cr, Nb-Mo, Nb-W, and Nb-Re alloys were essentially single phase. A small amount of an acicular precipitate was observed in the microstructure of the Nb-Ti, Nb-Mo and Nb-W alloys. This is evidently a carbide, since the carbon content of the base materials used to prepare the binary alloys was in excess of the solubility limit in the testing temperature range. Examination of Nb-Al alloys has not been completed.

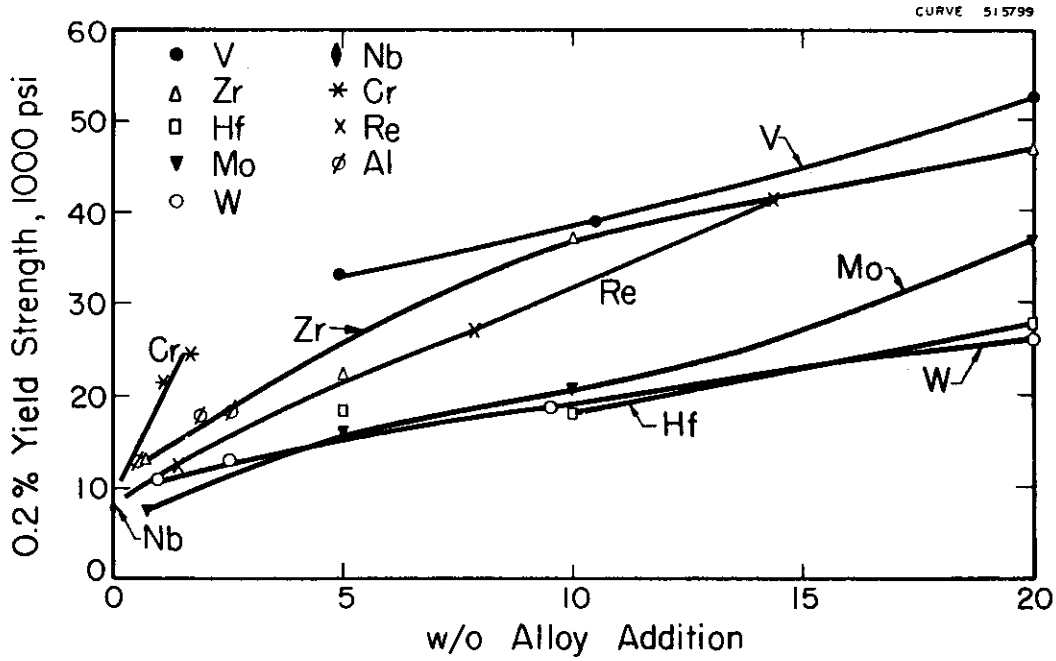

Fig. 29—Effect of binary alloy additions on the yield strength of niobium at 1095 C (2000 F)

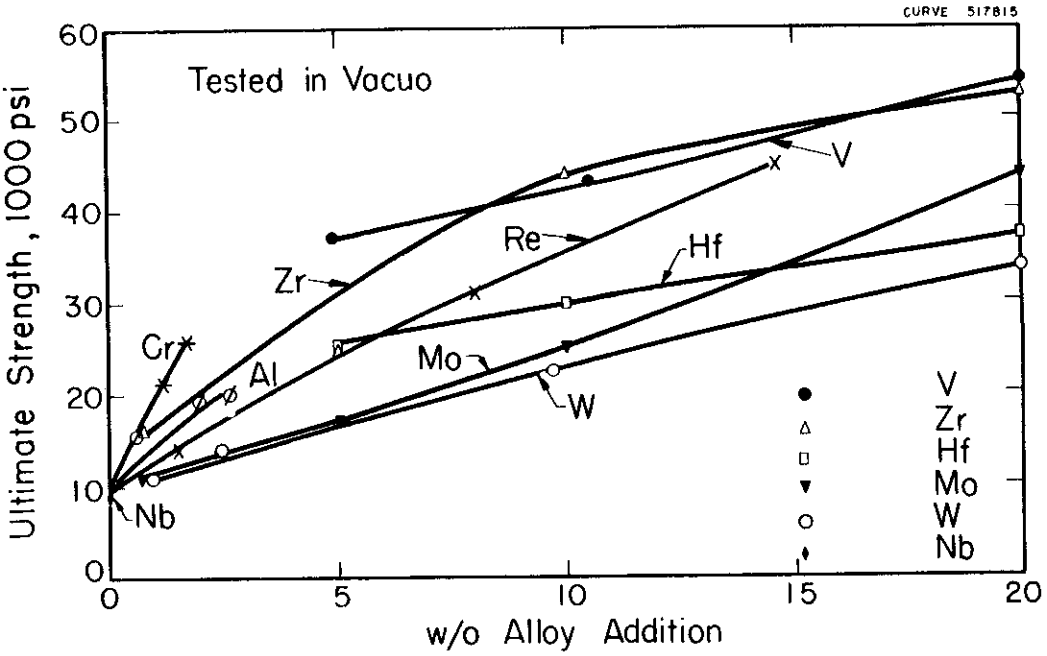

Fig. 30—Effect of binary alloy additions on the ultimate tensile strength of niobium at 1095 C (2000 F)

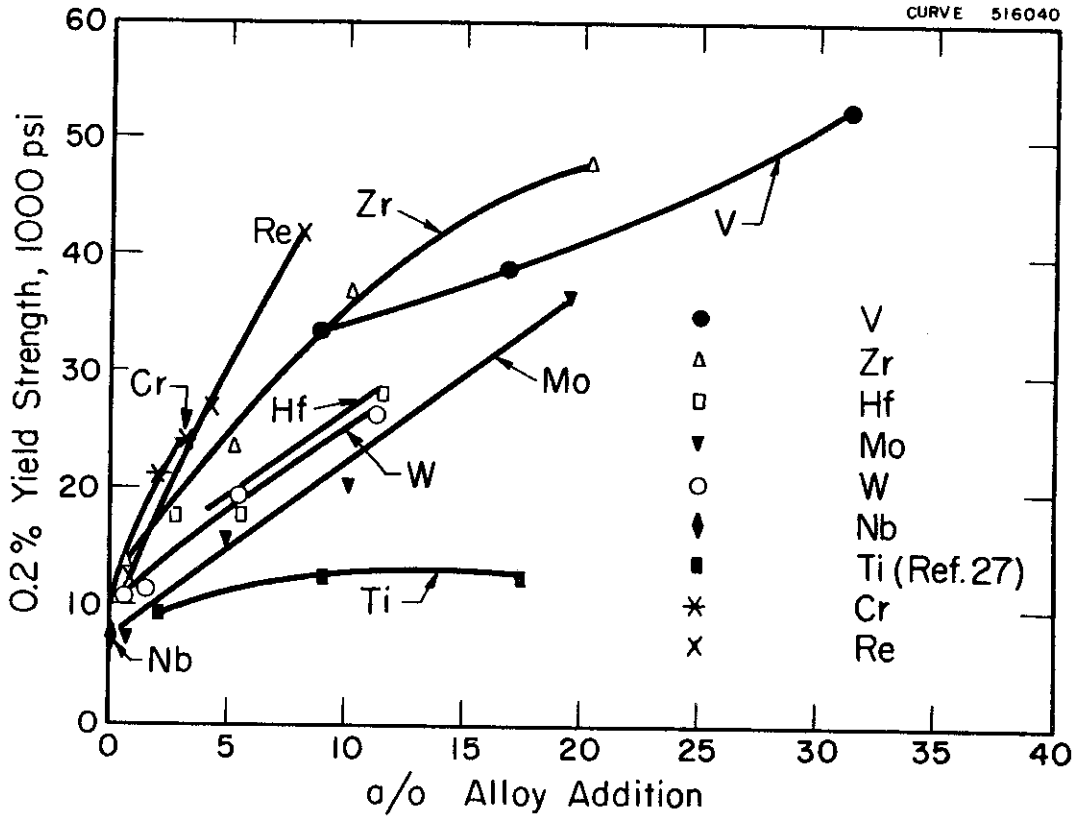

Fig. 31—Effect of binary alloy additions on the yield strength of niobium at 1095 C (2000 F).

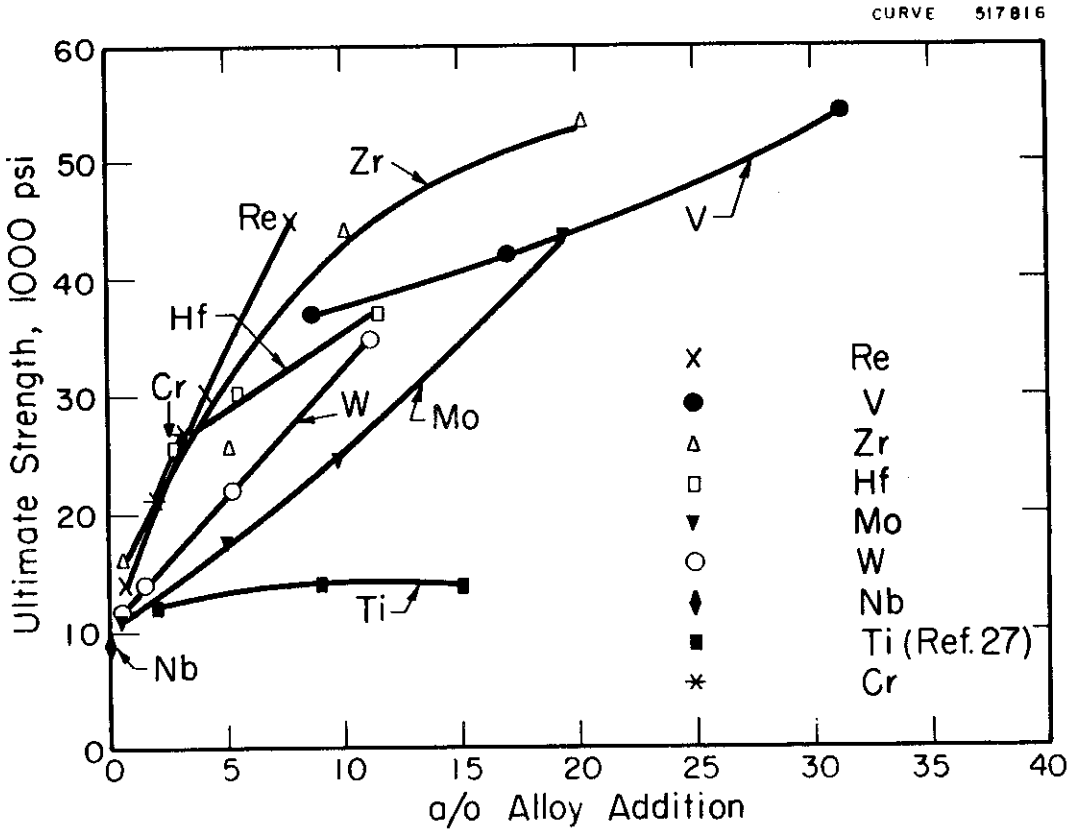

Fig. 32—Effect of binary alloy additions on the ultimate tensile strength of niobium at 1095 C (2000 F).

Deformation twins were observed in Nb-Ti alloys tested at low temperatures. Figure 33 shows twins adjacent to the fracture surface of a Nb-20 Ti alloy (NC-195) tested in tension at -196 C. As shown in Figure 33, the fracture was entirely intergranular.

All the Nb-Zr alloys showed a considerable quantity of second phase in the microstructure, as illustrated in Figure 34. This phase is evidently the decomposition product of the body-centered cubic Nb-Zr solid solution, according to the phase diagram of Rogers and Atkins.[32] Grain boundary cracking was observed in Nb-Zr alloys tested at 1095 C (2000 F), as shown in Figure 34.

Properties of Ternary and Quaternary Alloys

A number of ternary and quaternary alloys evaluated on the basis of workability and tensile properties. These alloys were prepared in the same manner as the binary alloys discussed previously.

Fabrication. The results of working ternary and quaternary alloys are listed in Table 14. Workability generally ranged from poor to fair. The best results were obtained with Nb-Mo-V and Nb-W-V alloys. Quaternary additions of zirconium to these alloys resulted in poorer rolling characteristics.

Earlier work in this program indicated that alloys containing over 10 w/o vanadium had poor ductility at 1095 C (2000 F). The observed tensile failures were completely intergranular. The "hot short" condition was apparently associated with the presence of a grain boundary film, possibly a vanadium oxide. Attempts were made to eliminate this grain boundary film by the addition of Al and Y to niobium-vanadium alloys. However, these alloys were completely unworkable.

The generally low yield of useable material obtained from the ternary and quaternary alloys should not be considered discouraging, considering the non-ideal working procedures used. Rolling an irregular as-cast button at 1200-1300 C is a rather severe workability test. Much better results would be expected with higher ingot breakdown temperatures and more favorable working procedures such as extrusion. Results described later in this report indicate this to be the case.

Mechanical Property Data. Tensile data for ternary and quaternary alloys are listed in Table 15. Attractive high temperature strength and good ductility were exhibited by the Nb-5V-5Mo and Nb-7.5W-5V alloys. The room temperature ductility

Fig. 33 – Deformation twins in Nb–20 Ti alloy (NC-195). Annealed 1 hour at 1600 C prior to testing at –196 C. 100X

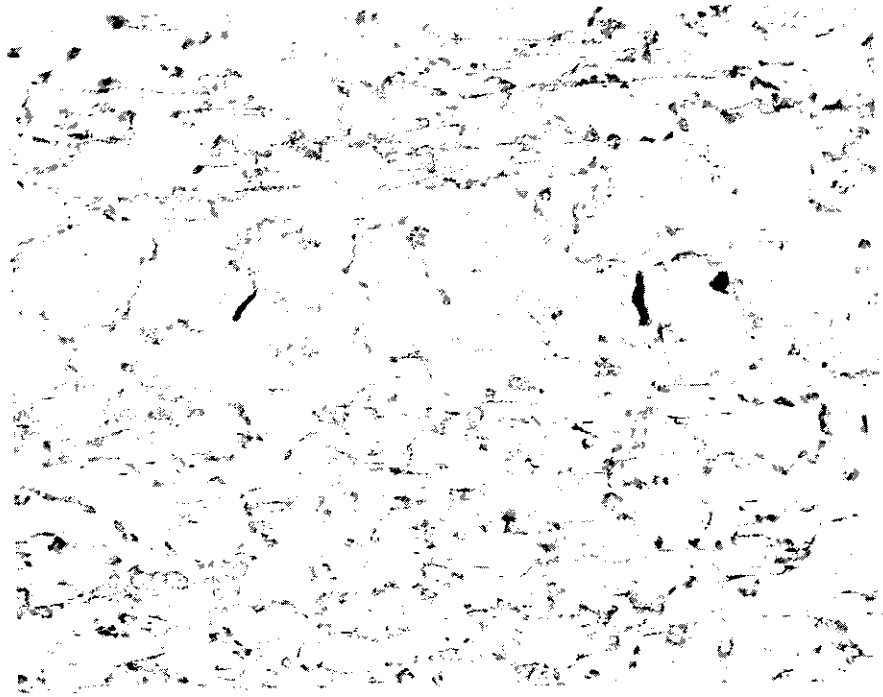

Fig. 34 – Microstructure of Nb–20 Zr alloy (NC–242) Annealed 1 hour at 1600 C prior to testing at 1095 C. 100X

Table 14. Results of Working Ternary and Quaternary Niobium-Base Alloys

Heat No.	Nominal Composition (w/o)	As-Cast Hardness (VPN)	Results of Hot Rolling[a]
NC-255	Nb-5 Mo-5 Hf	193	F
NC-263	Nb-7.5 Mo-7.5 Hf	239	P
NC-155	Nb-5 V-5 Mo	245	G
NC-264	Nb-5 V-5 Mo-1 Zr	255	P
NC-261	Nb-5 V-5 Mo-0.5 Zr	268	F
NC-181	Nb-5 V-5 Mo-1 Zr	255	P
NC-262	Nb-5 W-5 V	253	F
NC-254	Nb-7.5 W-5 V	246	F
NC-259	Nb-5 W-5 V-1 Zr	254	P
NC-240	Nb-5 V-5 Zr	244	P
NC-232	Nb-10 V-1.5 Al	342	NG
NC-233	Nb-20 V-0.5 Y	319	NG
NC-260	Nb-5 Hf-5 V	237	P
NC-281	Nb-5 W-5 V-5 Hf	266	P

(a) Workability Results: E - no cracks; G - minor surface cracks; F - small cracks, essentially sound
P - large cracks; NG - cracked up after small reduction

Table 15. Tensile Properties of Niobium Ternary and Quaternary Alloys

Specimen No.	Nominal Composition (w / o)	Test Temperature °C	Test Temperature °F	0.2% Yield Strength (psi)	Ultimate Strength (psi)	Elongation (%) Uniform	Elongation (%) Total	Reduction in Area (%)	Annealed Hardness (VPN)	Recrystallized Grain Size (ASTM No.)
NC-155-1	Nb-5 V-5 Mo	RT	RT	77,200	95,000	22.8	28.7	36.6	234	4-5
NC-155-2	Nb-5 V-5 Mo	1095	2000	37,300	40,100	0.7	43.5	54.2		4-5
NC-181-1	Nb-5 V-5 Mo-1 Zr	RT	RT	Defective Specimen						
NC-181-2	Nb-5 V-5 Mo-1 Zr	1095	2000	50,500	53,500	0.9	5.0	6.2	254	6
NC-262-1	Nb-5 W-5 V	RT	RT	87,300	97,200 *	0	3.6	6.1		
NC-262-2	Nb-5 W-5 V	1095	2000	35,700	36,100	0.3	37.2	71.5		
NC-254-1	Nb-7.5 W-5 V	RT	RT	89,500	125,800 *	0	21.9	17.1		5
NC-254-3	Nb-7.5 W-5 V	1095	2000	41,000	43,200	0.7	30.7	57.9		5
NC-259-1	Nb-5 W-5 V-1 Zr	RT	RT	84,600	104,500	25.4	32.4	45.5		
NC-259-2	Nb-5 W-5 V-1 Zr	1095	2000	46,500	50,500	1.4	18.6	42.5		
NC-260-1	Nb-5 Hf-5 V	RT	RT	75,500	94,200	22.0	30.7	51.1		
NC-260-3	Nb-5 Hf-5 V	1095	2000	45,000	48,000	1.7	18.2	30.8		
NC-240-1	Nb-5 V-5 Zr	1095	2000	45,600	49,600	1.2	5.2	28.0	227	6
NC-281-1	Nb-5 W-5 Hf-5 V	1205	2200	42,400	46,800	1.1	4.0	4.2		5-6

* True stress at fracture

of these alloys was also quite high. The addition of 1 w/o Zr to the Nb-V-Mo and Nb-W-Mo significantly improved elevated temperature strength. The highest strength alloy tested was Nb-5W-5Hf-5V. This sample had a 46,800 psi ultimate strength of 1205 C (2200 F). The elevated temperature properties of the alloys are compared in the bar graph of Figure 35.

The microstructure of the Nb-W-V and Nb-V-Mo alloys were clean single phase. Figure 36 shows a microstructure representative of all these alloys. Additions of zirconium to Nb-W-V and Nb-Mo-V alloys resulted in the formation of a finely dispersed second phase. This phase has not been identified as yet.

Properties of Interstitial Containing Alloys

The results of mechanical property tests carried out earlier in this program[24] indicated that oxygen additions may have a significant effect on the high temperature properties of certain niobium base alloys. The initial work was done with Nb-Zr, Nb-Hf, and Nb-Ti-Zr-Hf alloys which had been contaminated with oxygen during melting. The elevated temperature strength of these alloys appeared to be much higher than could be attributed to solid strengthening alone. In the current program, attempts were made to duplicate the mechanical properties of the high oxygen alloys and to gain some insight as to the actual strengthening mechanism. The effect of carbon additions on the properties of several alloys was also investigated.

Fabrication. The results of rolling interstitial containing alloys are listed in Table 16. Several alloys which contained no intentional oxygen or carbon additions are included for comparative purposes. High oxygen levels were obtained either by using high oxygen niobium powder as the base material (Lot KM-2, Table 9), or by adding NbO to the melting charge. Carbon was added as Nb_2C. As shown in Table 16, oxygen and carbon additions did not materially reduce the workability of Nb-Hf, Nb-Zr, and Nb-Ti-Zr-Hf alloys. The hot rolling characteristics of all the alloys were generally very good.

Mechanical Property Data. Tensile data for several of the initial high oxygen alloys (NC-29 and NC-32) are listed in Table 17. Contamination during melting increased the oxygen level of these alloys to over 0.14 w/o. Comparative data on low oxygen alloys of the same compositions (Nb-5Hf and Nb-1Ti-1Zr-5Hf, NC-184 and NC-183 respectively) are also given in Table 17. All of the alloys listed in this table were tested in the fully recrystallized condition. These data show that the high oxygen alloys have much higher tensile strengths at 1095 C (2000 F) than the low oxygen samples. The high strength of the oxygen containing alloys strongly

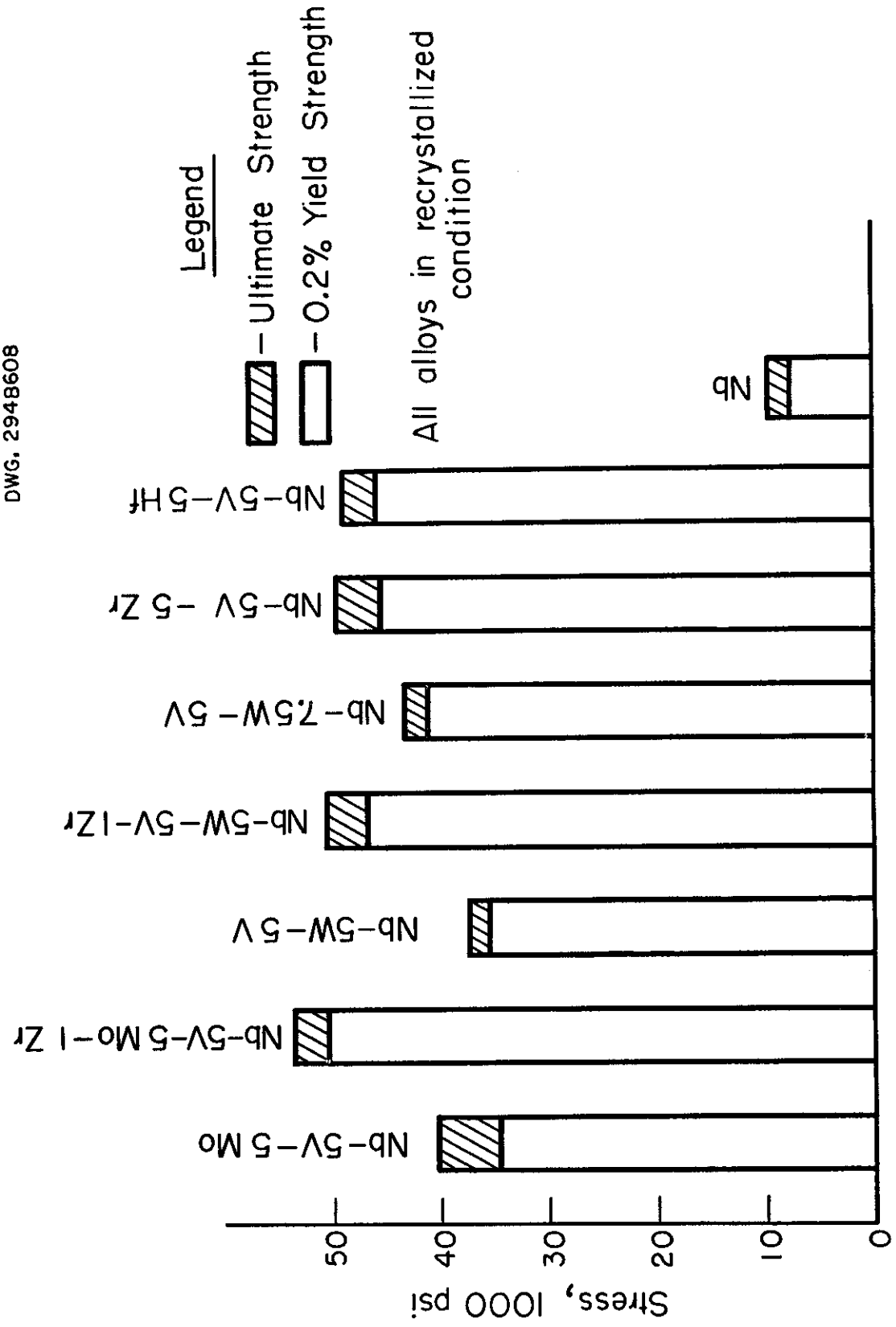

Fig. 35—Effect of ternary and quaternary alloy additions on the 1095 C (2000 F) tensile strength of niobium.

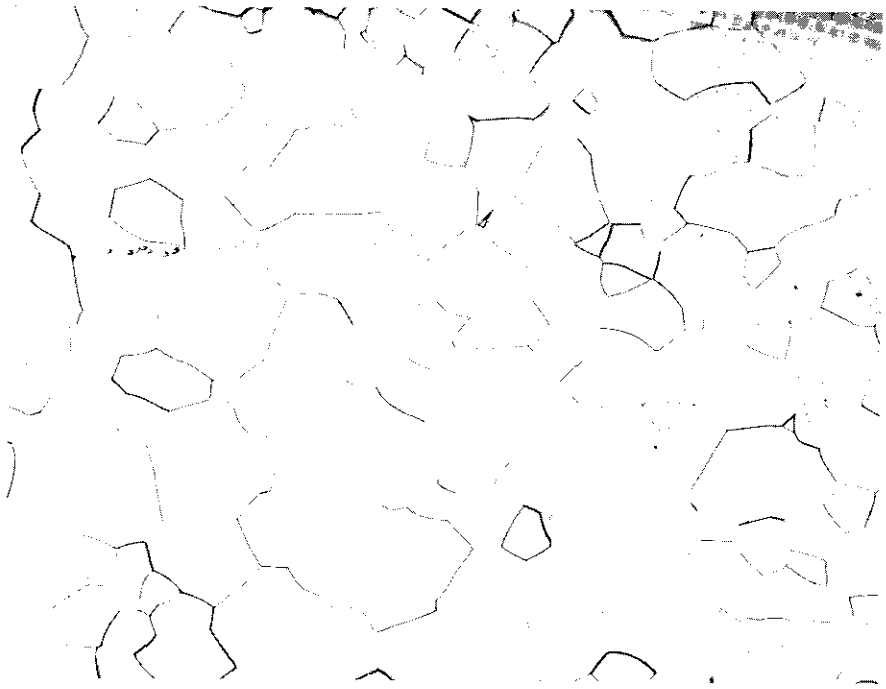

Fig. 36—Microstructure of Nb-5V-5 Mo alloy (NC-155) Annealed 1 hour at 1600 C prior to testing at 1095 C. 100X

Table 16. Results of Working Interstitial Containing Alloys

Heat No.	Nominal Composition (w/o)	As-Cast Hardness (VPN)	Results of Hot Rolling[(a)]
NC-184	Nb-5 Hf	143	G
NC-182	Nb-5 Hf-0.15 O_2	153	G
NC-250	Nb-5 Hf-0.08 O_2	173	F
NC-284	Nb-5 Zr-0.08 O_2	167	G
NC-183	Nb-1 Ti-1 Zr-5 Hf	165	G
NC-185	Nb-1 Ti-1 Zr-5 Hf-0.15 O_2	152	G
NC-230	Nb-5 Hf-0.1 C	154	F
NC-231	Nb-5 Hf-0.2 C	151	G
NC-229	Nb-5 Zr-0.1 C	179	G
NC-239	Nb-5 V-0.1 C	270	F

(a) Workability Results: E - no cracks; G - minor surface cracks; F - small cracks, essentially sound; P - large cracks; NG - cracked up after small reduction. (Rolled at 1200-1250 C)

TABLE 17. TENSILE PROPERTIES OF INTERSTITIAL CONTAINING NIOBIUM ALLOYS

Specimen No.	Nominal Composition (w/o)	Analysis (w/o)	Test Temperature C	Test Temperature F	0.2% Yield Strength (psi)	Ultimate Strength (psi)	Elongation (%) Uniform	Elongation (%) Total	Reduction in Area (%)	Remarks
NC-184-1	Nb-5 Hf	0.040 C	RT	RT	33,100	50,500	17.1	25.2	58.4	No intentional
NC-184-2	Nb-5 Hf	<0.04 O_2	1095	2000	18,400	25,500	4.9	14.4	57.8	O_2 addition
NC-29-1	Nb-5 Hf+O_2	4.84 Hf 0.193 O_2	RT	RT	52,500	69,500	17.2	30.2	62.4	Contaminated
NC-29-2	Nb-5 Hf+O_2	0.023 N_2	1095	2000	46,500	46,540	0.2	11.2	53.0	During Melting
NC-182-1	Nb-5 Hf+0.15 O_2	0.179 O_2	RT	RT	27,700	42,100	16.0	25.7	64.8	Oxygen added
NC-182-2	Nb-5 Hf-0.15 O_2		1095	2000	20,000	34,750	2.2	20.3	60.5	as NbO
NC-182-3	Nb-5 Hf-0.15 O_2		1205	2200	22,000	25,000	2.2	25.1	100	
NC-250-1	Nb-5 Hf-0.08 O_2	0.067 O_2	RT	RT	48,200	63,550	18.5	24.3	46.0	High Oxygen
NC-250-3	Nb-5 Hf-0.08 O_2	0.028 C	1095	2000	47,300	49,200	0.7	6.2	10.4	Base Material
NC-250-4	Nb-5 Hf-0.08 O_2		1205	2200	35,500	36,000	0.3	9.2	64.2	
NC-183-1	Nb-1 Ti-1 Zr-5 Hf	0.038 C	RT	RT	41,000	57,700	16.0	25.7	64.8	No intentional
NC-183-2	Nb-1 Ti-1 Zr-5 Hf	<0.04 O_2	1095	2000	26,600	30,300	2.2	20.3	60.5	O_2 addition
NC-32-1	Nb-1 Ti-1 Zr-5 Hf+O_2	0.149 O_2	RT	RT	53,750	76,800	18.7	26.4	41.5	Contaminated
NC-32-2	Nb-1 Ti-1 Zr-5 Hf+O_2		1095	2000	46,500	49,320	1.1	25.2	59.0	During Melting
NC-185-2	Nb-1 Ti-1 Zr-5 Hf-0.15 O_2	0.171 O_2	1095	2000	26,300	33,100	3.9	15.0	49.5	Oxygen added as NbO
NC-284-1	Nb-5 Zr-0.08 O_2		RT	RT	47,750	64,150	21.7	31.6	57.6	High oxygen
NC-284-3	Nb-5 Zr-0.08 O_2		1095	2000	31,200	36,800	1.9	19.8	41.2	Base Material
NC-284-4	Nb-5 Zr-0.08 O_2		1205	2200	23,000	27,800	3.8	42.0	62.3	
NC-230-1	Nb-5 Hf-0.1 C		RT	RT	31,300	53,900	20.7	24.7	40.0	Carbon added as
NC-230-3	Nb-5 Hf-0.1 C		1095	2000	26,000	35,220	1.2	16.7	32.5	Nb_2C
NC-231-1	Nb-5 Hf-0.2 C		RT	RT	38,300	57,200	13.3	18.5	64.6	Carbon added as Nb_2C
NC-229-1	Nb-5 Zr-0.1 C		RT	RT	41,150	61,200	16.9	23.8	55.5	Carbon added as Nb_2C
NC-239-1	Nb-5 V-0.1 C		RT	RT	83,350	100,000*	0	1.0	1.6	Carbon added as
NC-239-2	Nb-5 V-0.1 C		1095	2000	33,300	33,600	0.1	25.4	61.9	Nb_2C
NC-26-1	Nb-5 V	4.86 V	RT	RT	74,400	86,150	16.3	27.3	72.3	No intentional
NC-26-2	Nb-5 V	0.038 O_2	1095	2000	33,500	36,900	0.8	37.4	----	carbon addition

* True stress at fracture.

suggests that the oxygen reacts with alloy addition (s) to form a dispersed phase or phases which are effective in increasing the elevated temperature strength. Attempts were made to duplicate the mechanical properties of the initial series of alloys which had been contaminated with oxygen during melting. The following alloys were prepared and tested:

NC-182	Nb-5Hf-0.15 O_2
NC-185	Nb-1Ti-1Zr-5Hf-0.15 O_2

Oxygen was added to the melting charge as NbO. As shown in Table 17, the elevated temperature tensile strength of these alloys (NC-182 and NC-185) was somewhat higher than that of the samples without intentional oxygen additions. However, the strengths were still below those of the initial series of high oxygen alloys. Subsequently Nb-5Hf and Nb-5Zr alloys were melted using relatively high oxygen niobium powder as the base material (Lot KM-2, Table 9). As shown in Table 17, the Nb-5Hf alloy (NC-250) had properties almost identical with those of the initial high oxygen sample (NC-29), even though the oxygen content was only 0.067 w/o. These results suggest that having the oxygen already in solution in the base metal resulted in a more favorable distribution of the dispersed phase than when oxygen was added as NbO. The Nb-5Zr alloy (NC-284) had properties considerably below those of the Nb-5Hf alloy, although the strength was higher than would be expected merely from solid solution strengthening alone.

Phase Identification Studies. Phase separation and identification work was initiated in an attempt to provide information on the strengthening mechanism operative in the high oxygen alloys. Residues were extracted from several of the alloys. The procedure used was as follows: The sample was first prepared by grinding and polishing all areas that were in contact with the leaching solution. This was done to prevent an uneven attack which might have resulted in flaking of metal from the surface of the sample. The polished specimen was cleaned in benzene and thorough rinsed in methanol.

The solution used for the separation of the residues was prepared by adding 10 ml of liquid bromine and 10 grams of tartaric acid to 90 ml of methanol in a 250 ml beaker.[28] The polished specimen was suspended in the liquid by means of a platinum wire. The container was then covered with a polyethylene sheet and the specimen allowed to remain in the liquid until a sufficient amount of the residue was obtained for X-ray analysis. This usually required a period of 24 hours. The specimen was then removed and lightly rinsed with methanol. The residues were separated from the methanol-bromine solution by centrifuging and decanting. After the particles had been removed from the solution, they were

washed with methanol until the decanted liquid was clear. The residues were dried at 100 C for a half hour and then transferred to a container.

The separated residues were submitted for X-ray identification. The results obtained are summarized in Table 18. X-ray analysis showed that HfO_2

Table 18. X-ray Identification of Phases Extracted from Niobium Base Alloys

Sample No.	Composition (w/o)	Phases Present
NC-257	Nb-0.06 O_2	Nb_2C + small amount of NbC
NC-29	Nb-5Hf-0.193 O_2	HfO_2 + small amount NbC
L-311	Nb-5Hf (low oxygen)	Nb + HfC
NC-10	Nb-1Ti-1Zr-1Hf-0.059 O_2	HfO_2 and/or ZrO_2
NC-250	Nb-5Hf-0.067 O_2	HfO_2

was present in the Nb-5Hf-0.193 O_2 alloy (NC-29). To determine if the oxide was being formed as a result of the extraction process, residues were obtained from a vacuum levitation melted Nb-5Hf alloy (L-311), which had a very low oxygen content. As shown in Table 18, analysis of residues extracted from this sample did not show the presence of any oxide, indicating that the extraction process did not result in the formation of any extraneous phases.

Analysis of alloy NC-250 (Nb-5Hf-0.067 O_2) also showed the presence of HfO_2. Data for alloy NC-32, containing Nb-1Ti-1Zr-5Hf-0.149 O_2), is not available. However, results on alloy NC-10, Nb-1Ti-1Zr-1Hf-0.059 O_2, showed the presence of HfO_2 and/or ZrO_2. These results strongly suggest that the dispersion of HfO_2 and possibly ZrO_2 in niobium alloys significantly improves high temperature strength.

At the present time the role of interstitial elements in elevated temperature strengthening of niobium base alloys has not been fully determined.

It is obvious from the data of Table 17 that oxygen level, per se, is not the controlling factor in achieving greatly improved high temperature strength, since almost identical properties were obtained in Nb-5Hf alloys with oxygen levels of 0.067 and 0.193 w/o. The carbon and nitrogen contents of the base materials used for all the oxygen containing alloys were quite comparable. At present, electron micrographs are being obtained to determine the nature and distribution of the phases present in these alloys. However, this work has not reached a point where unambiguous conclusions can be drawn.

Carbon Containing Alloys. Preliminary mechanical property data for alloys with intentional carbon additions are given in Table 17. The addition of 0.1 w/o carbon increased the 1095 C yield strength of a Nb-5 Hf alloy from 18,400 psi to 26,000 psi, without decreasing low temperature ductility. Elevated temperature testing of other Nb-Hf-C and Nb-Zr-C alloy is in progress. As shown in Table 17, the addition of 0.1 w/o carbon to a Nb-5V alloy did not increase high temperature strength, but drastically reduced room temperature ductility. It should be noted that the alloys with intentional carbon additions were processed in the normal manner, i.e., hot rolled at 1200-1300 C, and annealed 1 hour at 1600 C prior to testing. The effect of varying heat treatment on the high temperature properties of carbon containing alloys is being investigated.

Consumable Electrode Arc Melted Alloys

In order to provide sufficient material for more extensive evaluation of promising compositions, a number of niobium alloy ingots were prepared by the consumable electrode arc melting process, using the procedures outlined previously in this report. Ingot breakdown was accomplished by high energy rate extrusion (Dynapak). The acquisition of a Dynapak unit by the Westinghouse Blairsville Plant provided a good opportunity to evaluate the potential of this process for primary working of high strength refractory metal ingots. The extrusion work described in this report was carried out on Westinghouse funds to supplement the contract effort.

High Energy Rate Extrusion. Dynapak, manufactured by Convair Division, General Dynamics Corporation, is a device capable of producing high energies, 28,000 to 430,000 foot-pounds, within short distances, 12 to 24 inches. High energies are generated in extremely short times, on the order of 5 to 10 milliseconds. One of the attractive features of this device is that it does not require a massive foundation, since all the energy it generates is dissipated within the device itself. Its relatively small size makes it ideal for laboratory or pilot plant installation.

Description of Equipment. The Dynapak derives its power from the controlled adiabatic expansion of a gas at high pressure. The heart of the Dynapak is the triggering device which allows a given volume of gas at high pressure to act on the driving piston almost instantaneously. A clear picture of the operation of the Dynapak can be obtained by following a complete operational cycle using the simplified schematic diagram shown in Figure 37.

The Dynapak is mounted on recoil devices (12) in such a manner that the active part of the machine is allowed to operate as a free body. When the Dynapak is used as an extrusion press the piston and column assembly (4) are forced to the rear of the back-up or low pressure chamber (1) by gas at low pressure usually 100 psi for the model 1200. The working gas at pressures up to 2000 psi is introduced into the high pressure chamber (2) and is separated from the piston by the firing mechanism (3). The amount of energy made available for the extrusion process is directly proportional to the gas pressure in the high pressure chamber (2). Activation of the firing mechanism (3) allows the high pressure gas to pass through the orifice plate and act on the whole surface of the piston (4) creating a large unbalanced force which drives the piston (4), weights (5), and ram (6) forward. Since the machine is essentially a free body a reaction force equal to the force driving the piston acts on the cushion piston (14) and causes it to move rearward along with the back bolster plate (13), tie rods (11), front bolster plate (10) and die assembly (8, 9). This reaction mass (8,9, 10, 11, 12, 13, 14) is much larger than the mass of the weighted ram assembly (4,5, 6) and therefore moves at a proportionally lower velocity. As the piston moves forward the driving pressure begins to decrease adiabatically while the back-up pressure in the low pressure chamber (1) increases also adiabatically. The net pressure difference across the piston continues to drive the ram forward while the reaction force continues to drive the reaction mass rearward. After traveling several inches the ram attains a high velocity relative to the die assembly. In the extrusion operation a billet (7) in the die container (8) receives the full impact of the ram and if all conditions are favorable the billet extrudes through the die (9). Hydraulic fluid pumped into the low pressure chamber returns the piston to its original position.

From the description of the apparatus given above, it is apparent that the initial pressure must be selected carefully before the extrusion process proceeds. There is no opportunity to adjust pressure once the Dynapak has been fired. If, for a given set of conditions, the initial pressure is too low, the billet will not extrude completely. If the pressure is too high, the billet will extrude completely and leave the die at a high velocity. With a high exit velocity it is very difficult to decelerate the extrusion without damage.

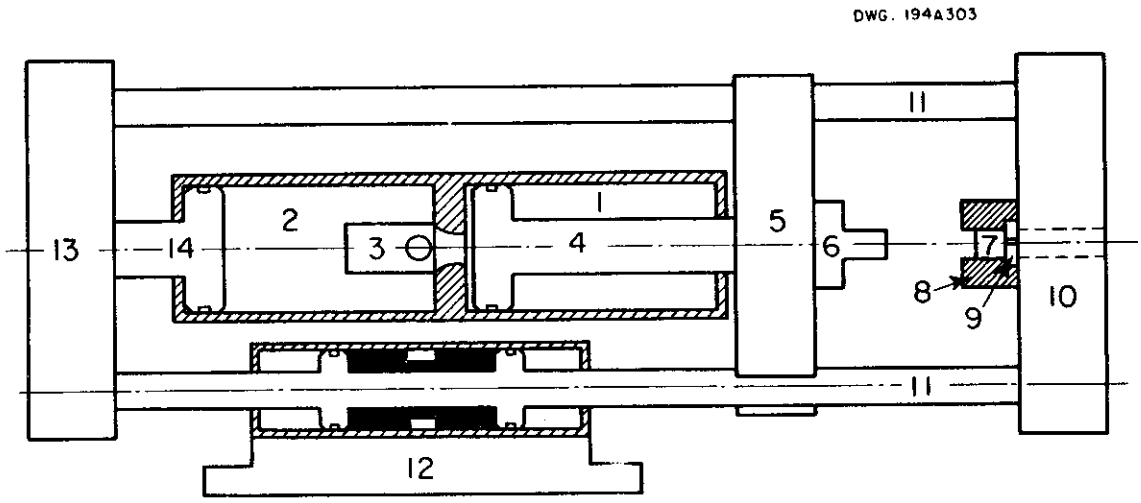

1 Back-up Chamber
2 High Pressure Chamber
3 Firing Mechanism
4 Piston & Column
5 Weights
6 Ram
7 Billet
8 Billet Container
9 Extrusion Die
10 Front Bolster Plate
11 Tie Rods
12 Recoil Mechanism
13 Rear Bolster Plate
14 Cushion Piston

Fig. 37–Schematic diagram of Dynapak

At the present time, the proper extrusion conditions must be selected empirically, since all the variables which enter into the process cannot be evaluated. With a given material the variables include: initial pressure, extrusion ratio, die geometry, die lubricant, billet length, stroke length, and ram weights. Weights may be added to the Dynapak ram to increase momentum, with a corresponding decrease in ram velocity. In the current study stroke length, ram weights and extrusion temperature were kept constant. Extrusion ratio varied slightly (4:1 to 6:1). Billet length depended upon the yield of useful material from the as-melted ingot. The billet lengths ranged from about 2.5 to 3.5 inches. The major variables which were investigated in the evaluation program were initial (firing) pressure, die geometry, and die lubricant.

Experimental Procedure. Ingots for extrusion were melted into 1-7/8 inch diameter water cooled copper crucibles. After cropping top and bottom, the ingots were machined to 1.75 inch diameter. The machined ingots (billets) were heated prior to extrusion in an induction furnace located adjacent to the Dynapak. A flowing argon atmosphere was maintained within the furnace enclosure to minimize contamination during the heating cycle. A photograph of the induction coil and coil enclosure is shown in Figure 38. The billets were supported vertically within the furnace an alumina pedestal. A niobium or tantalum sheet was placed on top of the pedestal to prevent interaction of the billet with the alumina.

Billet temperatures were measured with an optical pyrometer which was sighted through an observation port in the top of the furnace enclosure. Extrusion temperature was maintained at 1600 C. When the billet reached temperature, the coil enclosure was removed and the billet was removed from the coil and placed in the container. Transfer time was generally less than 5 seconds. The Dynapak was fired immediately after the billet was placed in the container. The billet was extruded through the die and caught in a receiving tube packed with expanded mica.

Extrusion Results. The results of Dynapak extruding niobium alloy billets are summarized in Table 19. Initial extrusion attempts were made using a simple circular shear die, which was essentially a flat disc with a hole bored through the center. The shear die was recommended by the Dynapak manufacturer. No lubricant was used in the first experiments. As shown in Figure 39, the first two extrusions (VAM-21 and 22) did not extrude completely through the die, although the section of VAM-22 which did extrude was sound. Billet VAM-21 suffered a shear failure on exit from the die.

The next group of billets were extruded using a die with a 120^{O} entrance angle. The various die configurations used are shown in Figure 40. Again the

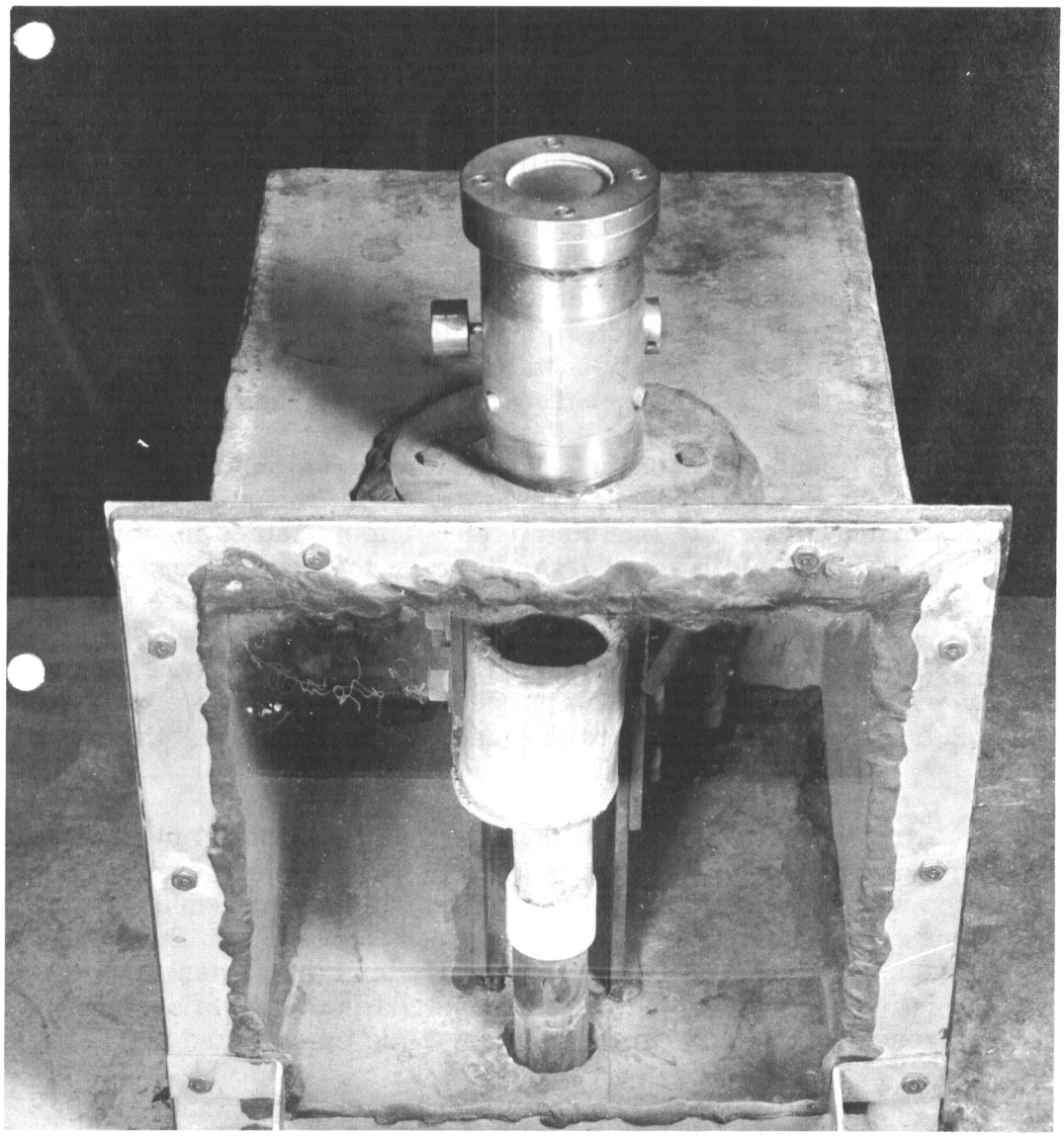

Fig. 38 – Induction furnace for Dynapak extrusion billets.

TABLE 19. DYNAPAK EXTRUSION DATA FOR NIOBIUM ALLOYS*

Heat No.	Nominal Composition (w/o)	Billet Length (Inches)	Extrusion Ratio	Firing Pressure (psi)	Die** Type	Lubricant	Remarks
VAM-24	Nb	2.80	6:1	1750	SI	Aquadag	Extruded completely. Hit end of receiving tube and deformed seriously.
VAM-21	Nb-10Mo-10 Hf	2.50	5.5:1	1500	S	None	Incomplete Extrusion. Extrusion parted
VAM-22	Nb-5V-5Mo-1 Zr	3.18	5.5:1	1950	S	None	Incomplete Extrusion
VAM-23	Nb-20 Zr	2.94	5:1	1750	S1	None	Incipient Melting. Billet did not extrude
VAM-25	Nb-5V-5Mo	3.12	5:1	1500	S1	None	Incomplete Extrusion
VAM-26	Nb-5V-5Mo-1 Zr	3.22	6:1	1700	S1	Aquadag	Incomplete Extrusion
VAM-29	Nb-10W-5V-1 Zr	2.81	4:1	1850	S2	Glass Wool on Die Glass Power on Container	Extruded Completely
VAM-31	Nb-4 V	2.69	4:1	1700	S2	Same as VAM-29	Extruded Completely
VAM-32	Nb-8 V	3.40	4:1	1600	S2	Same as VAM-29	Extruded Completely
VAM-34	Nb-5Zr-0.1 C	2.80	4:1	1750	S2	Same as VAM-29	Extruded Completely
VAM-28	Nb-10W-7.5Hf-0.1 C	3.38	4:1	1850	SBD	Glass Wool on Die Achesion FH 420 on Container	Extruded Completely
VAM-30	Nb-4 V	3.25	4:1	1800	SBD	Same as VAM-28	Extruded Completely
VAM-36	Nb-10W-7.5Hf-0.1 C	2.75	4:1	1800	SBD	Same as VAM-28	Extruded Completely
VAM-37	Nb-7.5W-3V-0.075 C	2.75	4:1	1800	SBD	Same as VAM-28	Extruded Completely

* All billets extruded at 1600 C except VAM-23, which was in excess of 1800 C

**See Figure 40 for die configurations

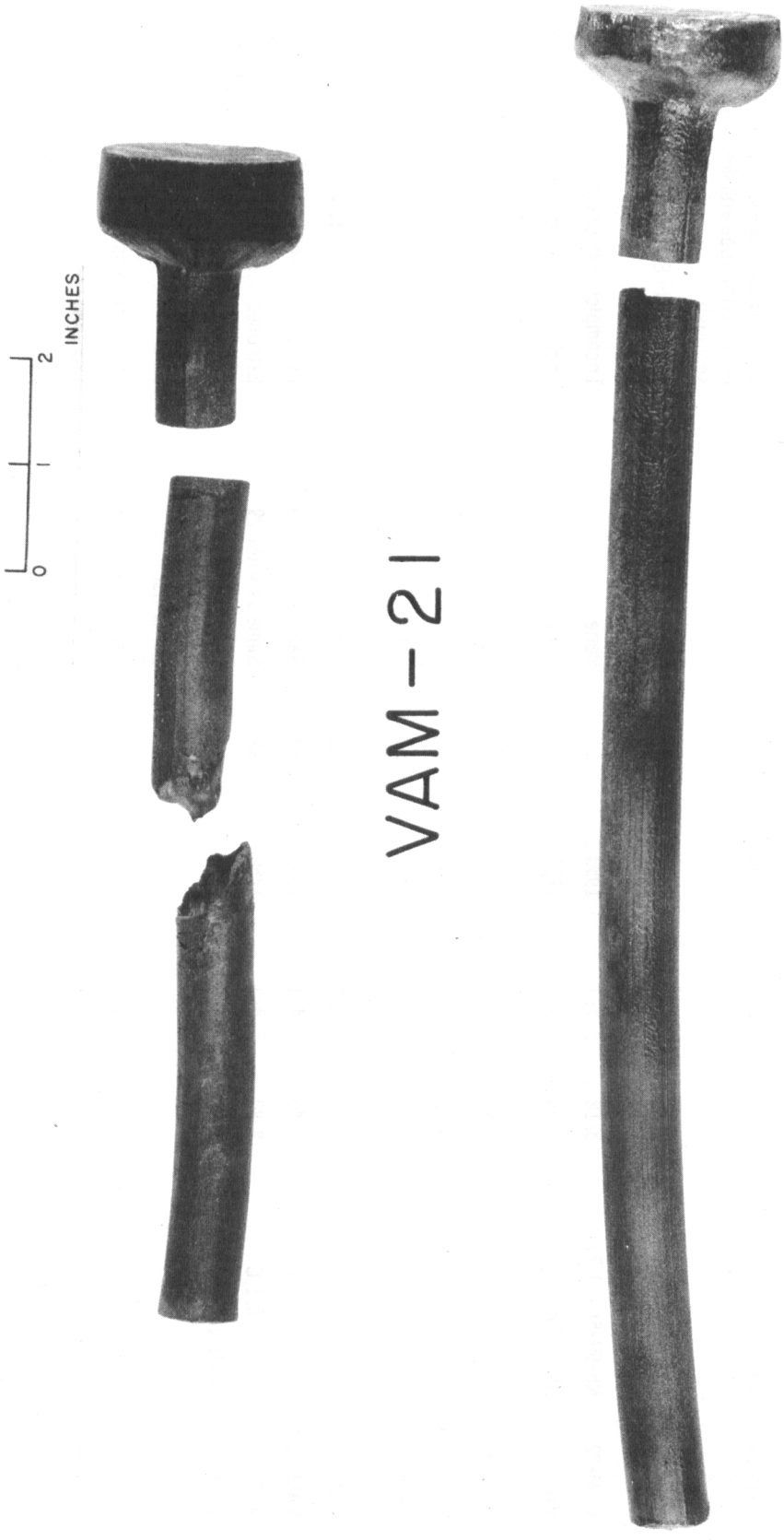

Fig. 39— Results of Dynapak extruding niobium alloys.

DWG. 2948609

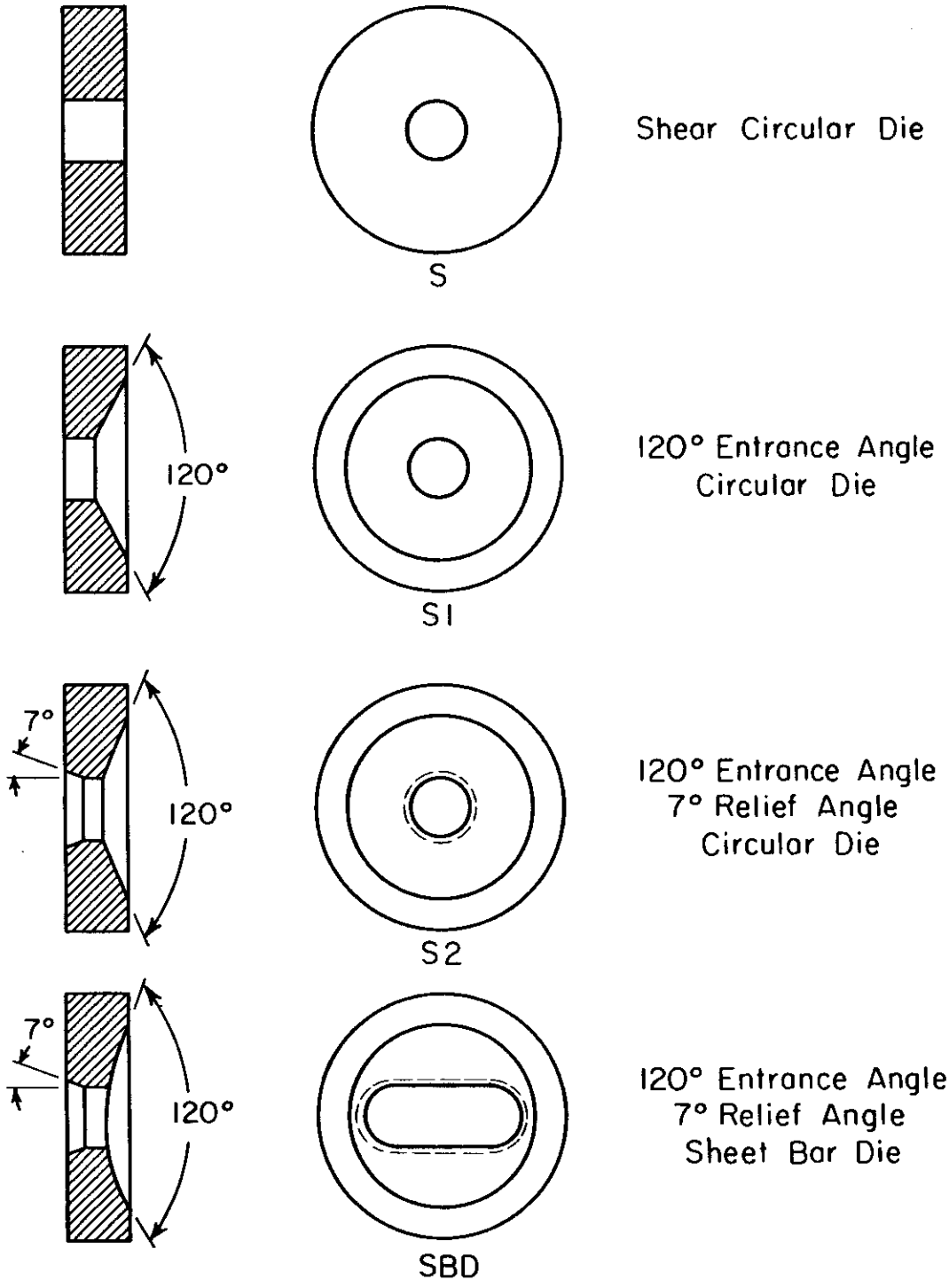

Fig.40—Configuration of dynapak extrusion dies

billets did not extrude completely through the die, with the exception of the pure niobium billet, VAM-24. This specimen passed through the die and struck the end of the receiving tube, deforming severely in the process. The third group of billets (VAM-29, 31, 32, and 34) were extruded using a die with a 120^{o} entrance angle and 7^{o} relief, as shown in Figure 40. These billets were coated with a glass slurry prior to heating. A glass wool pad was placed on the die face, and the container was also coated with a glass slurry. All of these billets extruded successfully, as shown in Figure 41. The final group of billets (VAM-28, 30, 36, and 37) were extruded to sheet bar. Glass was also used in this case. The sheet bar extrusions were quite satisfactory, as shown in Figure 42.

The results of Dynapak extrusion were very encouraging. Useful material was obtained from all of the billets with the exception of VAM-23, which was inadverently overheated and melted during extrusion.

The adoption of a die with a 120^{o} entrance angle and 7^{o} relief, plus the use of a glass lubricant provided very satisfactory results. The yield of useful material was quite high. Only very minor nose bursts were encountered. The extrusion pipe at the tail of the extrusion was generally very short. No serious die problems were encountered. The die and ram material was Latrobe VDC tool steels, hardened to 42-46 R_c. If a complete extrusion was obtained initially, a die could usually be used at least twice without excessive die wash.

Secondary Working. All of the extrusions with the exception of the sheet bar samples were forged to approximately 1/2 inch diameter rod. The as-extruded material was ground to remove the contaminated surface layer, and then forged in swage dies at 1200 C. Initially, the samples were heated in a retort inserted in a gas fired furnace and forged in air. Argon was passed through the retort during the heating cycle to minimize contamination. The alloys processed in this manner (VAM-21, 22, 25, and 26) forged fairly well. However, oxygen contamination occurred when the samples were exposed to air, leading to excessive surface cracks. Subsequently, the remaining extrusions were coated with window glass to minimize contamination during forging. This procedure gave very good results. The sheet bar extrusions are currently being surface ground prior to rolling to sheet.

Mechanical Property Data. Available mechanical property data for the consumable electrode melted alloys are listed in Table 20. Most of the samples were tested in the extruded, forged, and stress relieved condition. The specimens were stress relieved by annealing in vacuum for 1 hour at 1095 C (2000 F). Several

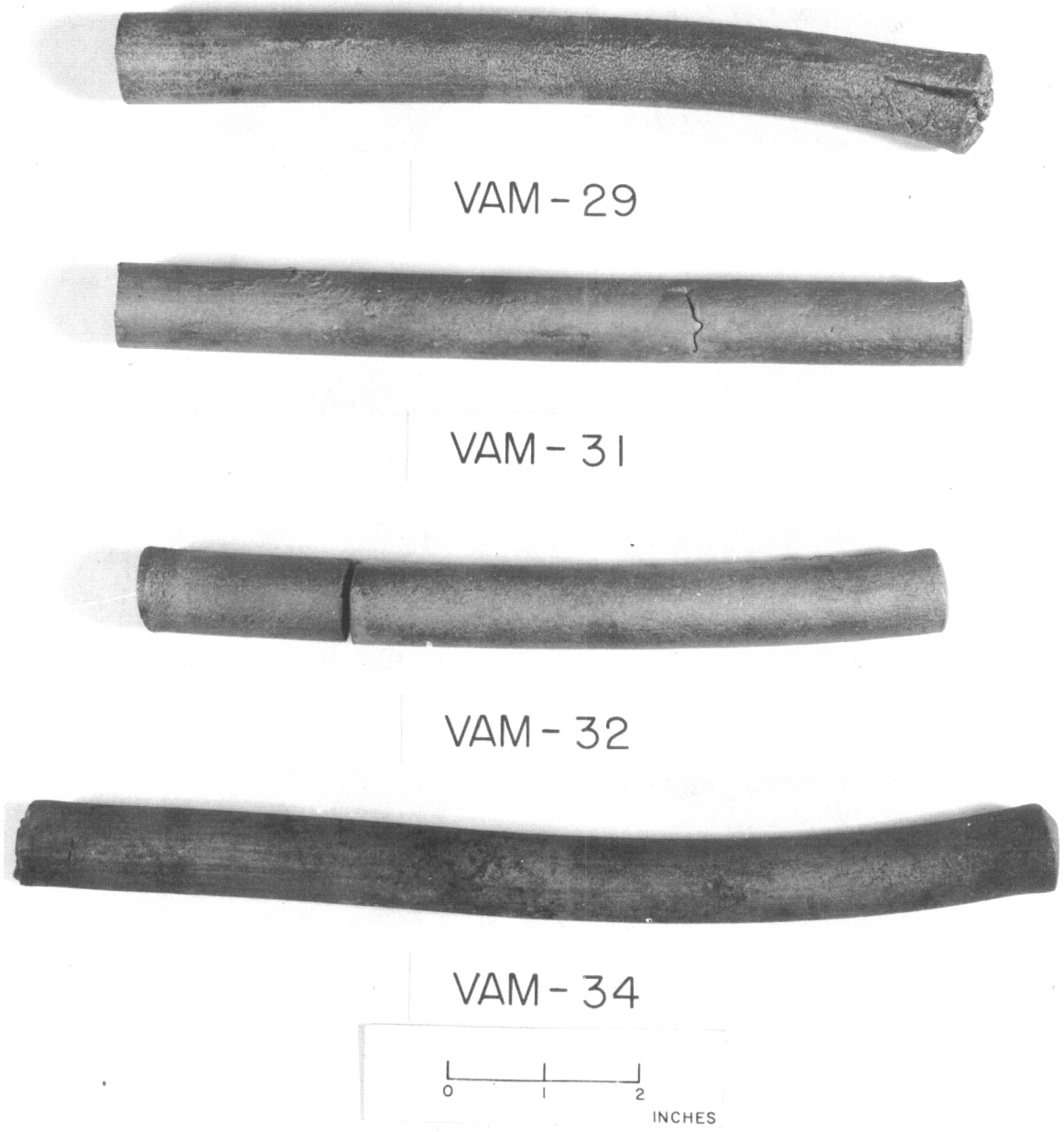

Fig. 41 — Results of Dynapak extruding niobium alloys.

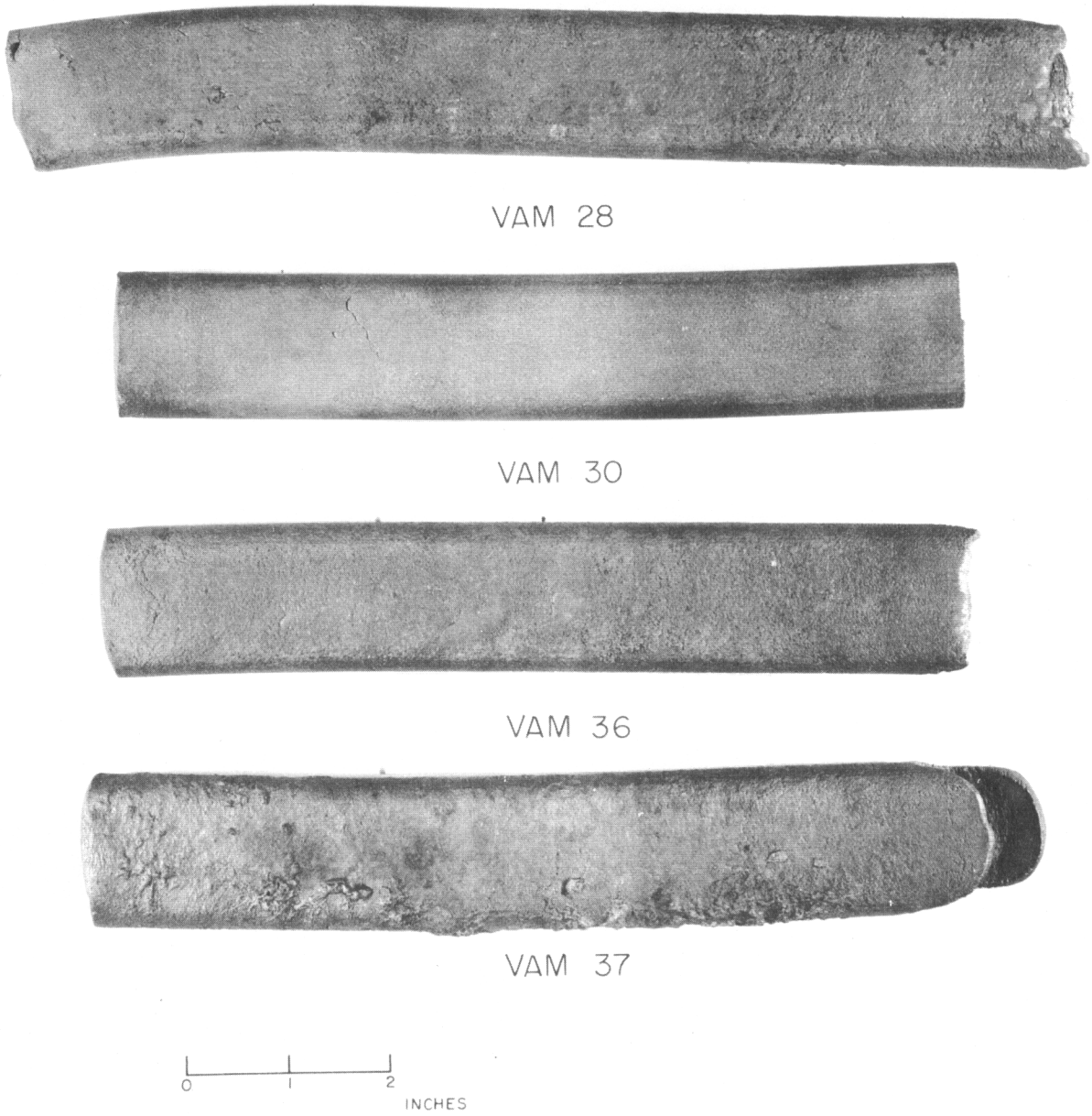

Fig. 42– Dynapak extruded niobium alloy sheet bars.

TABLE 20. TENSILE PROPERTIES OF CONSUMABLE ELECTRODE MELTED ALLOYS

Specimen No.	Nominal Composition (w/o)	Test Temperature C	Test Temperature F	0.2% Yield Strength (psi)	Ultimate Strength (psi)	Elongation (%) Uniform	Elongation (%) Total	Reduction in Area (%)	Condition
VAM-21A	Nb-10Mo-10 Hf	RT	RT	94,000	109,400	16.7	38.9	72.0	Extruded forged, and stress-relieved*
VAM-21	Nb-10Mo-10 Hf	1093	2000	40,000	52,700	3.9	19.5	64.9	Extruded and stress-relieved
VAM-22D	Nb-5V-5Mo-1 Zr	RT	RT	83,000	101,300	19.8	34.9	70.4	Extruded, forged, and stress-relieved
VAM-22B	Nb-5V-5Mo-1 Zr	1093	2000	42,400	47,400	3.0	41.8	51.1	Extruded and stress-relieved
VAM-22A	Nb-5V-5Mo-1 Zr	1205	2200	34,200	35,440	1.7	35.1	86.2	Extruded and stress-relieved
VAM-22D	Nb-5V-5Mo-1 Zr	1315	2400	18,400	20,000	1.9	62.2	94.4	Extruded, forged, and stress-relieved
VAM-26-7	Nb-5V-5Mo-1 Zr	RT	RT	87,600	111,400	19.2	31.4	65.6	Extruded, forged, and stress-relieved
VAM-26-8	Nb-5V-5Mo-1 Zr	RT	RT	77,250	113,400[(a)]	0	16.6	14.3	Extruded, forged, and recrystallized**
VAM-26-5	Nb-5V-5Mo-1 Zr	980	1800	65,400	70,000	2.3	36.7	60.3	Extruded, forged, and stress-relieved
VAM-26-2	Nb-5V-5Mo-1 Zr	1095	2000	45,800	53,400	1.5	37.5	77.0	Extruded, forged, and stress-relieved
VAM-26-1	Nb-5V-5Mo-1 Zr	1205	2200	37,800	41,740	1.6	35.2	78.2	Extruded, forged, and stress-relieved
VAM-26-3	Nb-5V-5Mo-1 Zr	1205	2200	39,200	40,500	0.7	3.8	9.9	Extruded, forged, and recrystallized
VAM-26-6	Nb-5V-5Mo-1 Zr	1315	2400	23,500	28,000	1.8	57.0	91.3	Extruded, forged, and stress-relieved
VAM-26-4	Nb-5V-5Mo-1 Zr	1315	2400	23,900	25,700	0.7	8.2	9.9	Extruded, forged and recrystallized

(a) True stress at fracture

* Stress relieved 1 hour at 1095 C

**Recrystallized - 1 hour at 1800 C

TABLE 20. TENSILE PROPERTIES OF CONSUMABLE ELECTRODE MELTED ALLOYS (Cont'd)

Specimen No.	Nominal Composition (w/o)	Test Temperature C	Test Temperature F	0.2% Yield Strength (psi)	Ultimate Strength (psi)	Elongation (%) Uniform	Elongation (%) Total	Reduction in Area (%)	Condition
VAM-25-3	Nb-5V-5 Mo	RT	RT	93,000	109,200	20.3	42.6	86.5	Extruded, forged, and stress-relieved
VAM-25-1	Nb-5V-5 Mo	1095	2000	36,200	40,080	1.7	56.3	93.3	Extruded, forged, and stress-relieved
VAM-25-2	Nb-5V-5 Mo	1205	2200	26,100	28,300	2.5	60.6	92.9	Extruded, forged, and stress-relieved
VAM-29-1	Nb-10W-5V-1 Zr	RT	RT	106,600	127,300	11.9	14.9	25.2	Extruded, forged, and stress-relieved
VAM-29-3	Nb-10W-5V-1 Zr	1095	2000	59,500	64,800	1.7	30.4	42.4	Extruded, forged, and stress-relieved
VAM-29-6	Nb-10W-5V-1 Zr	1205	2200	38,500	44,500	2.1	49.0	89.4	Extruded, forged, and stress-relieved
VAM-29-5	Nb-10W-5V-1 Zr	1315	2400	26,200	29,450	1.7	34.2	70.4	Extruded, forged, and stress-relieved
VAM-29-4	Nb-10W-5V-1 Zr	1370	2500	19,600	22,600	1.2	44.0	87.1	Extruded, forged, and stress-relieved

of the specimens were recrystallized by annealing for 1 hour at 1800 C prior to testing. Available chemical analysis data for the consumable electrode arc melted alloys are listed in Table 21.

Table 21. Chemical Analysis of Consumable Electrode Arc Melted Alloys

Heat No.	Nominal Composition (w/o)	Analysis (w/o) Mo	W	V	Zr	Hf	O	N	C
VAM-21	Nb-10Mo-10Hf	10.29	-	-	-	9.07	0.049	0.011	0.029
VAM-22	Nb-5V-5Mo-1Zr	6.07	-	4.27	0.88	-	0.060	0.013	0.039
VAM-26	Nb-5V-5Mo-1Zr	4.97	-	3.84	1.16	-	-	-	0.022
VAM-25	Nb-5V-5Mo	4.83	-	4.47	-	-	0.042	0.025	0.033
VAM-29	Nb-10W-5V-1Zr	-	7.07	6.09	0.97	-	0.060	-	0.033

The following designations have been applied to the alloys listed in Table 21.

B-11	Nb-10Mo-10Hf
B-55	Nb-5V-5Mo
B-66	Nb-5V-5Mo-1Zr
B-77	Nb-10W-5V-1Zr

These alloy designations will be used for the sake of simplicity in further discussion.

All of the alloy exhibited very satisfactory room temperature ductility when tested in the worked and stress relieved condition. Elevated temperature properties were also very attractive, particularly for alloys B-66 and B-77. These alloys have considerably greater strength than the commercial niobium-base alloys D-31 (Nb-10Mo-10Ti) and FS-82 (Nb-33Ta-0.75 Zr).[30] The short time elevated temperature tensile properties compare quite well with the high strength Nb alloys F-48 (Nb-15W-5Mo-1Zr) and Cb-74 (Nb-10W-5Zr).[30] On a strength-weight basis the properties of B-66 are even more attractive, since it has a

lower density than either F-48 or FS-82. (The calculated density of B-66 is 0.30 lbs/in^3)

As shown in Table 20, annealing alloy B-66 at 1800 C prior to testing lowered ductility at both low and high temperatures, without appreciably changing high temperature strength. The mode of fracture of the annealed tensile samples at elevated temperature was mixed shear and grain boundary. The room temperature failures were complete transgranular cleavage. As shown in Figure 43, the microstructure of alloy B-66 after annealing at 1800 C is single phase. However, after testing at 1205 C (2200 F) and 1315 C (2400 F), carbide precipitation was observed within the grains and at grain boundaries (Figure 44). Extensive carbide precipitation was not observed in alloys stress relieved for 1 hour at 1095 C (2000 F) prior to testing. These results suggest that the presence of grain boundary carbides is very detrimental to elevated temperature ductility.

The effect of temperature on the elevated temperature properties of the consumable electrode arc melted alloys are shown in Figure 45. The properties exhibited by alloys B-66 and B-77 are quite encouraging, particularly in view of their generally good working characteristics. Further work to more fully assess the potential of these alloys for high temperature structural use appears to be warranted.

Hot Hardness Data

Preliminary hot hardness data were obtained on pure niobium and several niobium base alloys. The hot hardness measurements were obtained in a unit constructed at the Westinghouse Research Laboratories. The samples were supported on a molybdenum anvil, located inside a molybdenum wound furnace. Hardness impressions were made with a sapphire pyramid indenter, mounted in a molybdenum extension shaft. All hardness impressions were made in vacuum at pressures below 5×10^{-5} mm of Hg.

Hardness data for recrystallized electron beam melted niobium in the range from room temperature to 1000 C (1832 F) are shown in Figure 46. The apparent hardness peak near 300 C is probably associated with strain aging. Hot hardness data for several alloys are listed in Table 21. In several instances, hot hardness and mechanical property data are available for the same alloy. The correlation between hot hardness and 0.2% yield strength at 1095 C (2000 F) is shown in Figure 47. As can be seen, the correlation is excellent. Additional hot hardness measurements on several alloys are in progress.

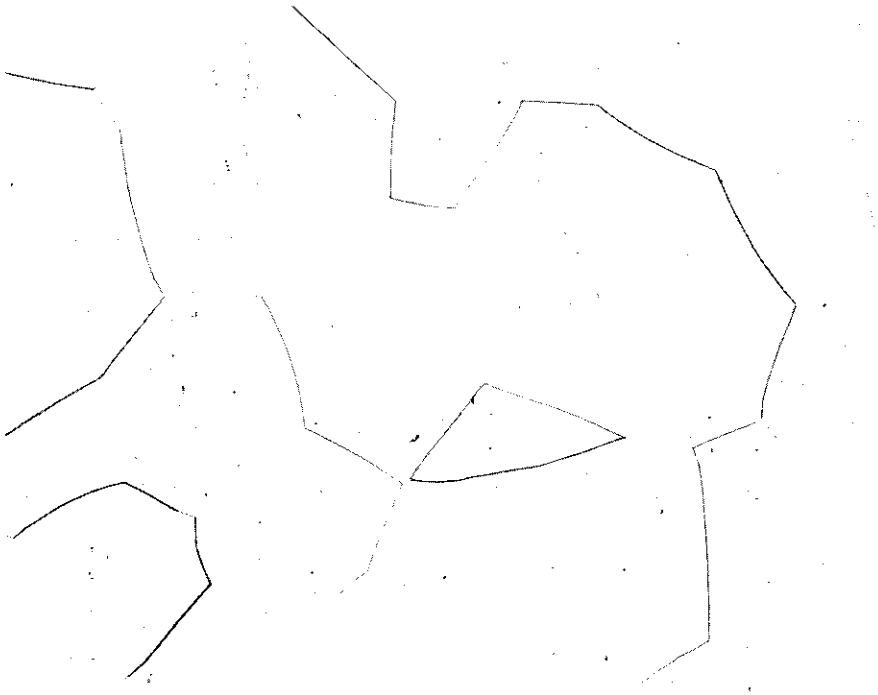

Fig. 43 – Microstructure of Nb–5V–5Mo–1Zr alloy (VAM-26) Annealed 1 hour at 1800 C 100X

Fig. 44 – Microstructure of Nb–5V–5Mo–1Zr alloy (VAM-26) Annealed 1 hour at 1800 C prior to testing at 1205 C 100X

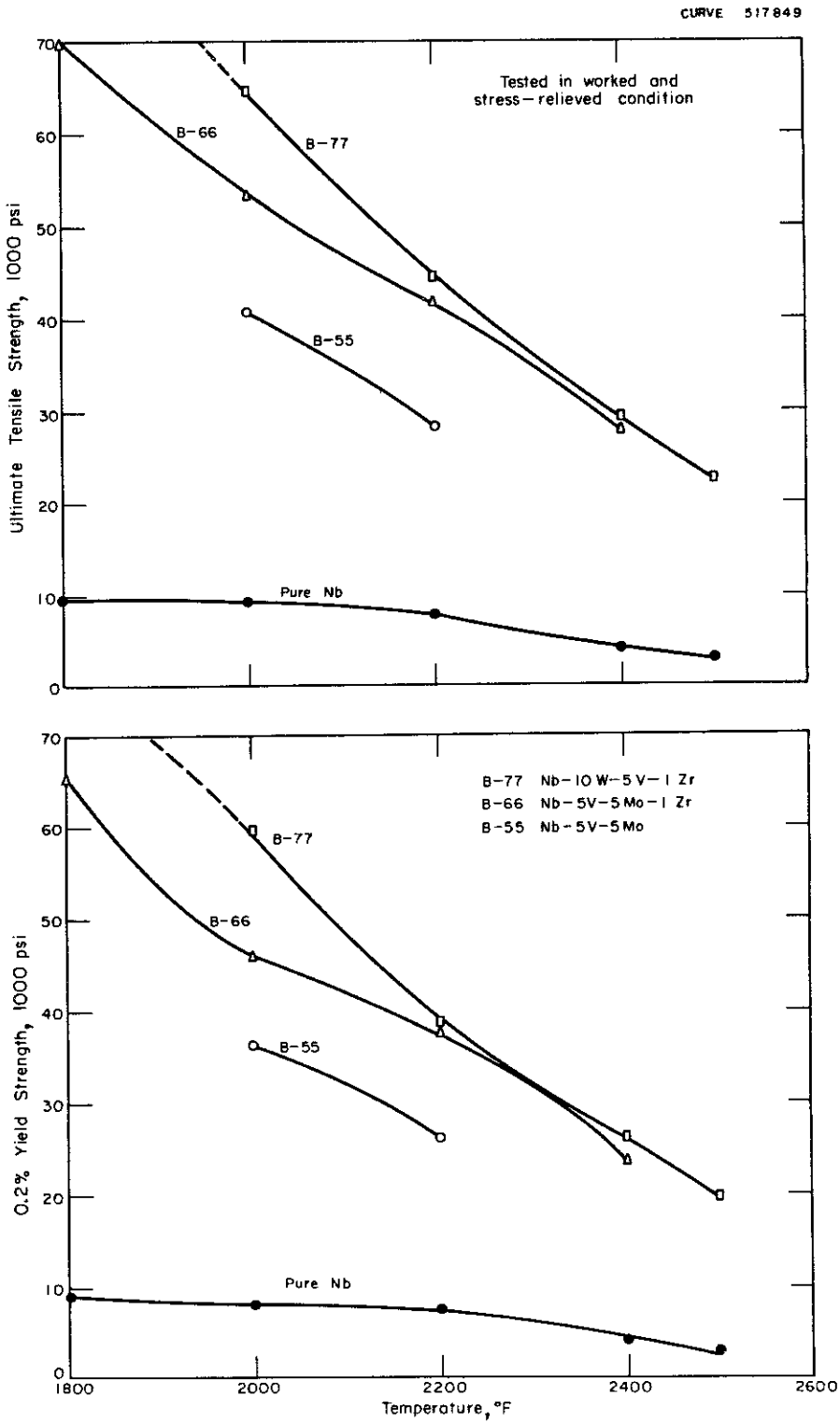

Fig. 45- Elevated temperature tensile properties of consumable electrode arc melted alloys.

Table 22. Hot Hardness Data

Specimen No.	Nominal Composition (w/o)	Condition[a]	Test Temperature (°C)	Test Temperature (°F)	Load (kg)	Hardness (VPN)
VAM-21	Nb-10Mo-10 Hf	As extruded	1000	1830	5	174
VAM-22	Nb-5V-5Mo-1 Zr	As extruded	1000	1830	5	144
VAM-26	Nb-5V-5Mo-1 Zr	As extruded	1095	2000	5	133
VAM-26	Nb-5V-5Mo-1 Zr	Extruded and stress relieved	1095	2000	5	134
NC-170 *	Nb-5V-5 Mo	Cast and Homogenized	980	1800	5	118
NC-170 *	Nb-5V-5 Mo	Cast and Homogenized	1095	2000	2.5	103
NC-171 *	Nb-10V-10 Mo	Cast and Homogenized	980	1800	5	172
NC-171 *	Nb-10V-10 Mo	Cast and Homogenized	1095	2000	2.5	159
NC-172 *	Nb-15V-15 Mo	Cast and Homogenized	1095	2000	2.5	185
NC-169 *	Nb-5V-5 Zr	Cast and Homogenized	980	1800	5	140
NC-169 *	Nb-5V-5 Zr	Cast and Homogenized	1095	2000	2.5	135

* 20 gram button

(a) Stress relieved 1 hr. at 1095 C, Homogenized 12 hours at 1800 C

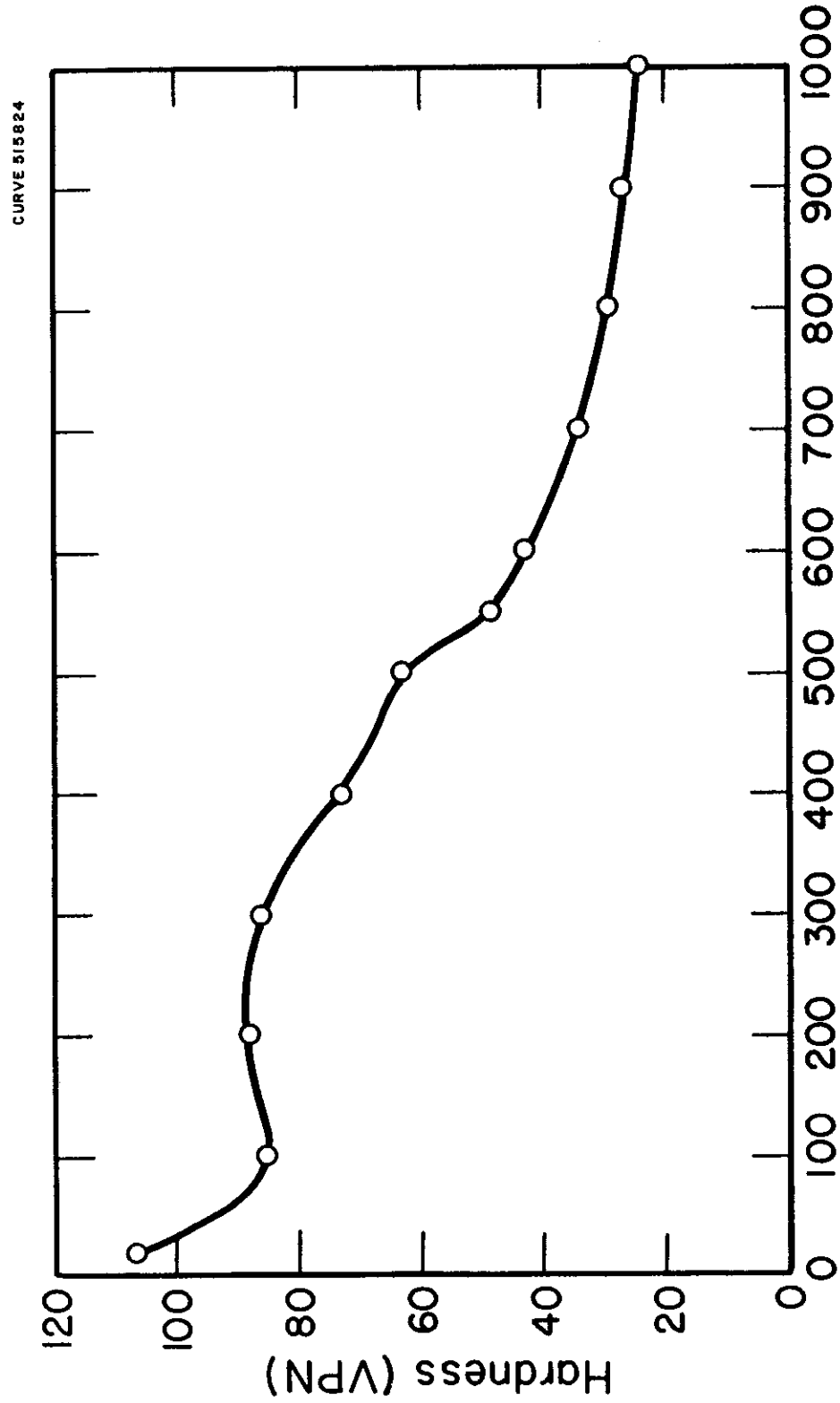

Fig.46-Elevated temperature hardness of niobium.

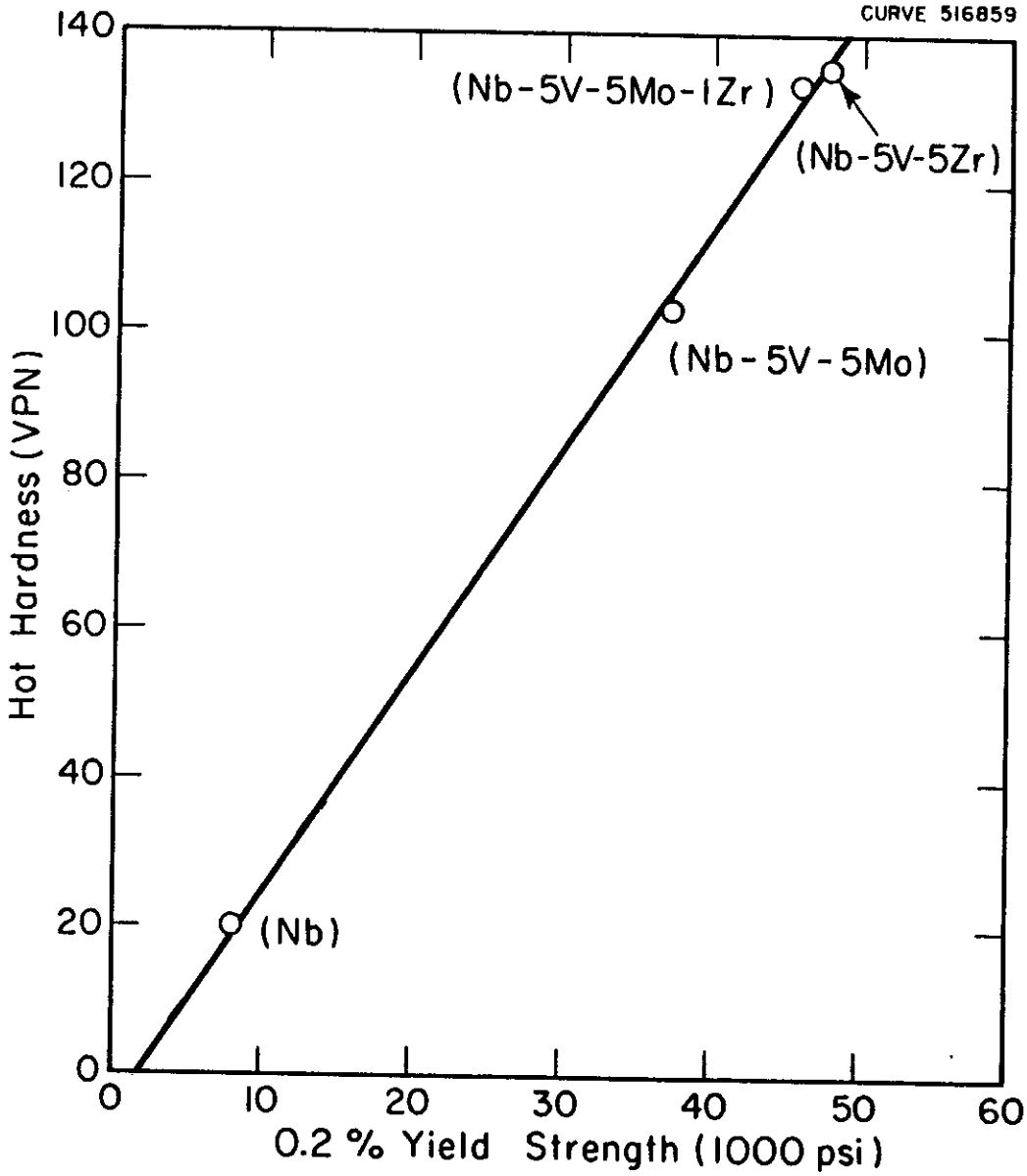

Fig.47 – Correlation of hot hardness and yield strength for niobium alloys at 1095C (2000F)

WELDING

Welding studies were carried out in conjunction with the alloy development program. During a preliminary study, a number of elements were selected as possible additions to niobium which would improve the mechanical properties without damaging those properties necessary for welding. The method of selecting these elements was discussed in earlier reports.[29, 25] The elements selected and the suggested range of compositions to be tried are shown in Table 23. The circled compositions are those which have been examined. The vertical lines indicate suggested composition limits.

Welding studies involved making bead-on-plate welds using a tungsten arc in a chamber which had been purged by evacuation and back filled with helium. Filler metal was not used. The welds were started and stopped on the plate. This technique develops relatively high stresses in and around the weld and provides a qualitative indication to the degree of hot cracking which will be encountered in the material. The strength of the weld metal was also examined using high-temperature tensile tests.

The effect of alloying elements on the ductile-to-brittle transition temperature was studied using a bend test. Bend specimens were cut transverse to the longitudinal axis of the weld and deflected with the top surface in maximum tension. The ductile-to-brittle transition is described as the amount of deflection and stress obtained at the outer fiber as a function of the test temperature. Welds were tested over the range -196 C to +300C.

The alloys studied in this portion of the investigation were an extension of those studied and reported earlier.[25, 29] The binary alloys of Nb with Ti, Hf, Zr, W, Mo, and V have been examined. In addition, several ternary alloys have been examined in the Nb-Mo-Hf and Nb-V-Mo systems. In all of these alloys, carbon, oxygen, and nitrogen are present in limited amounts. It is known that these interstitial elements may cause large differences in the mechanical properties of the material either as individual elements or in the presence of some of the getter elements such as Hf or Zr. However, these effects will be the subject of a later investigation.

Welding Tests

Welding was done in a closed chamber under one atmosphere of helium so that the changes in mechanical properties which result from contamination by oxygen and nitrogen were avoided. It was shown earlier that both oxygen and

Table 23. Alloys Selected for Welding Studies

Element	Alloy Addition (w/o) 0.5	1	2	5	10	20	40
Alloys with Neutralizers							
Ti	X	(X)	X	(X)	(X)	(X)	
Hf	(X)	(X)	X	(X)	(X)		X
Zr	(X)	(X)	X	(X)	(X)	X	
U	-	-	-	-	-	-	-
Alloys with Strengtheners							
Mo		X		(X)	X	X	
Ti		(X)		(X)	(X)	(X)	
Ta		X		X	X	X	
W		(X)		(X)	(X)	X	
V		(X)		(X)	X	X	
Zr	-	-	-	-	-	-	-
Alloys with Probable Poor Weldability							
Co		X	X	X	X		
Cr		X	X	X	X	X	
Th		X	X	X	X	X	
Al	X	X	X	X	X	X	

Ternary Alloys

Nb-Mo-Ti	85 - 7.5 - 75.
Nb-Mo-Hf	91.5 - 7.5 - 1, 90.5 - 7.5 - 2, 87.5 - 7.5 - 5, (85 - 7.5 - 7.5,) 82.5 - 7.5 - 10.

nitrogen affect the ductile-to-brittle transition temperature, as well as other mechanical and metallurgical properties.[29, 25] The use of the closed welding chamber shown in Figure 48 prevents contamination by the atmosphere gases. This chamber is purged by evacuation to 5×10^{-5} mm Hg and then back filled with helium. Prior studies showed that there were no increases in the oxygen or nitrogen content of the material during the welding operation. Welding was done with a tungsten arc using the work as the anode (straight polarity). The work piece was moved under the arc by means of a table driven by a shaft through a vacuum seal in the chamber wall.

The alloys tested in this portion of the study are given with their chemical analyses in Table 24. The welding data are given in Table 25. The welding current was 80-100 amperes and the voltage was 15-17 volts. The welding speed was maintained at 0.3 cm/sec. (7 in/min) The arc length was preset at 3/32 inch, and the arc was started by means of a high-frequency spark.

The alloys tested were made in a nonconsumable arc melting furnace. The starting stock was Union Carbide roundels. (Table 9) The melting and fabricating techniques were described earlier in this report. The weld specimens were approximately 0.065 in. thick. The samples were ground after rolling and etched in a 60% HNO_3-40% HF solution. Prior to welding the pieces were annealed at 1500 C for 1 hour in vacuum.

The welds were examined for porosity using X-ray techniques. The radiographs of the welds are shown with their photographs in Figures 49-58. Welds in heats NC-127, NC-132, NC-263, and NC-258 were the only ones which showed porosity except those made in pure Nb.[24] However, in the recent tests the alloys containing Hf and the pure Nb heat were the only ones which showed porosity. Re-examination of the melting technique showed that the latter heats had been remelted to avoid segregation of the alloy addition. The remelting process provided a longer time for the completion of any reactions involving the liberation of gases. It is presumed that the gases which caused porosity were removed during the melting operation; hence, porosity did not occur during welding. The pure niobium sample (NC-258) was not remelted since alloy segregation was not expected. This sample did show porosity after welding confirming the effect of the remelting operation as a method of preventing weld porosity. The porosity in heat NC-263 containing 7.5 Hf and 7.5 Mo is the only exception. This weld showed only one void so that the remelting operation is almost completely effective in eliminating porosity.

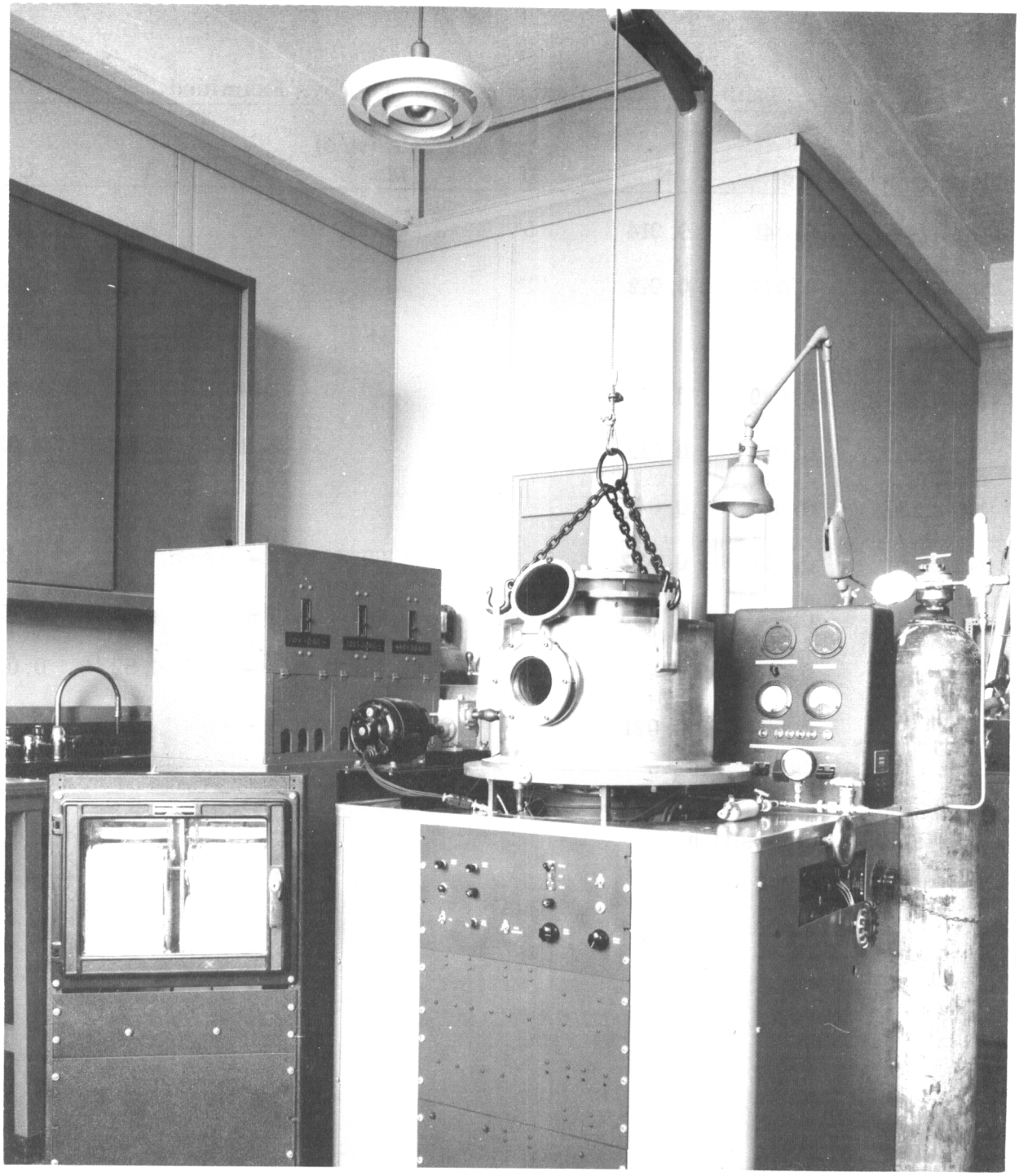

Fig.48 – Welding chamber

Table 24. Chemical Analyses of Alloys Examined

Heat	Analysis (w/o) 0	N	Hf	Mo	W	V	C
NC-127	0.041	0.014	5*	-	-	-	0.022 *
NC-132	0.077	0.012	10*	-	-	-	0.022 *
NC-191	-	-	-	5*	-	-	0.022 *
NC-194	0.049	0.014	-	-	10*	-	0.022 *
NC-131	0.077	0.012	-	-	8.75	5.01	0.022 *
NC-253	0.057	0.042	-	-	-	-	0.025 *
NC-255	0.055	0.022	5.40	4.89	-	-	0.025 *
NC-263	0.114	0.025	7.78	7.50	-	-	0.025 *
NC-264	0.057	-	-	5.00	-	4.82	0.025 *
NC-258	0.074	0.021	-	-	-	-	0.033

* Nominal Composition

Table 25. Welding Data

Heat No.	Nominal Composition (w/o)	Current (Amps)	Voltage (Volts)	Weld Speed (cm/sec)	Comments
NC-127	Nb-5Hf	75	19-17	0.3	Distortion caused voltage variation.
NC-132	Nb-10Hf	80	21	0.3	-
NC-191	Nb-5Mo	80	18	0.3	-
NC-194	Nb-10W	85	17-20	0.3	Distortion produced voltage variation.
NC-131	Nb-8.75W	85	15-18	0.3	Slight distortion
NC-253	Nb-5V	100	16-16.5	0.3	-
NC-255	Nb-5Hf-5Mo	90	18	0.3	-
NC-263	Nb-7.5Hf-7.5Mo	100	20-18	0.3	Slight distortion
NC-264	Nb-5V-5Mo	85	17	0.3	-
NC-258	Pure Nb	100	17	0.3	-

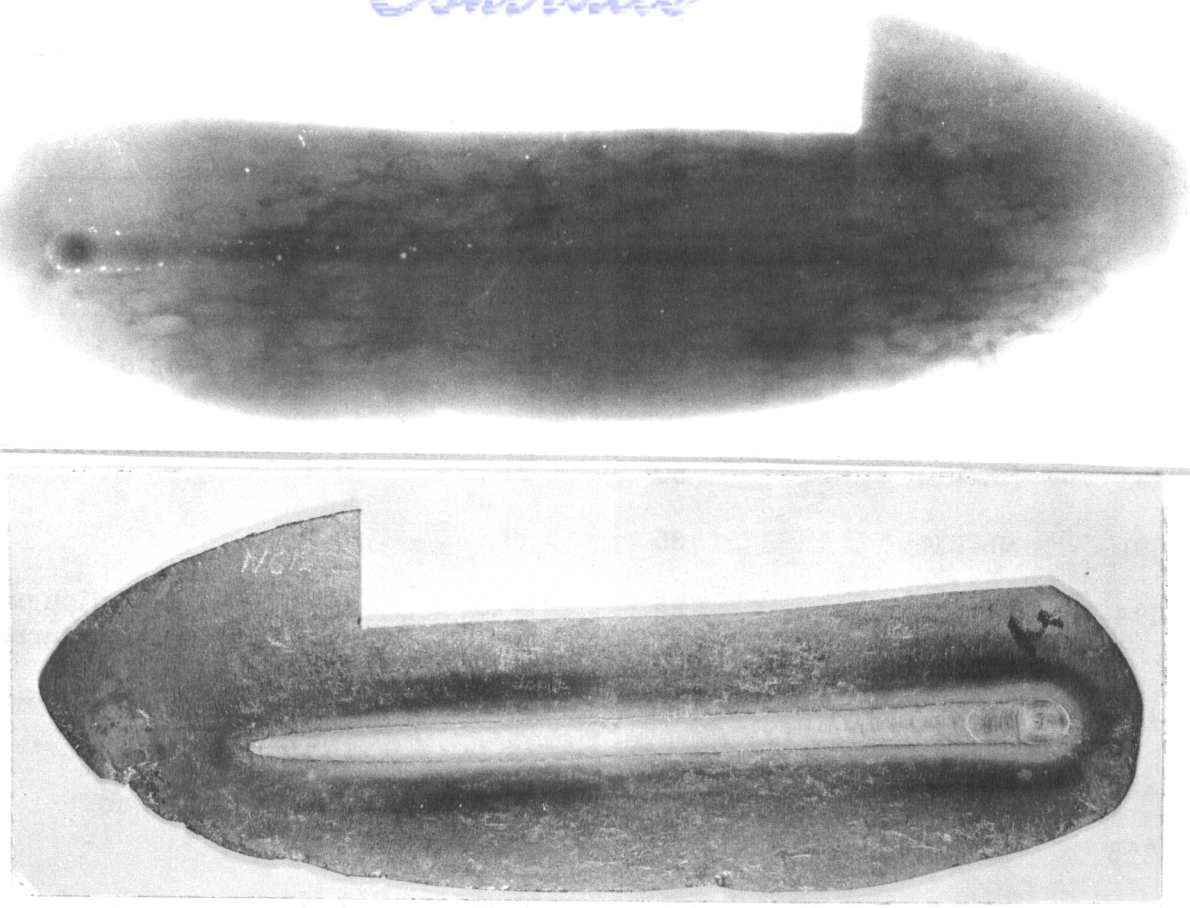

Fig. 49 – Weld in Nb-5 Hf alloy (NC-127)

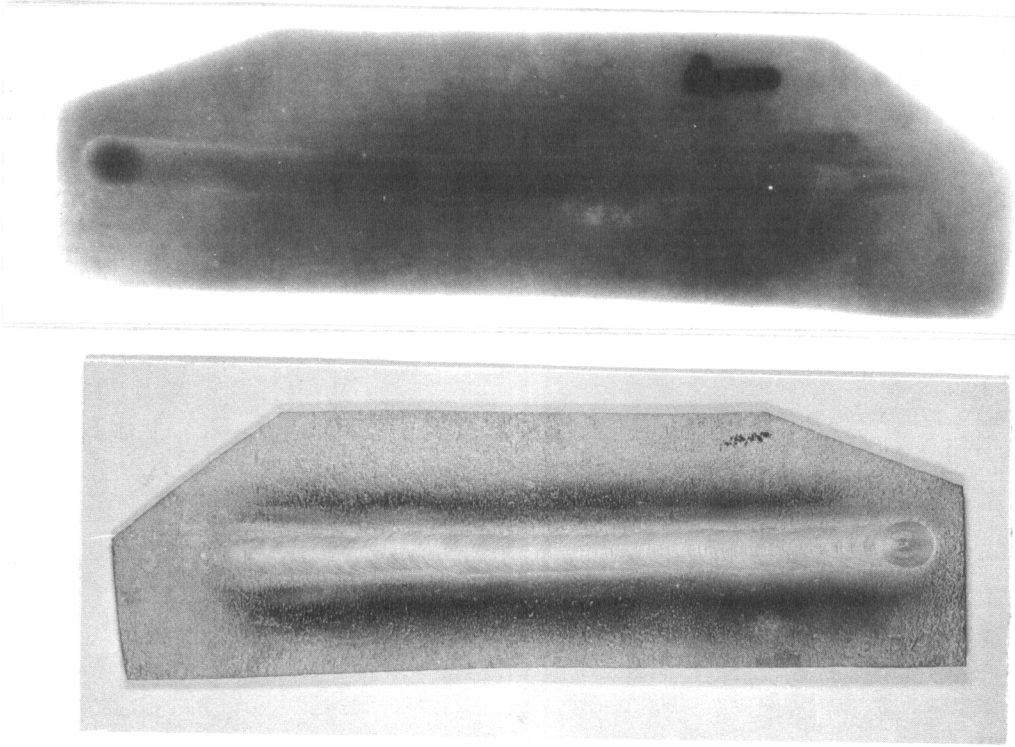

Fig. 50 – Weld in Nb-10 Hf alloy (NC-132)

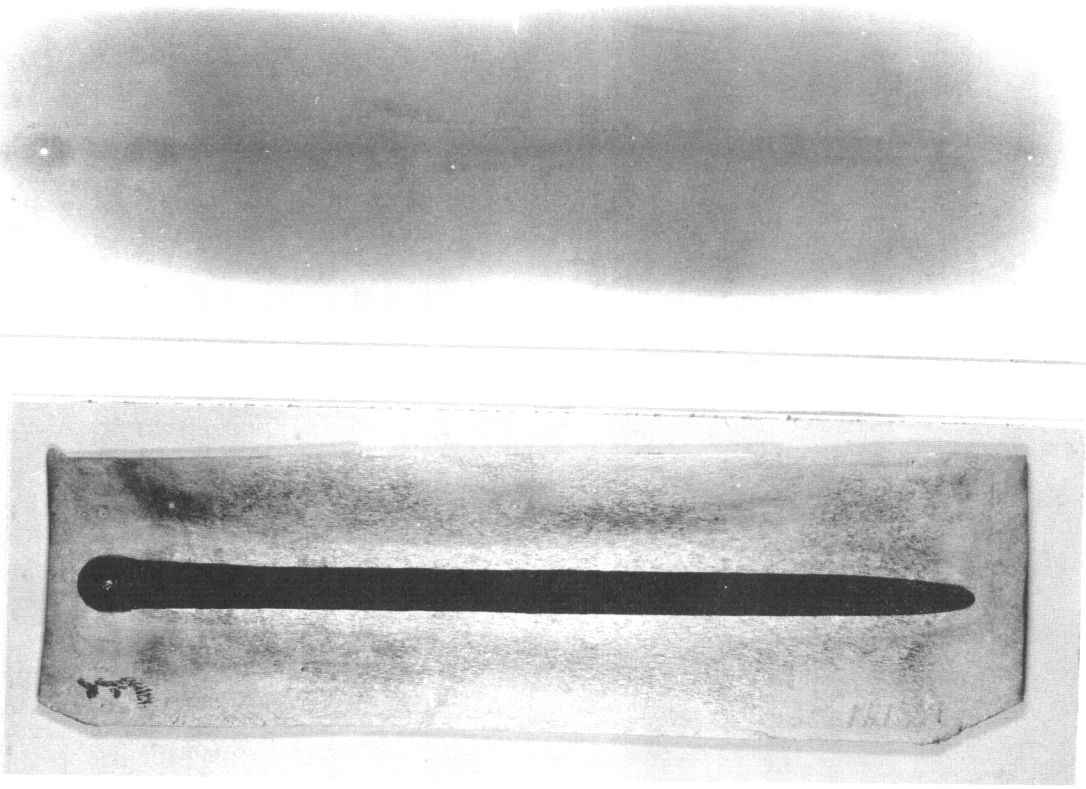

Fig. 51 – Weld in Nb–5 Mo alloy (NC – 191)

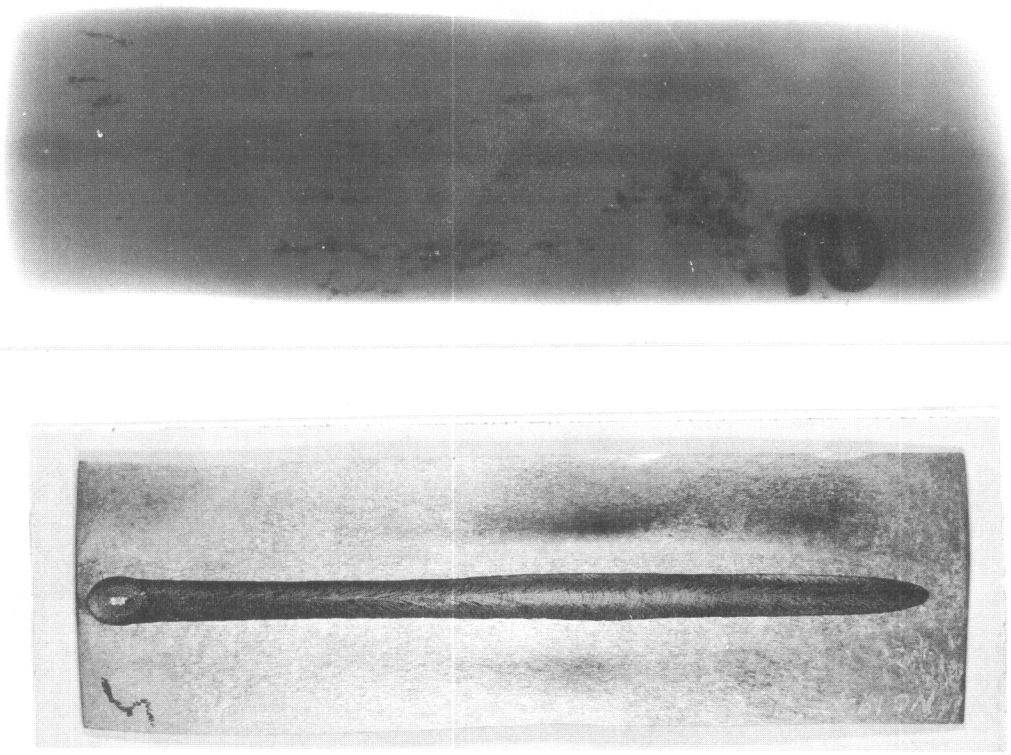

Fig. 52 – Weld in Nb-10W alloy (NC-194)

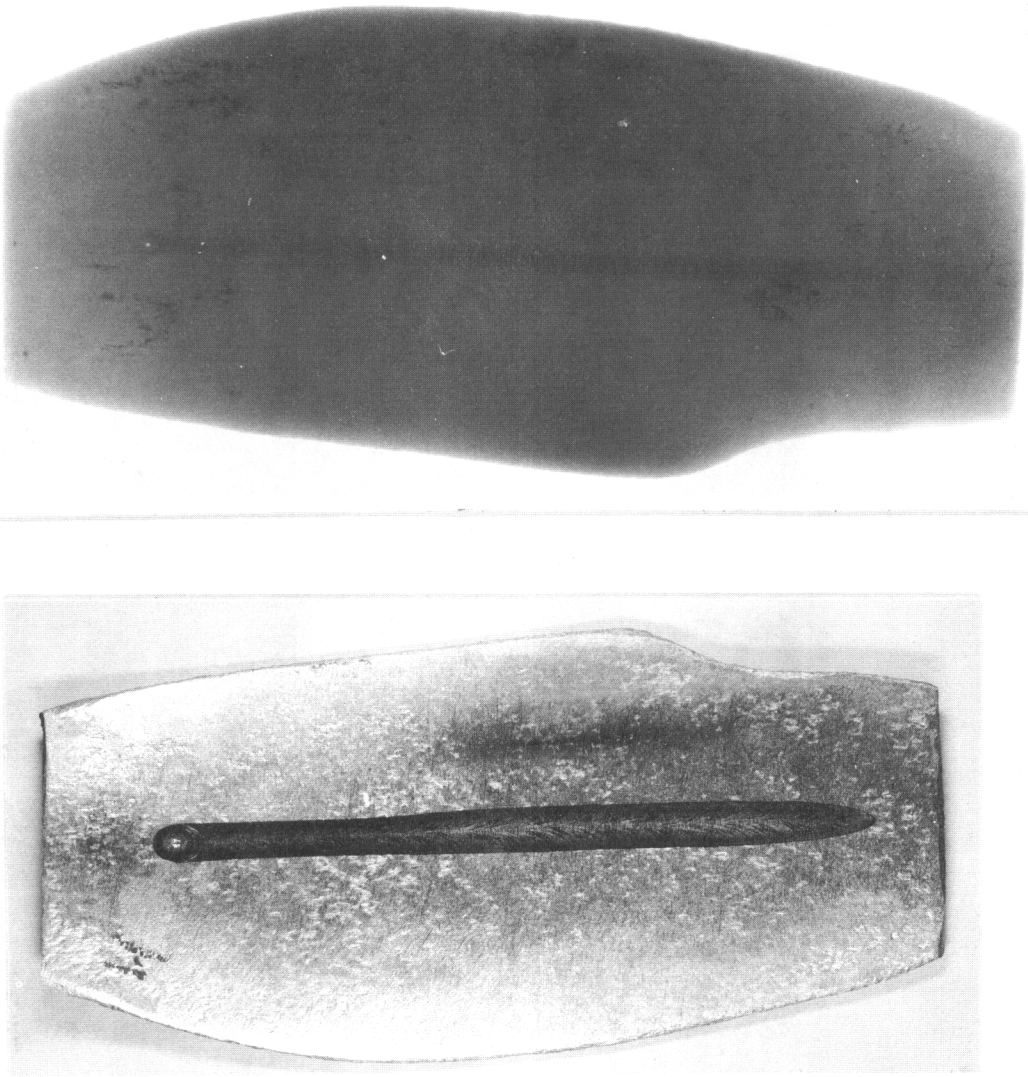

Fig. 53—Weld in Nb-8.75 W alloy (NC-131).

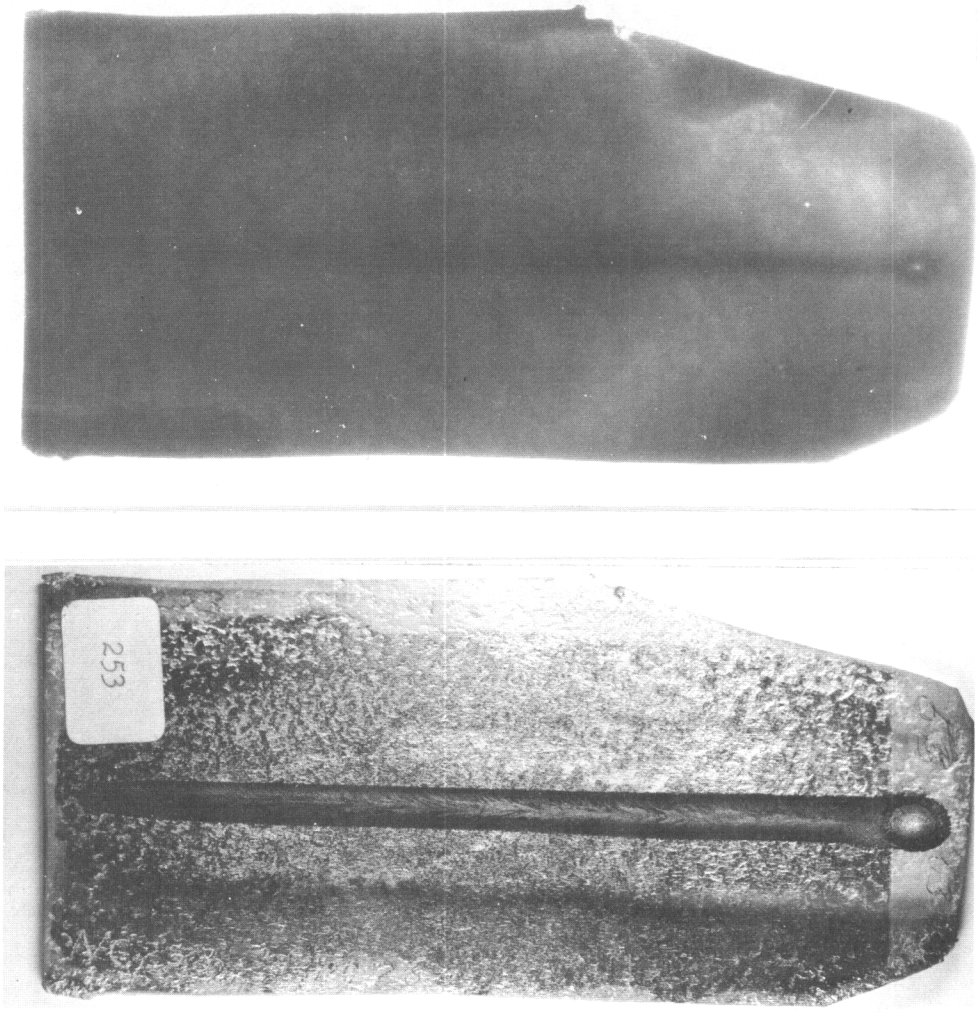

Fig. 54 - Weld in Nb-5 V alloy (NC-253)

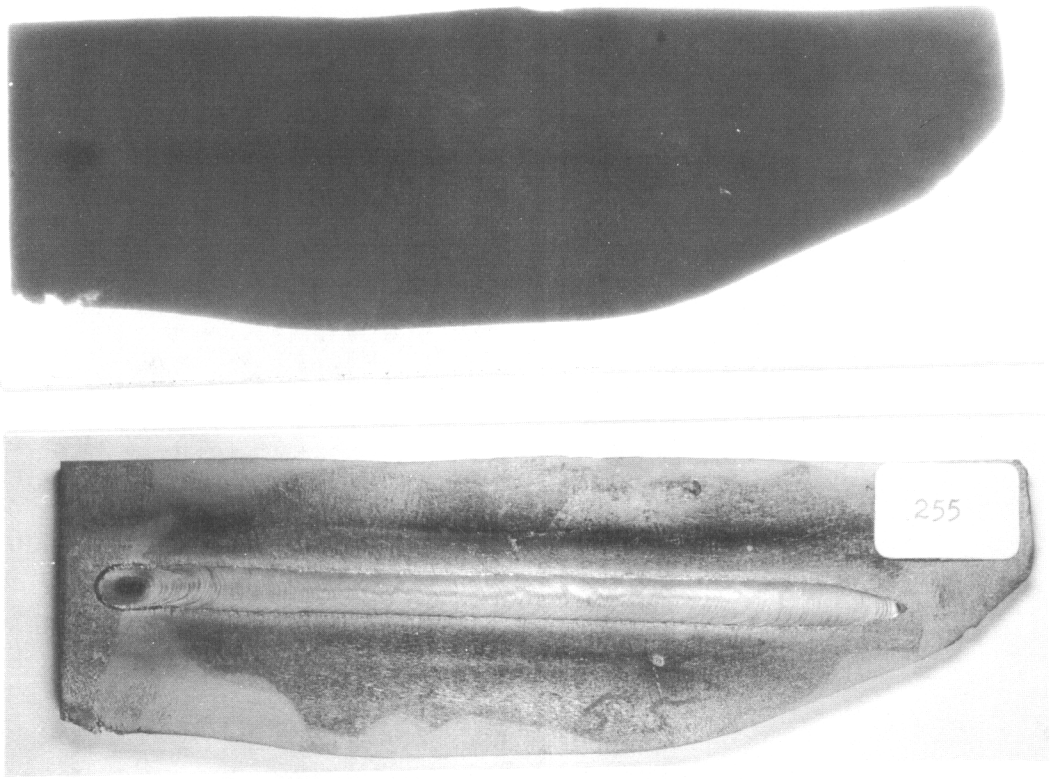

Fig. 55– Weld in Nb–5 Mo–5 Hf alloy (NC–255)

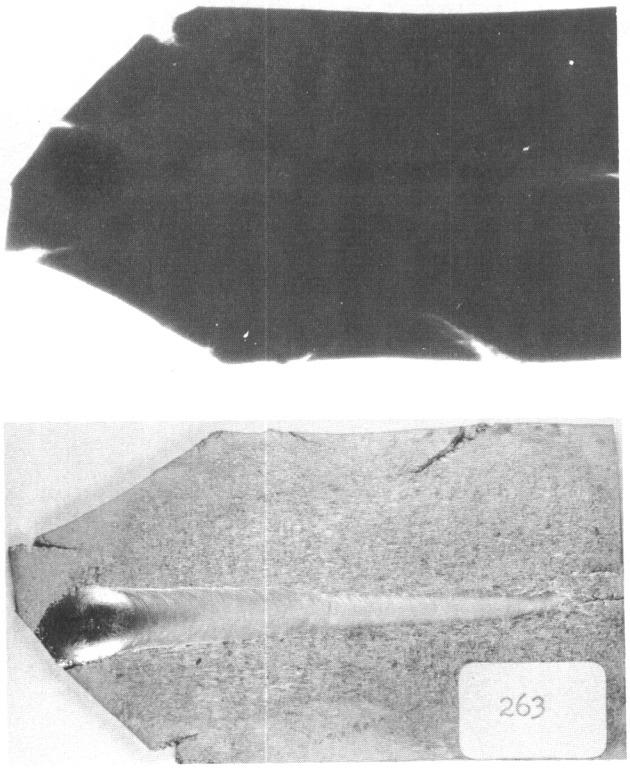

Fig. 56– Weld in Nb-7.5 Mo-7.5 Hf alloy (NC-263)

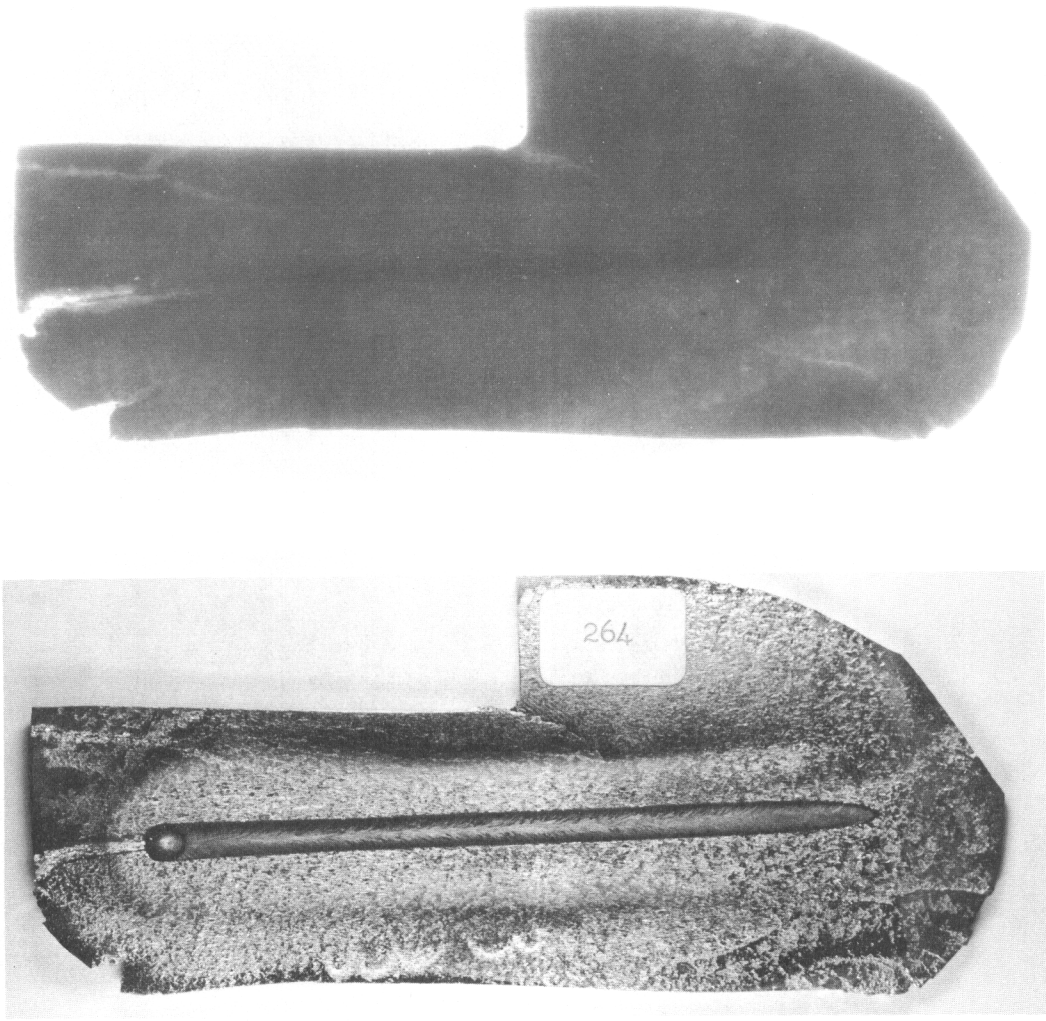

Fig. 57 – Weld in Nb-5 V-5 Mo alloy (NC-264).

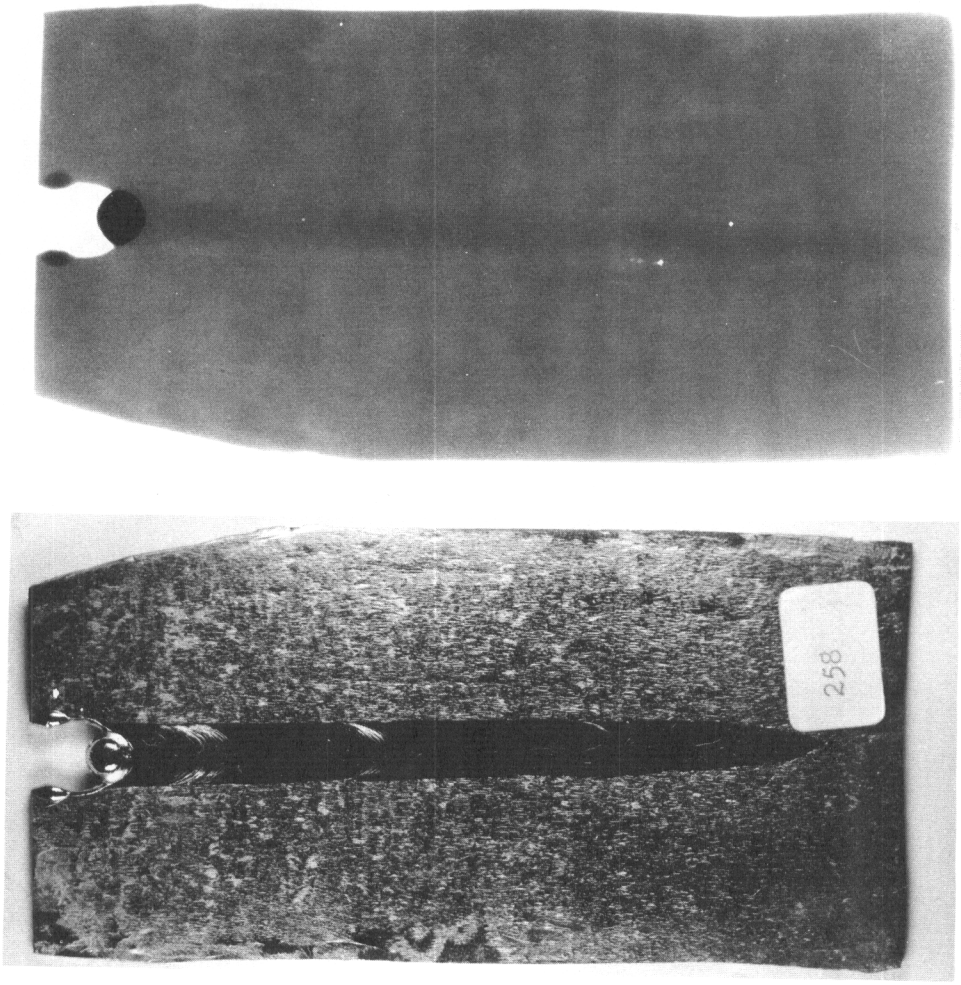

Fig. 58—Weld in pure niobium (NC-258)

Mechanical Properties

The welds were cut into specimens for bend and tensile tests. Due to the limited amount of material available, it was not possible to make both tensile and bend tests from the same sample. There were only three alloys where duplicate heats were available for testing for both the ductile-to-brittle transition temperature and the high temperature tensile strength. Tensile data were obtained for heats NC-258 (pure niobium), NC-131 (8.75 W); and NC-258 (5.01 V). The remaining heats were tested only in bending at relatively low temperatures.

The results of the bend tests on the heats in this portion of the study are shown in Figs. 59-66. These data are summarized with the results from earlier work[24] in Fig. 67. These results extend the earlier work and show that as the amount of alloy addition is increased the ductile-to-brittle transition temperature generally increases. However, the cases of Ti, Hf, and V are of particular interest. Earlier studies showed that additions of slightly more than 0.5 w/o Hf lowered the ductile-to-brittle transition temperature to below -196 C. However, the extension of the studies of Nb-Hf alloys have shown that further increases in the amount of Hf added to Nb will cause the transition temperature to rise rapidly. An addition of 5 w/o Hf raised the transition temperature to +50 C and 10 w/o Hf further increased the temperature to +200 C.

The addition of Ti first caused the transition temperature to increase to 0 C and then fall to below -196 C when the Ti addition exceeded 10 w/o. Additions of V cause a somewhat similar effect where a maximum in the transition temperature is reached at approximately 5 w/o after which the transition temperature begins to fall. The data in Fig. 67 indicate that further study should be made of Nb-V alloys with additions of V in excess of 6.8 w/o.

The three ternary alloys tested are also shown in Figure 67 for comparison. They have been arbitrarily placed in a location which accounts for their total alloy content. These alloys all had relatively high ductile-to-brittle transition temperatures. The 5 w/o Mo - 5 w/o Hf, and 5 w/o Mo - 5 w/o V alloys both showed ductile behavior only at temperatures above 150 C. The 7.5 w/o Mo-7.5 w/o Hf alloy was still brittle at the upper limit of the test fixture, 250 C, indicating that ductile behavior did not occur in this alloy until higher temperatures had been attained.

The data shown in Fig. 67 demonstrate that the use of alloying elements to improve the properties of niobium can have a large effect on the ductile-to-brittle transition temperature of the welds. All of the elements added caused the transition

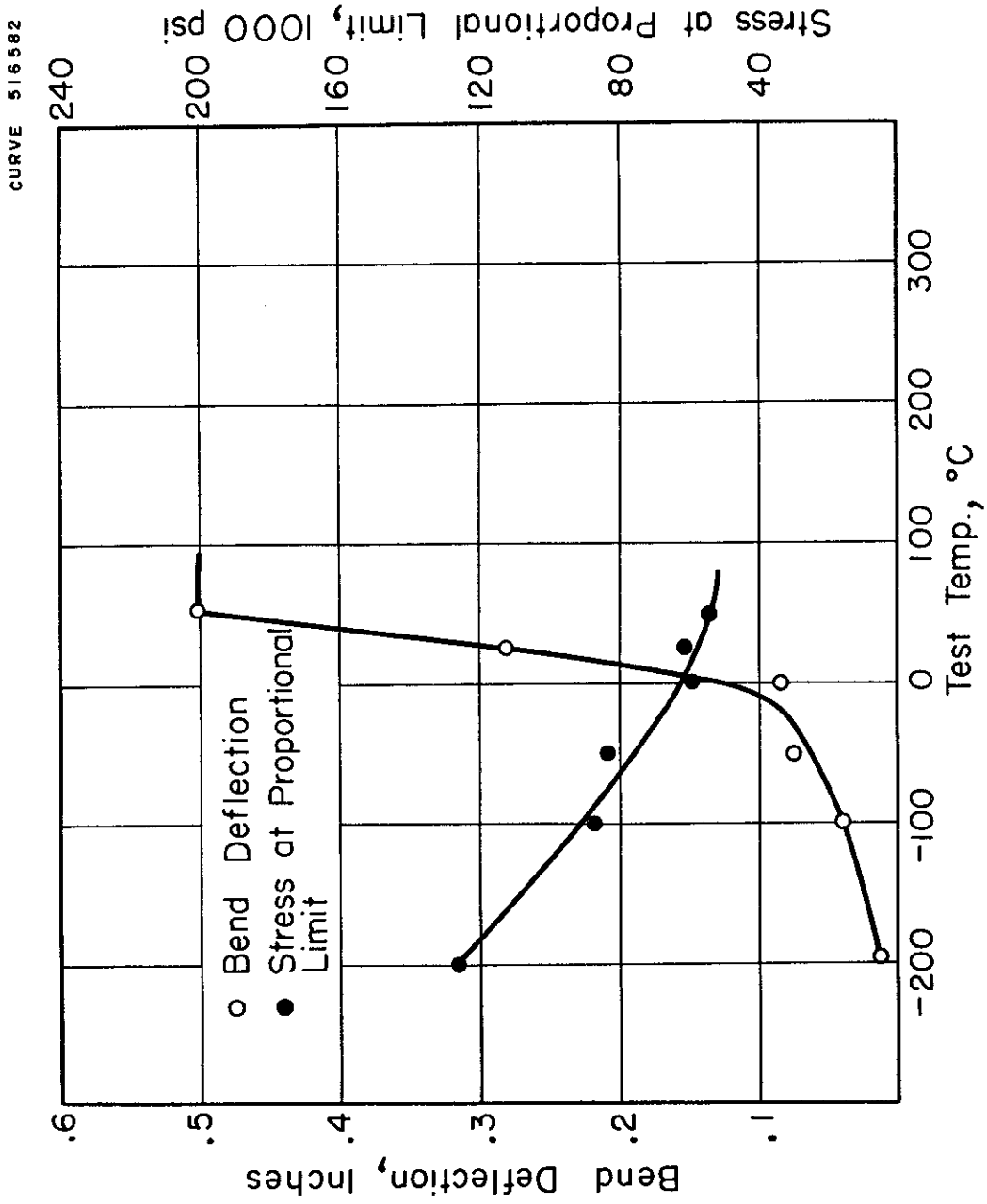

Fig.59- Bend data for weld in Nb-5Hf alloy (NC-127)

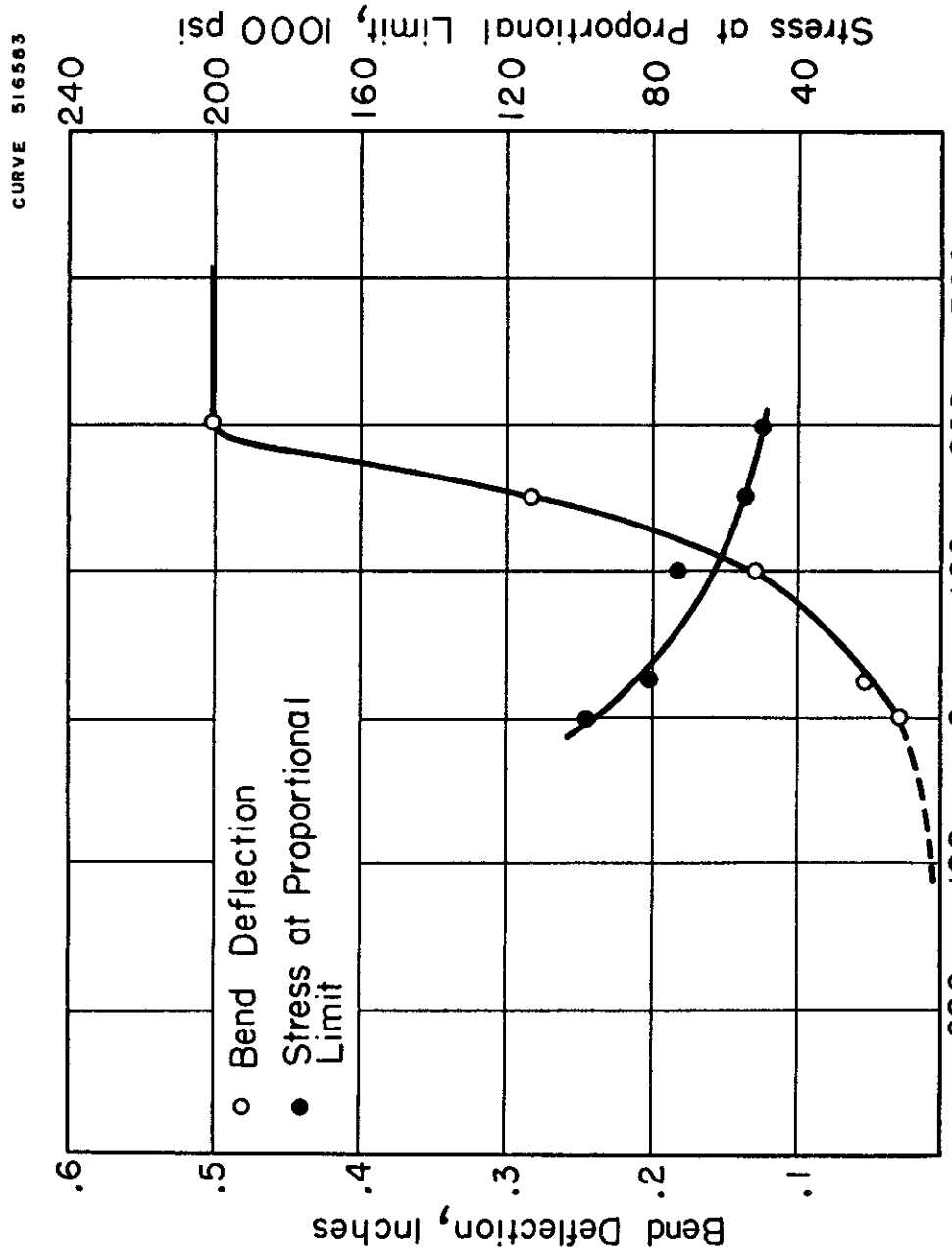

Fig. 60 - Bend data for weld in Nb-10Hf alloy (NC-132).

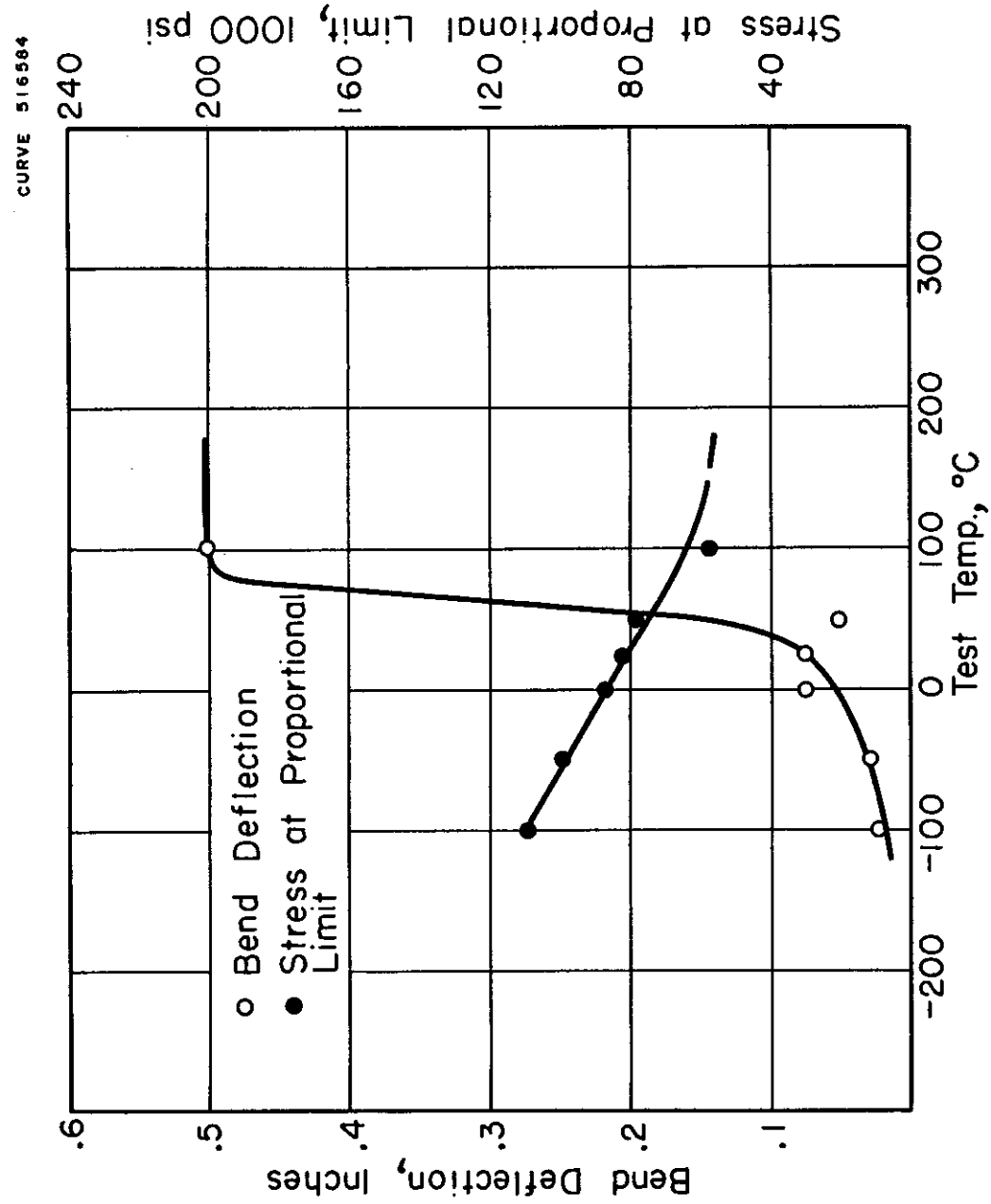

Fig. 61 – Bend data for weld in Nb-5Mo alloy (NC-191).

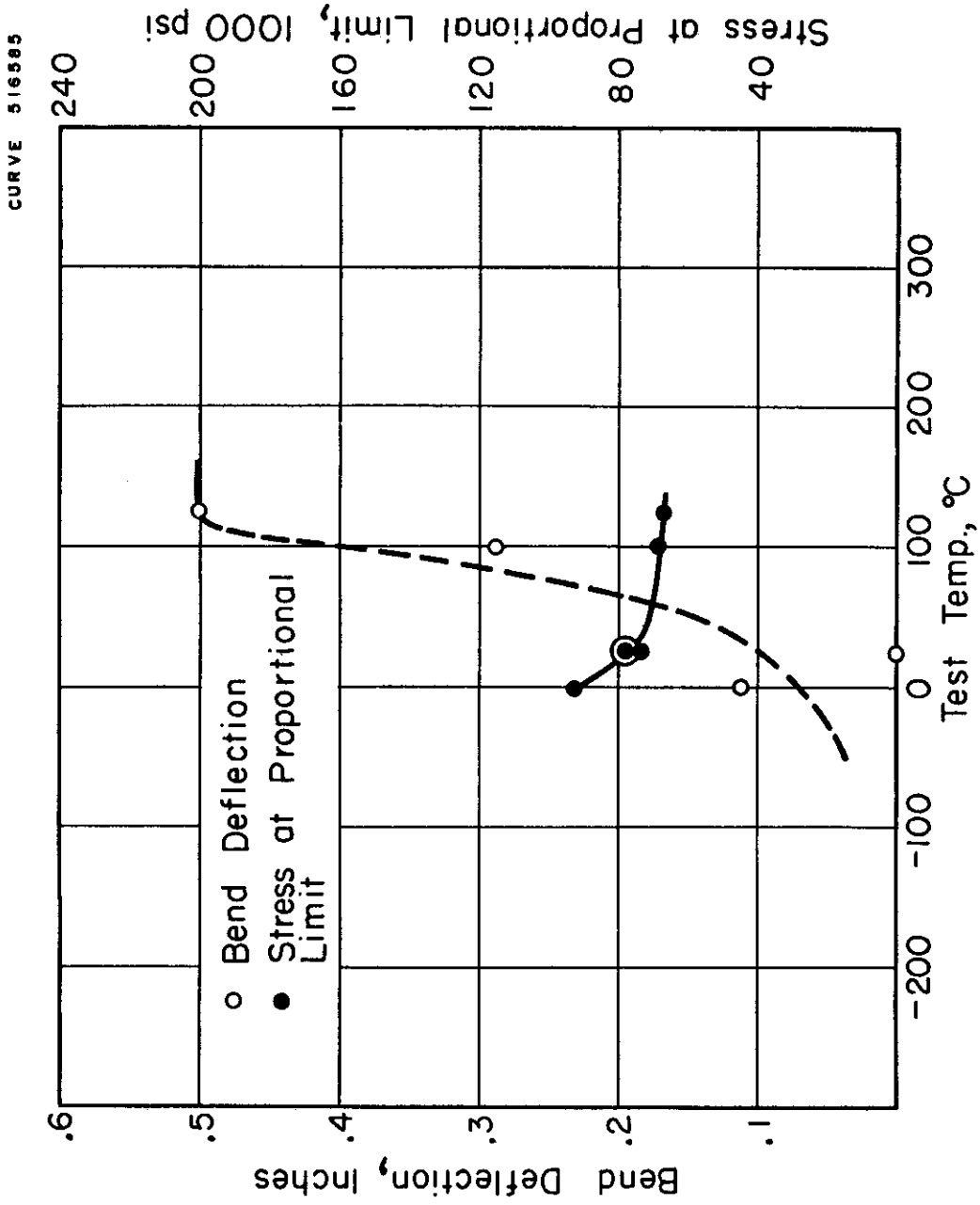

Fig. 62 – Bend data for weld in Nb-10W alloy (NC-194).

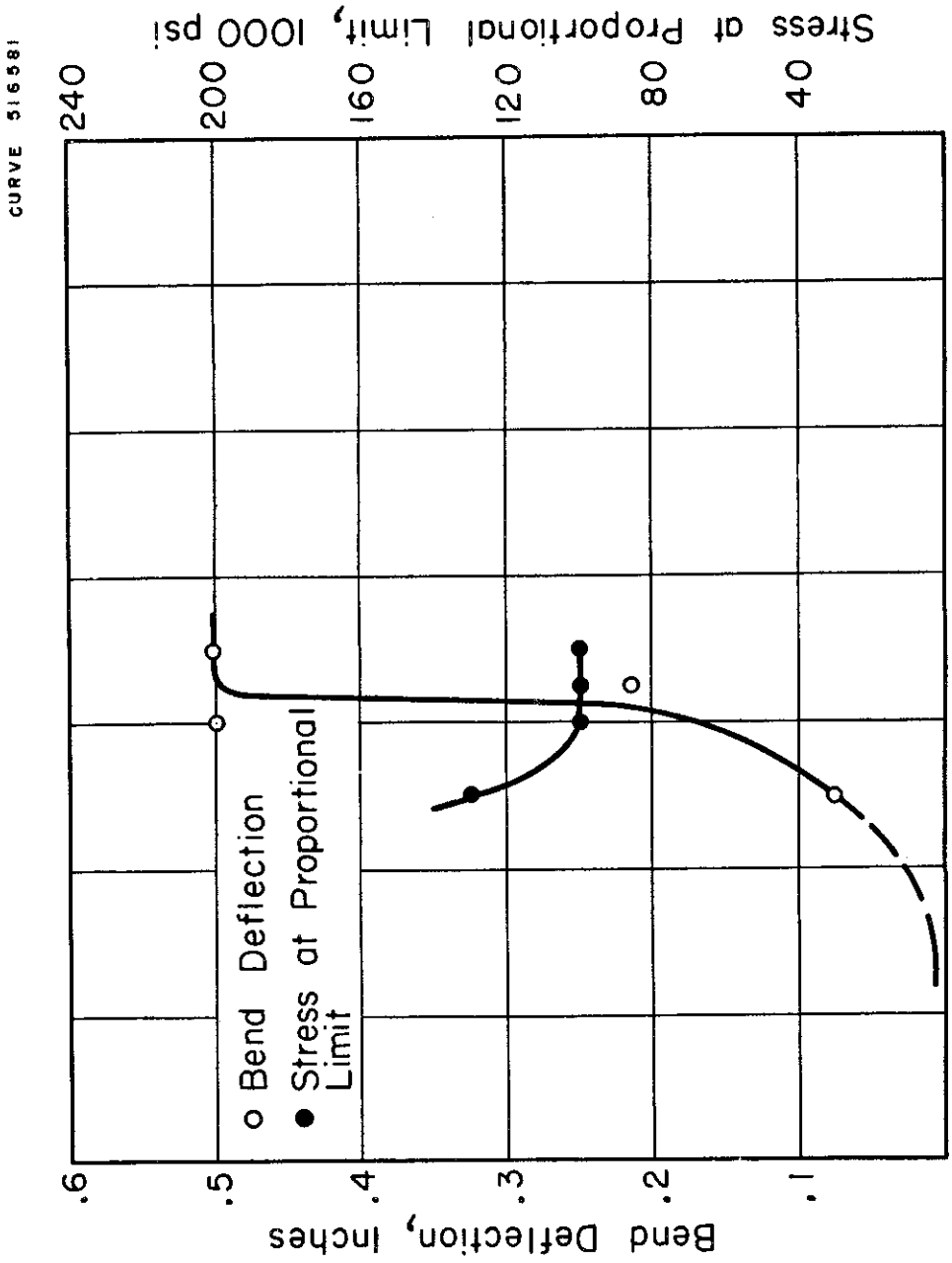

Fig. 63- Bend data for weld in Nb-5V alloy (NC-253).

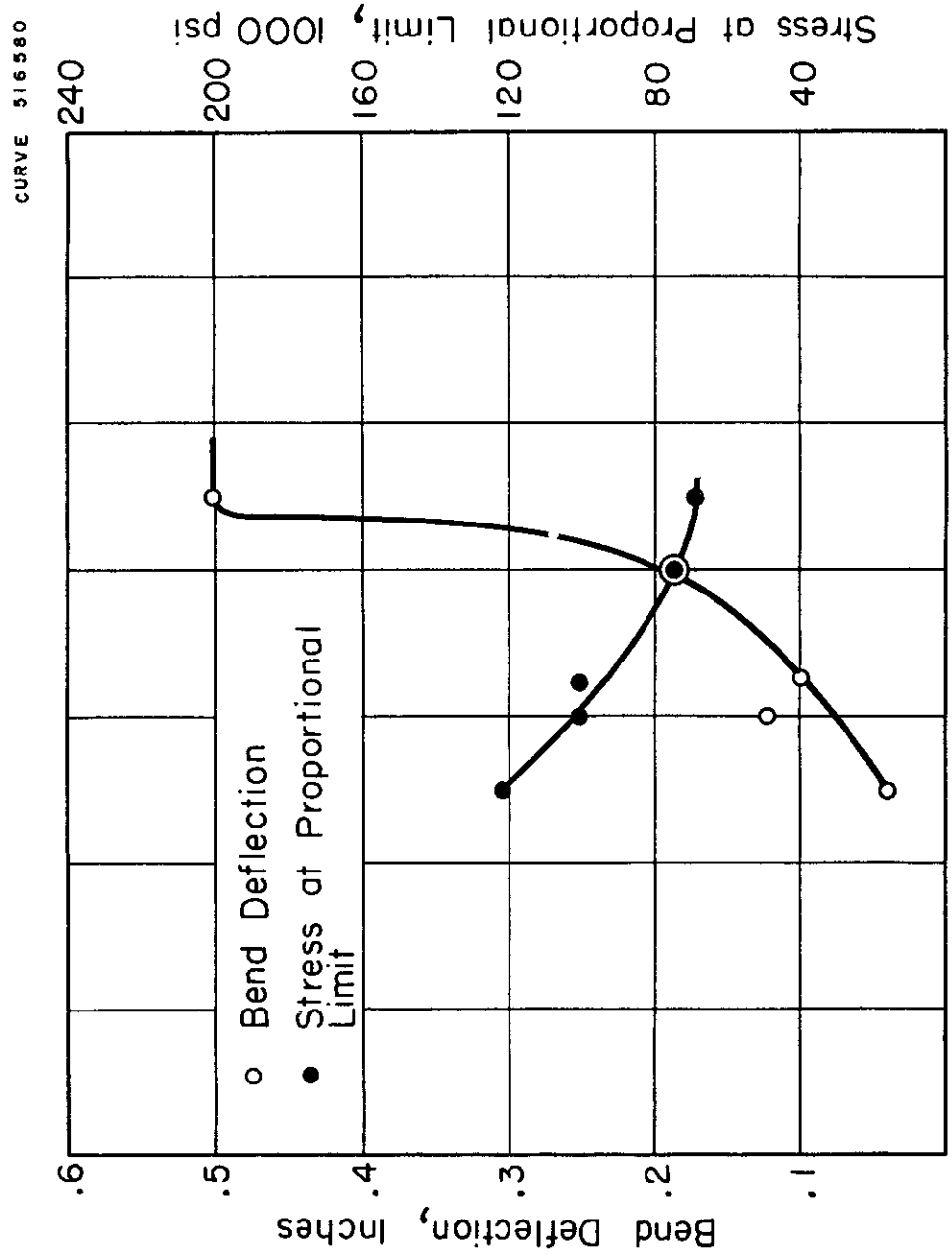

Fig.64 – Bend data for weld in Nb–5Mo–5Hf alloy (NC-255).

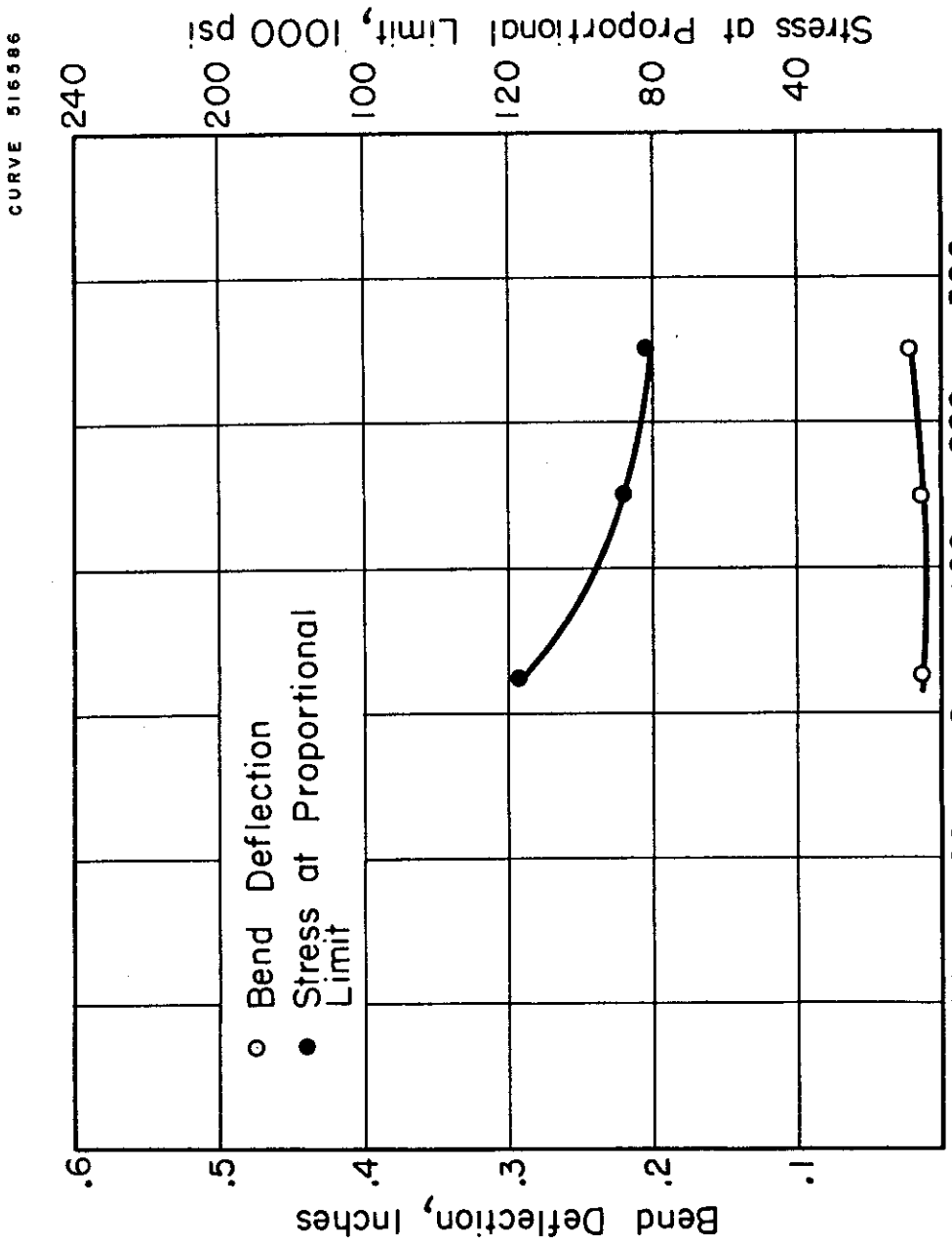

Fig. 65 – Bend data for weld in Nb-7.5 Mo-7.5 Hf alloy (NC-263).

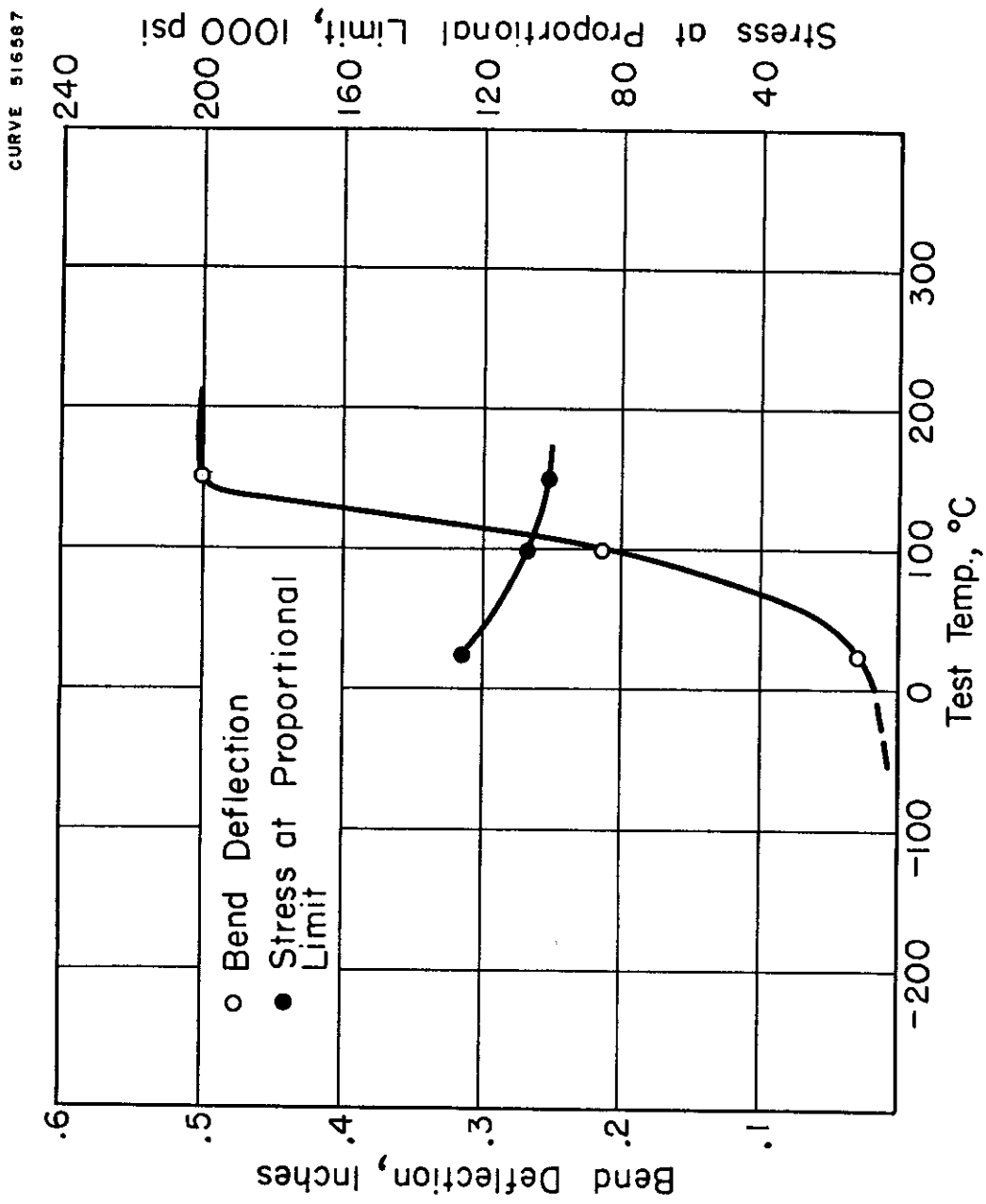

Fig. 66- Bend data for weld in Nb-5V-5Mo alloy (NC-264).

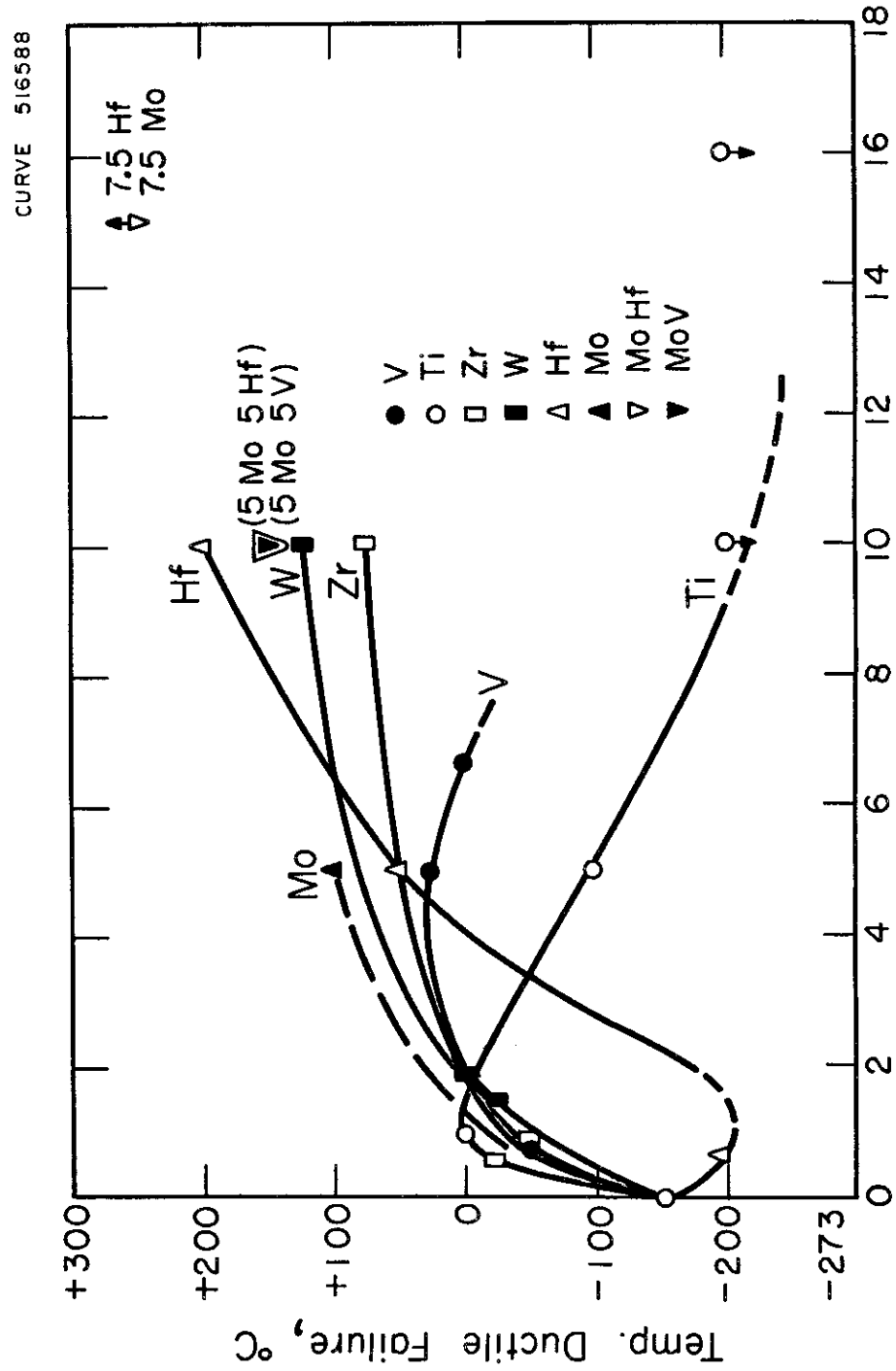

Fig. 67 – Effect of alloy additions on the bend ductility of niobium welds.

temperature to increase with the exception of Ti additions greater than 1.5 to 2 w/o and Hf additions of about 0.5 w/o. The reason for these differences are not fully understood. However, it is suspected that the effects of these elements and possibly some others may be related to the formation of oxides, nitrides, or carbides of a size and degree of coherency in a dispersion which cause the change in the mechanical properties.

The room temperature hardness was measured across the weld in many of the alloys studied. These data are shown in Figs. 68 to 71. The weld hardness data have been summarized in Fig. 72 from the present data and values given in an earlier work.[24] Comparison of the hardness data in Fig. 72 with the ductile behavior data in Fig. 67 indicates a correlation between composition and the ductile-to-brittle transition behavior. The data in Figs. 67 and 72 show that as the hardness increases the transition temperature increases and vice versa. The hardness change when Hf is added in amounts near 0.5 w/o does not correspond to the decrease found in the transition temperature in this alloy. This anomaly may be partly explained by the hardening effect caused by the formation of hafnium oxide in niobium. The hardening effects of oxides and nitrides in niobium are not fully understood at this time. However, it is believed that the combinations of the interstitial elements, oxygen, nitrogen, and carbon, with such elements as Ti, Hf, and Zrhave a strong effect on both the strength and ductility of the weld metal at both low and high temperatures. The work reported earlier on oxygen and nitrogen contamination effects was done on an alloy containing 0.5 w/o Zr.[24,25] It is suspected that the damage to the ductile-to-brittle transition temperature by interstitial elements in this alloy may have been increased by the presence of Zr. This difficulty is under investigation. If the combination of getter elements and the interstitial elements can cause changes in the weld metal mechanical properties, it will be necessary to use additional care with respect to contamination by oxygen and nitrogen when welding alloys containing elements such as Ti, Zr and Hf.

Metallographic Studies

The welds were sectioned and examined metallographically. Photomicrographs of pure Nb and some of the binary alloys are shown in Figs. 73-77. The 5 w/o V alloy, Fig. 74,appears to have very clean base material. There is no evidence of a precipitate, although both the oxygen and nitrogen are high, Table 24. The fused weld metal shows only the effect of dendritic coring during solidification. However, some porosity can be observed in this sample. Furthermore, there is evidence of grain boundary parting in the heat-affected base

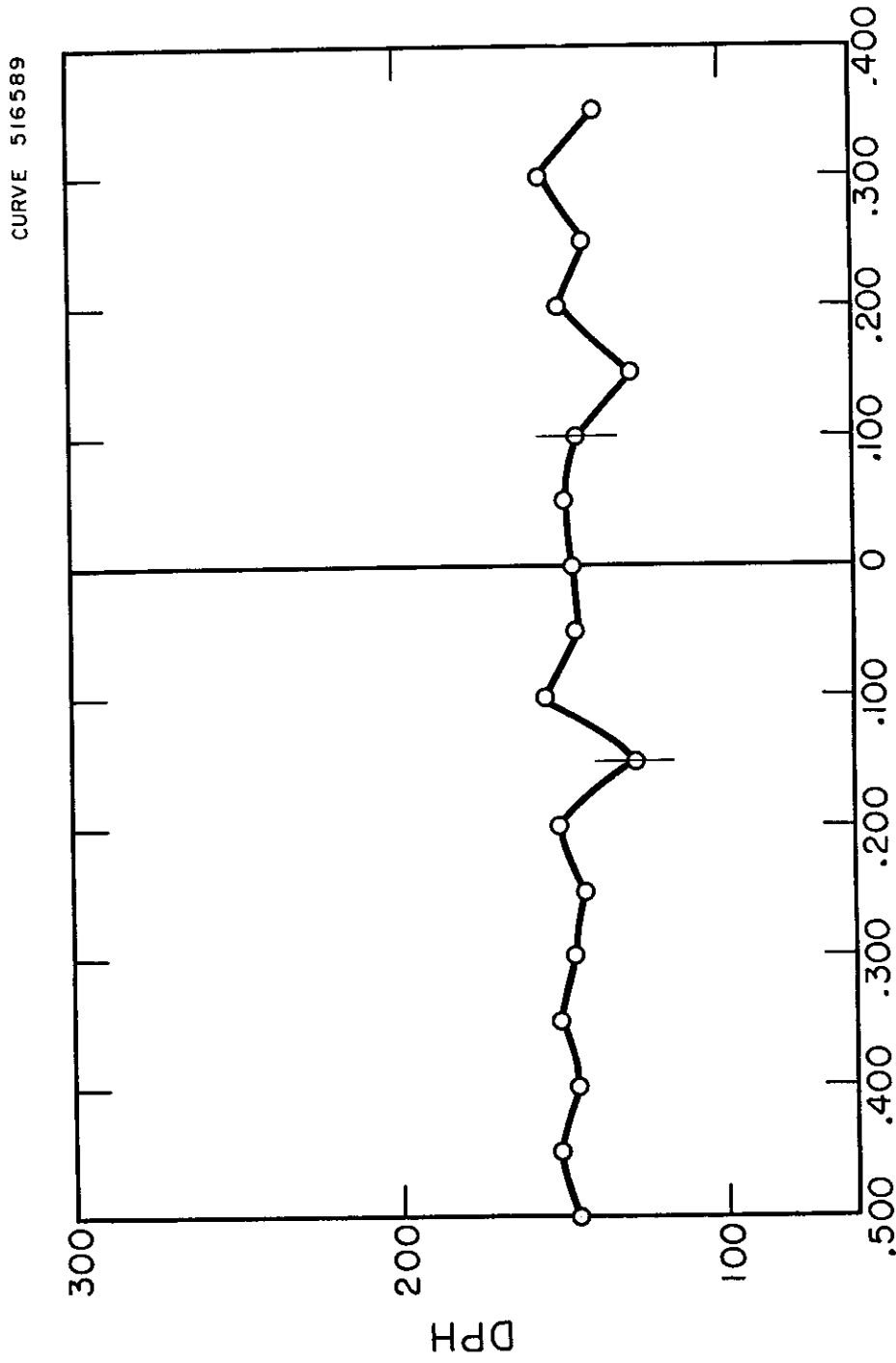

Fig.68-Weld hardness in pure Nb (NC-258).

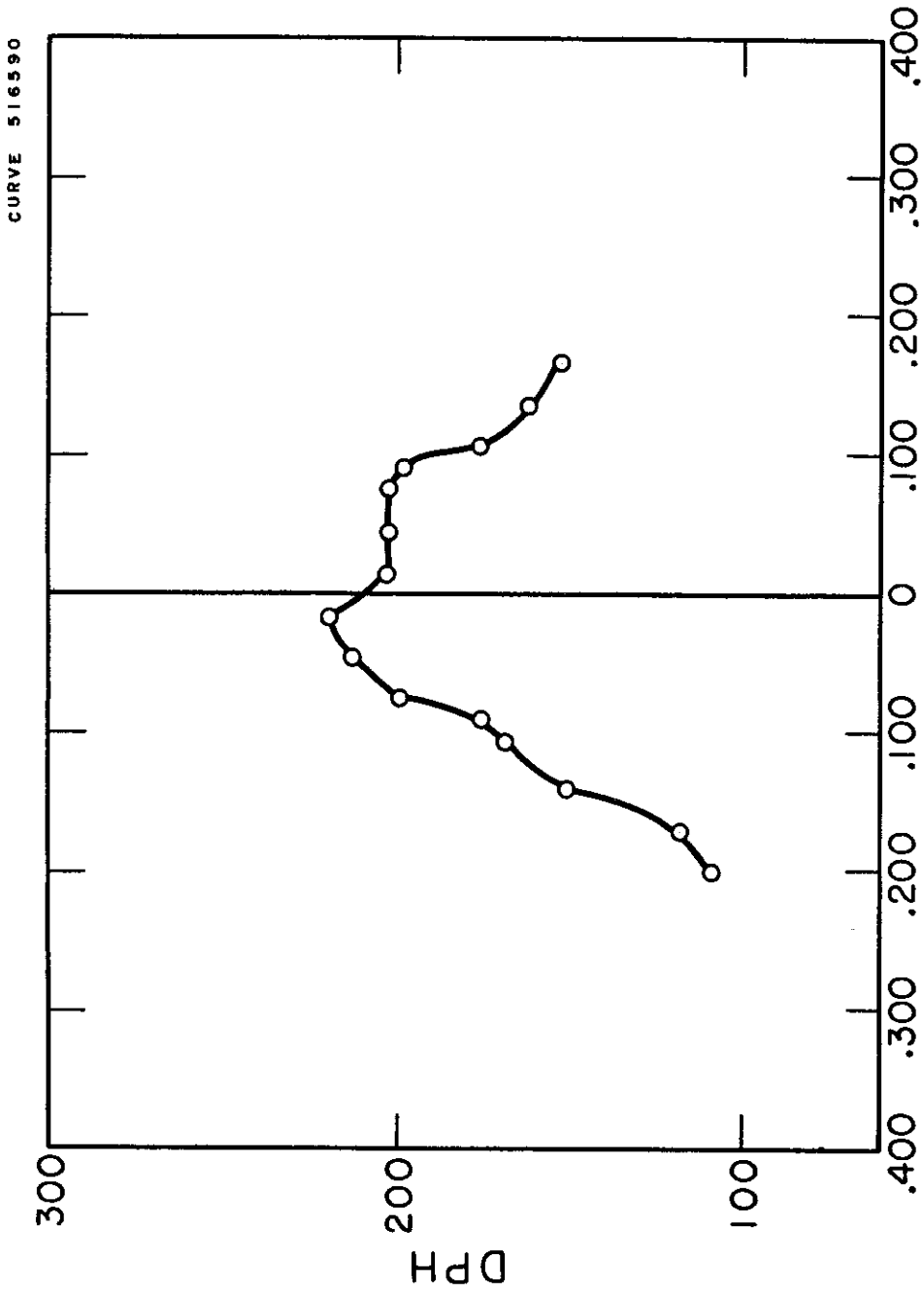

Fig.69– Weld hardness in Nb-10 Hf alloy (NC-132).

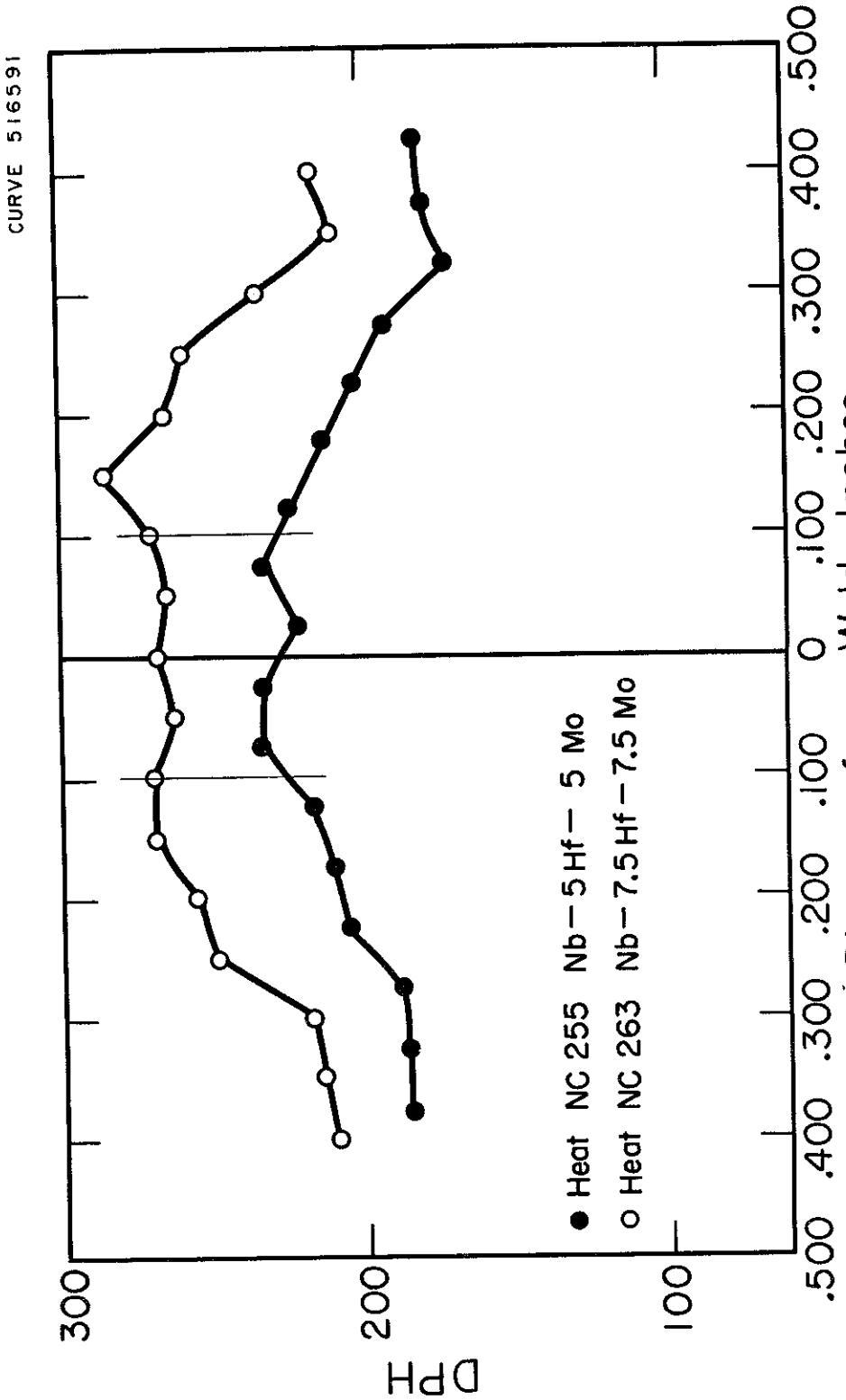

Fig. 70 - Weld hardness in Nb-Hf-Mo alloys.

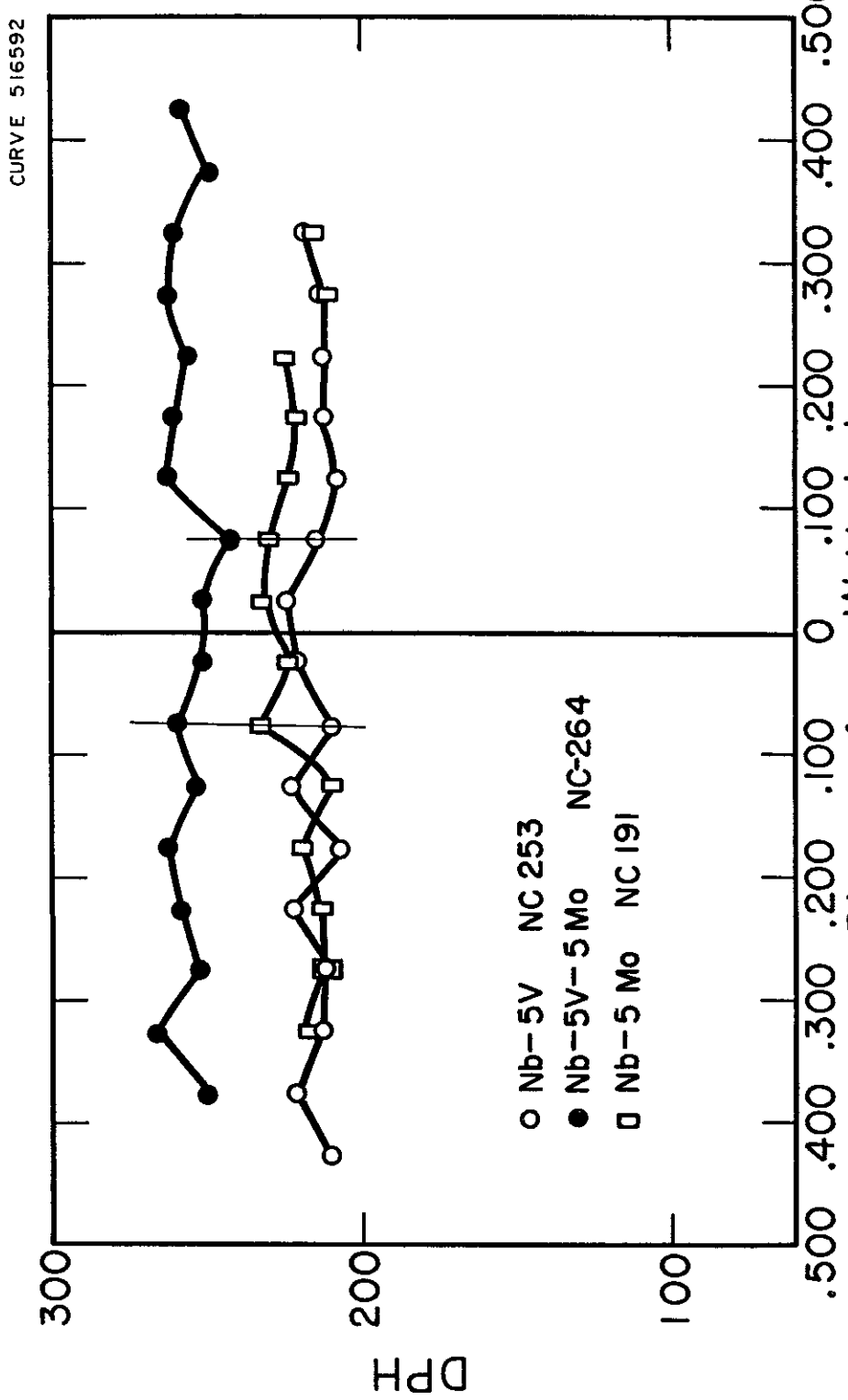

Fig. 71 – Weld hardness in Nb-V and Nb-V-Mo alloys.

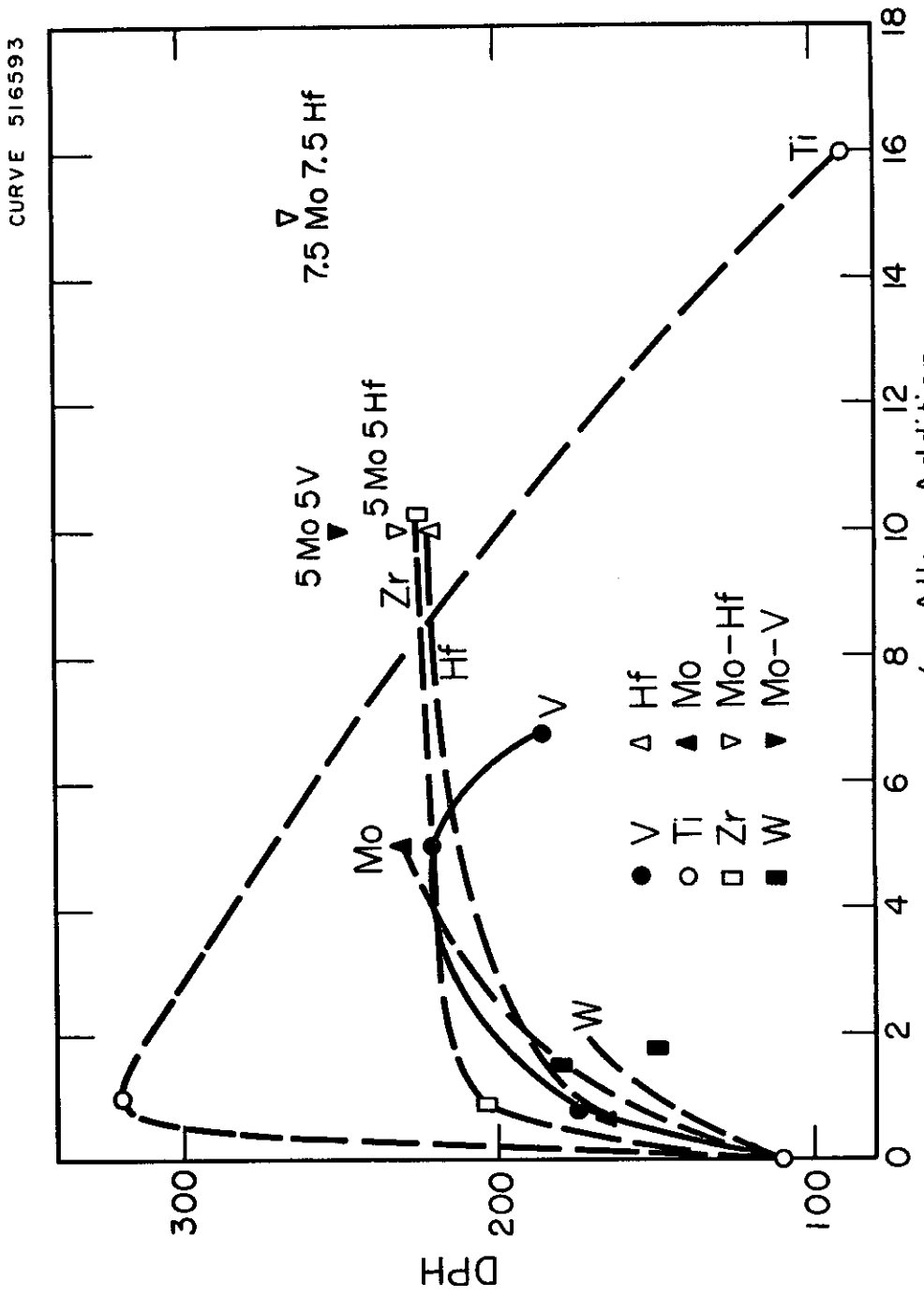

Fig. 72 – Peak weld hardness vs alloy content.

a) Base Metal 100 X

b) Weld Metal 100 X

Fig.73 – Microstructure of weld in pure Nb (NC-258).

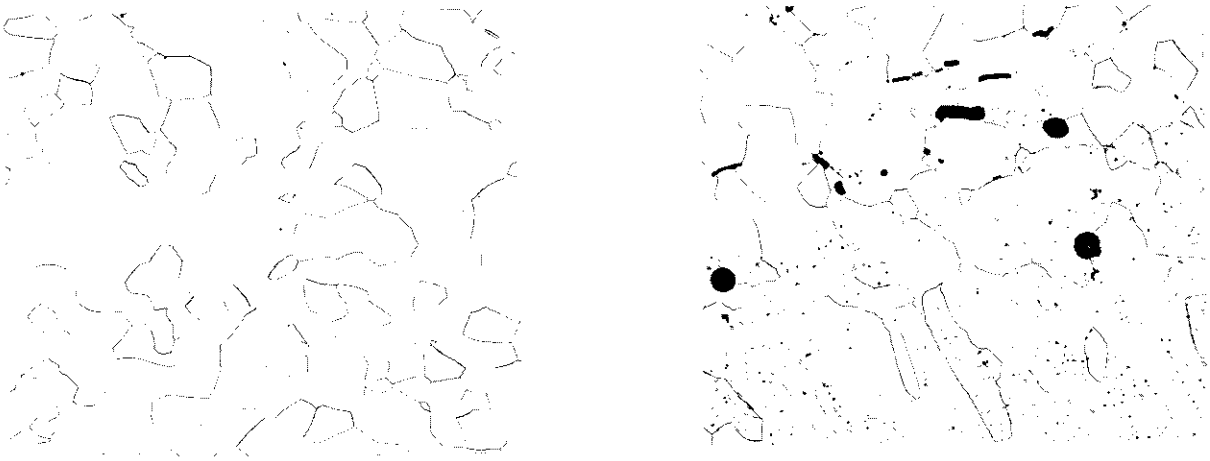

a) Base Metal 100X

b) Weld Metal 100 X

Fig. 74 – Microstructure of weld in Nb–5V alloy (NC-253).

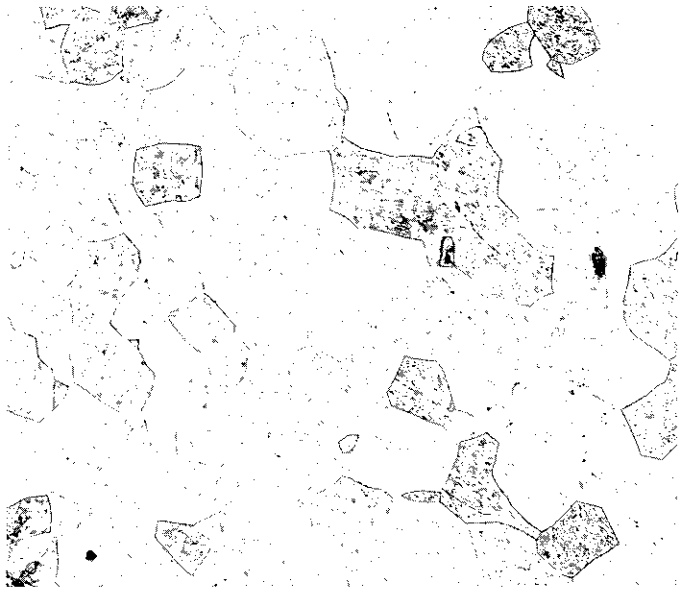

a) Base Metal 100 X

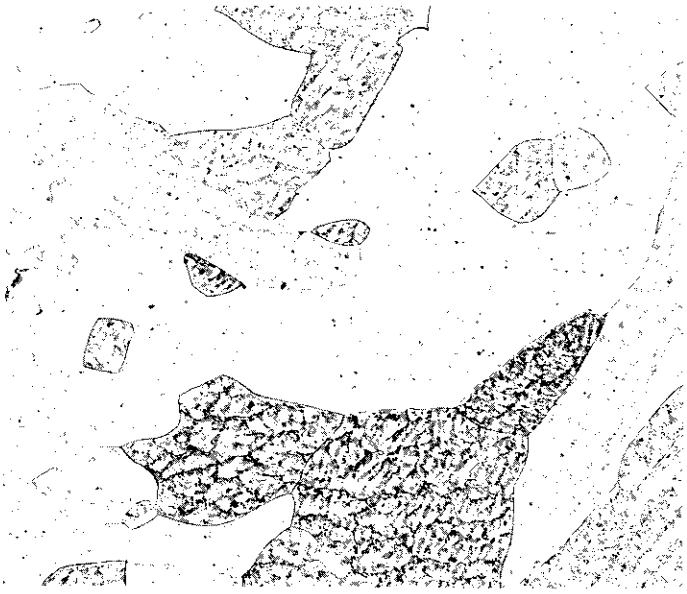

b) Weld Metal 100X

Fig. 75 – Microstructure of weld in Nb-10W alloy (NC-194).

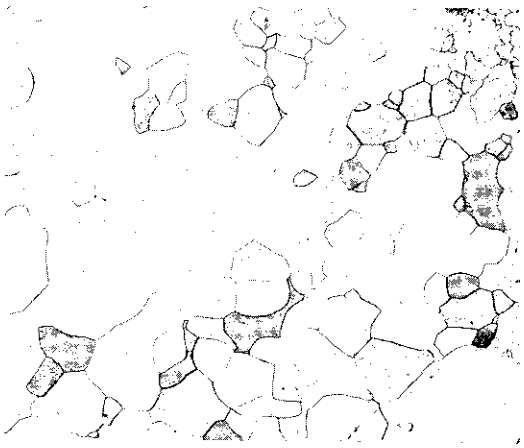

a) Base Metal 100X

b) Center of Weld 100X

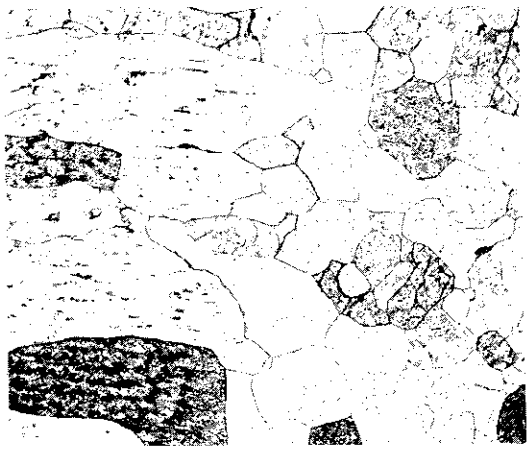

c) Weld Edge 100X

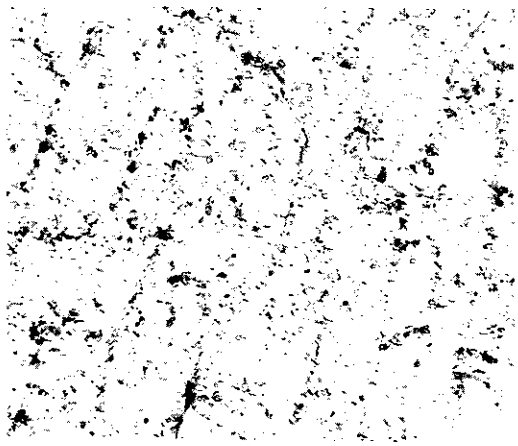

d) Weld 500 X

Fig. 76– Microstructure of weld in Nb–10 Hf alloy (NC–132).

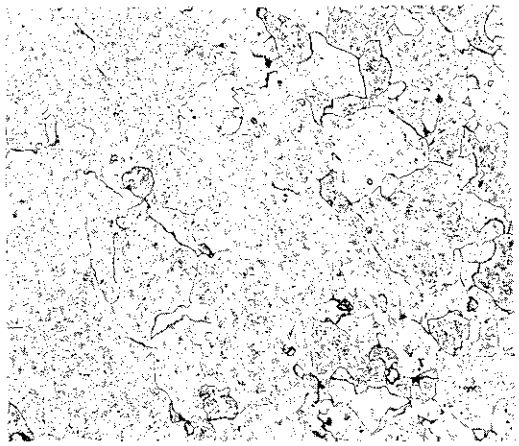

a) Base Metal 100 X

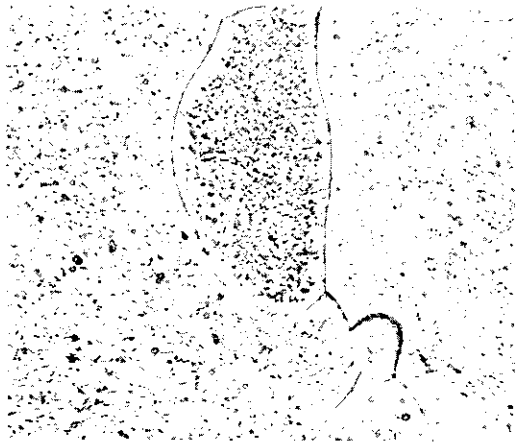

b) Base Metal 100 X

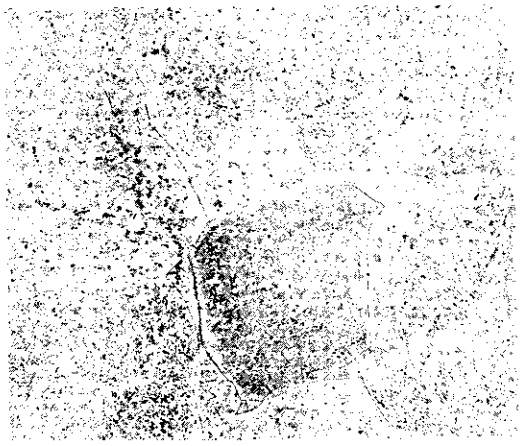

c) Weld Metal 100 X

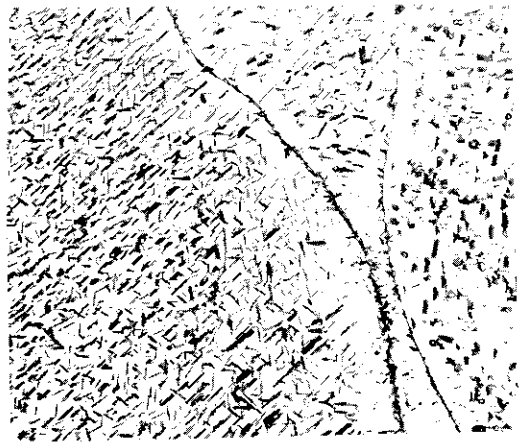

d) Weld Metal 100 X

Fig. 77—Microstructure of weld in Nb-5 Mo alloy (NC-191).

material. Grain boundaries appear to have been pulled apart due to thermal stresses. However, the ends of these micro cracks have been blunted by plastic deformation. The 5 w/o V alloy is the only one in which micro cracking in the base metal has been observed. This result indicates a susceptibility to hot cracking which was not suspected from previous work.

The 10 w/o W alloy showed a fairly normal dendritic coring effect in the weld metal. The presence of some precipitate is possible, but it cannot be definitely defined. If the precipitate exists in the weld metal, it occurs in the areas of dendritic segregation.

The needle type precipitate found in the 5 w/o Mo alloy suggests a carbide. However, the exact nature of these precipitates has not been determined. Extraction processes for use with the electron microscope are being used to identify the precipitates.

A heavy precipitate is in evidence in the 10 w/o Hf alloy. This precipitate seems to occur in the striation boundaries which have formed during solidification of the weld metal. It is believed that this precipitate is a hafnium containing carbide. The exact nature of this precipitate will also be determined.

The tensile properties of pure niobium, Nb-8.75 w/o W and Nb-5 w/o V alloys were determined at 1095 C (2000 F) in vacuum. The data are shown in Table 26. The data are compared with the properties of wrought recrystallized niobium and the 8.75 w/o W alloy are nearly the same. However, the yield strength of the weld metal in the Nb-5 w/o V alloy is only 80% of the base metal strength. The ultimate strength is slightly lower at 75% of the base metal strength. From these limited data, it appears that the joint efficiency in Nb and Nb alloy varies somewhere in the range between 75 and 100%, depending on the alloy composition.

Table 26. 1095 C (2000 F) Tensile Data - Weld and Base Metal *

Heat No.	Composition ** (w/o)	.2% YP (psi)	.5% YP (psi)	Ult. Strength (psi)	Uniform Elongation (%)	Fracture Strain (%)	Red. in Area (%)
NC-258	Pure Nb	9,400	10,180	10,180	0.5%	18.9%	46.4%
	O_2 0.074						
	N_2 0.021	(7800)*	(-)	(9200)	(1.8)	(38.4)	~(100%)
	C 0.033						
NC-131	Nb-8.75 W	18,400	20,300	21,500	1.2	15.4%	~100%
	O_2 0.077						
	N_2 0.014	(19,500)*	(-)	(22,400)	(1.6)	(41)	(66)
	C 0.05						
NC-253	Nb-5.01 V	26,600	27,700	27,700	0.5	34.2%	62.2%
	O_2 0.057						
	N_2 0.042	(33 500)*	(-)	(36,900)	(0.8)	(37.4)	(-)
	C 0.05						

* Base metal data in parentheses from other work.

** Applies to weld metal only.

The ductility of the weld metal is usually somewhat lower than the base metal when the strengths are equal.

Discussion

The weld specimens in the alloys tested showed no sign of gross hot cracking, however, the alloy containing 5 w/o V showed micro-cracks in the grain boundaries of the heat-affected zone. This cracking may be attributed to the presence of V_2O_3 which melts at 1977 C a temperature which is considerably lower than the melting point of the 5 w/o V alloy. Furthermore, V_2O_3 is readily oxidized to V_2O_5 which has a melting point of 670 C. It seems probable that the higher melting point oxide is the one involved since the loss in high-temperature properties would probably be excessive. The free energy values for V_2O_3 as compared to NbO_2 indicate that the oxide of vanadium would be present. This combination of factors indicated the presence of V_2O_3 as the caused of the boundary failure in the alloy containing vanadium. The presence of porosity as shown in Fig. 74 also indicates the presence of oxygen. An increase in the solubility for oxygen could be the reason for 5 w/o V, as shown in Fig. 67. The good hot strength properties of the Nb-V alloys could be used to advantage if a third element such as Hf or Ti were added to eliminate the V_2O_3 from the grain boundaries.

Summary

The addition of alloying elements to Nb in general increases the ductile-to-brittle transition temperature of the weld metal. The notable exceptions are Ti over 10 w/o, Hf between 0.5 and 1 w/o, and possibly V over 5 w/o. The mechanisms involved in these changes are not understood at this time.

There seems to be a reasonably close correlation between the room temperature hardness and the ductile-to-brittle transition temperature of the weld metal. The hardness, transition temperature and strength are related to the reactions between the alloying elements and the interstitial element to a large degree. Further study of the nature and dispersion of the precipitates is needed to established the hardening mechanisms. It is also apparent that the presence of oxygen and nitrogen in the welding atmosphere could influence the mechanical properties of the weld metal where alloying elements are present which could form precipitates with these elements.

REFERENCES

1. A. U. Seybolt, Journal of Metals, Vol. 6, 1954, p. 774.

2. R. P. Elliott, "Columbium-Oxygen System", ASM Preprint No. 143, 1959.

3. C. R. Tottle, "The Physical and Mechanical Properties of Niobium", Journal Institute of Metals, Vol. 85, 1956-57, p. 375.

4. B. F. Dyson, R. B. Jones, and W. J. McG. Tegart, "The Tensile Properties of High-Purity Niobium at Low Temperatures", J. Institute of Metals, Vol. 87, 1958-59, p. 340.

5. L. R. Williams and T. J. Heal, "The Consolidation, Fabrication and Properties of Niobium", Plansee Proceedings, 1958, Springer-Verlag, Vienna 1959.

6. R. T. Begley, et al., "Development of Niobium Base Alloys", WADC TR 57-344 Part II, December 1958.

7. H. R. Smith, C. Hunt, and C. W. Hanks, "The Development of Large Scale Electron Bombardment Melting and its Effect on the Composition of Metals and Alloys." Plansee Proceedings 1958, Springer-Verlag, Vienna, 1959.

8. W. F. Harris, "The Determination of Oxygen and Nitrogen in Niobium" Technology of Columbium (Niobium). John Wiley, New York, 1958.

9. W. F. Harris, W. M. Hickam, M. Loeffler, and C. Shaffer, "Quantitative Addition and Recovery of Oxygen Isotopes in Niobium". Accepted for publication by AIME.

10. C. Y. Ang and C. Wert, "Some Properties of Columbium Containing N_2," Journal of Metals, Vol. 197, 1953, p. 1032.

11. M. Hansen, Constitution of Binary Alloys, McGraw-Hill, New York, 1959.

12. E. T. Wessel, L. L. France and R. T. Begley, "Flow and Fracture Characteristics of Electron-Beam Melted Columbium". Presented at AIME Columbium Metallurgy Symposium, Hotel Sagamore, Lake George, New York, June 9-10, 1960.

13. H. A. Saller, J. T. Stacy and S. W. Porembka, Initial Investigation of Niobium and Niobium-Base Alloys, Battelle Memorial Institute Report No. BMI-1003, May 23, 1955.

14. W. H. Chang, "Strength Properties of Some Columbium-Base Alloys", Presented at Fall Meeting of Metallurgical Society AIME, Chicago, Nov. 2-5, 1959.

15. M. L. Pouchon, C. R. McKinsey, R. A. Perkins, and W. D. Forgeng, "The Solubility of Carbon and the Structure of Carbide Phases in Tantalum and Columbium", Reactive Metals, Vol. 2, Interscience Publishers, N. Y., 1959, p. 327.

16. R. P. Elliott, Niobium Phase Diagrams, Armour Research Foundation Report 2120-4, U. S. A. E. C. Contract No. AT(11-1)-515, May 6, 1959.

17. M. J. Manjoine, E. T. Wessel and W. H. Pryle, "Constant Strain Rate Testing Machine with Instantaneous Speed Change", ASTM Bulletin No. 226, Dec. 1957, p. 31.

18. E. T. Wessel and R. D. Olleman, "Apparatus for Tensile Testing at Sub-Atmospheric Temperatures", ASTM Bulletin No. 187, Jan. 1953, p. 56.

19. Betsy Anker and E. R. Parker, "Quantitative Substructure and Tensile Property Investigation of Nickel Alloys", AIME Trans., Vol. 200, 1954, p. 1155.

20. E. R. Parker and J. Washburn, "Effects of Impurities and Imperfections on Mechanical Properties", Impurities and Imperfections, American Society for Metals, 1955.

21. P. A. Beck, B. G. Ricketts and A. Kelly, "Subgrain Growth and Softening in Rolled Aluminum Crystals", AIME Trans. Vol. 215, p. 949, 1959.

22. C. A. Zapffe, F. K. Landgraf, and C. O. Worden, "Fractographic Study of Cast Molybdenum", AIME Trans., Vol. 180, p. 616, 1949.

23. E. T. Wessel and D. D. Lawthers, "Ductile-To-Brittle Transition in Niobium", in Technology of Columbium (Niobium) John Wiley and Sons, New York, 1958.

24. R. T. Begley and W. N. Platte, Development of Niobium-Base Alloys, WADC TR 57-344, Part IV, April, 1960.

25. R. T. Begley et al., Development of Niobium-Base Alloys, WADC TR 57-344, November 1957.

26. D. D. Lawthers and M. J. Manjoine, "The Effect of Testing Atmospheres on the Creep-Rupture Properties of Molybdenum Base Alloy" in High Temperature Materials, John Wiley and Sons, New York, 1959, pp. 486-497.

27. G. D. Gemmel, "Some Effects of Alloying on the Strength Properties of Niobium", Trans. AIME, Vol. 215, No. 6, December 1959, p. 898.

28. M. L. Pochon, C. R. McKinsey, R. A. Perkins, and W. D. Forgeng, "The Solubility of Carbon and Structure of Carbide Phases in Tantalum and Columbium" in Reactive Metals, Vol. 2, AIME, (W. R. Clough, ed.), Interscience Publishers, New York, 1959, p. 397.

29. R. T. Begley, et al., Development of Niobium-Base Alloys, WADC Technical Report 57-344, Part II, December, 1958.

30. Interim Report I, Contact No. AF 33(600)-39944, Manufacturing Methods for Columbium Alloy Forgings. Crucible Steel Company, November 30, 1959.

31. G. L. Miller, Tantalum and Niobium, Academic Press Inc., New York, 1959, p. 546.

32. B. A. Rogers and D. F. Atkins, "Zirconium-Columbium Phase Diagram" AIME Trans., Vol. 203, 1955, p. 1034.